An Assessment of Experimental Debris-Flow Scaling Relationships

JESSICA LAUREN HOLMES

An Assessment of Experimental Debris-Flow Scaling Relationships

Jessica Holmes

Thesis for MSc. (by Research)

Department of Geography, Durham University

2017

Declaration of Copyright

This thesis is the result of my own work and has not been submitted for consideration in any other examination. Material from the work of other authors, which is referred to in the thesis, is acknowledged in the text.

Jessica Holmes

Department of Geography, Durham University

2017

Acknowledgements

I would like to thank my supervisor, Jeff Warburton, for his continued support and guidance, and for sharing his expertise which made this research possible. I would also like to thank my dedicated flume helpers, Cameron Davies and my Dad, without whom I would have had no data to analyse, and no-one to share my excitement over levee formation with. Thanks also go to all of the laboratory staff who were extremely patient in answering my questions and assisting with my analysis, particularly Mervyn Brown and Michael Heslop who helped greatly with setting up the flume experiments.

Finally, I wish to thank my family and friends for their enduring support, encouragement and inspiration.

Abstract

This research tests empirically the theoretical assumption that scaling issues make small-scale flume debris flows unrepresentative of natural debris flows. Here, results from a small-scale debris-flow flume (8 m long, 0.2 m wide) were compared with similar experiments carried out using a large-scale USGS flume (95 m long, 2 m wide) and field observations. In total, 40 experiments were carried out at different slope angles (29°, 30°, and 31°) and different viscosities (from 0.001 Pa.s to 0.005 Pa.s) to provide a quantitative analysis of scaling relationships of debris flows of different sizes.

Dimensionless parameters, used for assessing debris-flow scaling, were typically within the range of natural debris flows: The Bagnold number was 73 – 1.9×10^{4}, the Savage number was 2×10^{-1} – 2.4×10^{2}, and the Friction number was 8×10^{1} – 4.7×10^{3}. The Savage number was larger than expected based on USGS data, but this is attributed to the larger value for grain-size/flow-depth. Inherent variability of debris-flow behaviour was highlighted in the basic characteristics such as mean deposit length (150.30±44.96 cm), mean width (50.10±4.86 cm), and mean velocity (3.88±1.35 m s^{-1}). Therefore, initial conditions are insufficient to make accurate predictions of debris-flow behaviour. There was considerable variation in flow behaviour with small changes in slope angle and viscosity. With each 1 degree change in slope, flow velocity increased by an average of 1.06 m s^{-1} and runout distance increased by an average of 16.35 cm. Small changes in viscosity (±0.002 Pa.s) altered the debris-flow rheology to such an extent that no lateral levees formed. Such effects can only be investigated in small-scale flumes which are free from the constraints of large flume models where initial conditions are difficult to vary.

Compared to natural and USGS flume debris flows, the reduced-scale debris-flow model used here provides results which broadly reproduce the behaviour of natural debris flows.

Contents

List of Figures

Chapter 1: Introduction and Background

Chapter 2: Methodology

Chapter 3: Results

List of Tables

List of Equations

Chapter 1: Introduction and Background

Chapter 2: Methodology

Chapter 4: Discussion

Chapter 1: Introduction and Background

A debris flow is a mixture of sediment saturated with water moving rapidly downslope under the influence of gravity (Anderson et al., 1969; Hungr, 1995; Blair, 1999; Chiarle et al., 2007), and these often occur in response to intense rainfall or snowmelt (Anderson et al., 1969; Blijenberg, 2007; Milne et al., 2012; Hu et al., 2015). Debris flows are highly destructive geomorphic events (Lorenzini and Mazza, 2004) owing to their high velocities and great erosive power (Iverson et al., 2011). Large debris flows have velocities which exceed 10 m s^{-1} and sediment volumes of up to 1 km^3 (Haas, 2016). They therefore control rates of hillslope erosion and longer-term landscape evolution (McCoy et al., 2013), and pose a major hazard to communities in mountainous areas where steep slopes are common (Shih et al., 1997). Although critical thresholds for debris flow initiation vary spatially (Burbank, 2002), most debris flows occur on slopes over 30˚ (Iverson et al., 2011) which is important in developing countries as often the poorest communities settle on steep hillslopes where land is available (UN Habitat, 2009). As such, geomorphic events such as debris flows present the greatest risk in developing countries (Petley et al., 2007), with single events causing multiple fatalities and damage to infrastructure. From 1950 to 2011, the median number of fatalities per deadly debris flow was 23 in developing countries, and 6 in developed countries (Dowling and Santi, 2014).

The largest debris flows often pose the greatest hazard, because the volume of the flow partly determines debris-flow impact forces (Ghilardi et al., 2001). For example, a high-intensity rainstorm in Japan triggered 107 debris flows and 59 shallow landslides in August, 2014, resulting in 74 deaths, as well as damage to 429 homes (Figure 1.2.1) (Wang et al., 2015). This highlights the importance of improving understanding of debris-flow dynamics in order to better

inform hazard management, as impact forces are often used to inform hazard management structures. Given that the frequency and magnitude of debris flows are likely to increase with climate change (Johnson and Warburton, 2003; Milne et al., 2012; Stoffel et al., 2014), debris-flow research that will allow for prediction and appropriate hazard management is becoming increasingly important.

Figure 1.1. Photograph of the Midori-ga-oka debris flow, one of 107 debris flows which were initiated in Japan on 20th August, 2014 in response to high-intensity rainfall, causing infrastructural damage and loss of life. (Wang et al., 2015).

Debris flows are unsteady, non-uniform geomorphic processes, making their initiation and flow behaviour difficult to predict (Iverson, 1997), which has implications for risk management in mountainous settlements (Roberds and Ho, 1997). Observation of natural debris flows is difficult due to the infrequent and sporadic nature of debris-flow initiation. Whilst there have been recent advances in

debris-flow observation, with video documentation of experimental flows (Logan and Iverson, 2007) and continuous monitoring of a select few natural debris flows (Berti et al., 2000; Marchi et al., 2002; McArdell et al., 2007; Badoux et al., 2009), it is difficult to infer debris-flow mechanics and processes from such limited data. As an alternative, debris-flow deposits have also been used to infer debris-flow processes and dynamics. However, again, this is problematic (Major and Iverson, 1999; Breien et al., 2007) as grain composition can undergo considerable change in the transition from fluid to deposit (Li et al., 2015). Laboratory models are therefore another approach used to inform the prediction of debris flows, and are used to carry out research at a reduced scale, as geomorphic processes often occur on scales too large to measure directly (Bennett et al., 2015). The use of numerical models where boundary conditions can be defined, and experimental debris flows which allow conditions to be controlled and replicated, is seen as vital to debris-flow research in the future (Turnbull et al., 2014).

1.1. Flume Experiments in Debris-Flow Research

The use of experiments in geomorphology is widespread and although criticised due to their inability to capture the true complexity of natural geomorphic events (Baker, 1996), debris-flow experiments in particular have been instrumental in the development of debris-flow research over recent years, as they allow measurements to be taken under controlled environmental conditions (Seeger et al., 2011). Unlike natural events where instrumentation is very costly as continuous monitoring is required due to the unpredictable nature and infrequency of debris flows, experimental debris flows, particularly those conducted on a reduced scale, can be carried out relatively cheaply and quickly. The reproducibility of experimental debris flows is also an advantage, as experiments

can be carried out with specific boundary conditions, whereas field experiments are unreproducible due to the idiosyncrasies of the environment (Iverson, 2015).

Debris-flow experiments can be carried out over a range of scales, from miniature flumes (e.g. Fairfield 2011), to small-scale flumes (e.g. Haas, 2016), to large-scale flumes, such as the USGS flume (e.g. Johnson et al., 2012), and debris-flow behaviour can be studied using a range of methodologies. These include chute experiments - or open channel flume experiments - which are the focus of this research and concentrate largely on the mobilisation and the importance of bed characteristics and boundary conditions on debris flows. Alternatively, centrifuge experiments are used to study debris-flow rheology (Bowman et al., 2010), and mathematical models, which have been widely used in developing understanding of the physical basis of debris flows, are frequently employed to predict debris-flow behaviour on particular slopes, to estimate erosion, and to inform the design of hazard management structures (Hungr, 2008; Deubelbeiss et al., 2011; D'Aniello et al., 2015; Turnbull et al., 2015). Table 1.1. shows some key characteristics of debris flows in large-scale experiments (USGS flume experiments) compared with debris flows in small-scale experiments. This demonstrates the differences in characteristics of debris flows over a range of scales, and therefore highlights the need for scaling relationships to be defined if debris flows of different scales are to be compared as there is considerable variation between debris flows of different scales.

Table 1.1. Characteristics of debris flows in large-scale experiments, small-scale experiments, and in natural debris flows. There is a "-" where there is a lack of data.

	Flume Dimensions				Flow Characteristics	
Experiment	**Slope angle (˚)**	**Width (m)**	**Length (m)**	**Depth (m)**	**Velocity (m s^{-1})**	**Flow Depth (m)**
Iverson et al., 2010	31	2	95	1.2	10-13	0.20
Iverson et al., 2011	31	2	95	1.2	-	-
Major, 1997	31	2	95	1.2	6-13	0.1-0.3
Haas. 2016	22-34	0.12	2	0.15	0.9-2.9	0.005-0.018
Cui et al., 2015	10-15	0.2	3	0.4	-	0.24-0.52
Sheidl et al., 2013	30	0.45	6.5	0.5	1.3*	0.024-0.160
Bettalla et al., 2012	0-38	0.33	1.5	0.15	1.24-3.35	0.016-0.039
Fairfield, 2011 (same flume as this study)	15-30	0.2	8	0.1	0.02-1.97	0.003-0.12
Typical range for natural debris flows	<30	-	-	3	0.1-20	0.1-10

*Average value

Debris-flow experiments can be carried out using a range of apparatus. This includes rotating drums - predominantly used for rheological studies - (Kaitna and Rickenmann, 2007; Kaitna et al., 2007; Sosio and Crosta, 2009), conveyor belt flumes (Hirano and Iwamoto, 1981; Hubl and Steinwendtner, 2000), recirculating flumes (Mainali and Rajaratnam,1994; Larcher et al., 2007), and open channel flumes, similar to the one used in this research (Van Steijn and Coutard, 1989; Davies, 1994; Weber and Rickenmann, 1999; Parsons et al., 2001; Fairfield, 2011; Procter, 2011; Hurlimann et al., 2015; Haas, 2016).

Large debris-flow flumes, such as the USGS flume, H. J. Andrews Experimental Forest, Oregon (Iverson et al., 1992), are useful due to their large scale which minimises scaling issues (Iverson et al., 2011) (Figure 1.2). However, it is difficult to redefine boundary conditions such as debris-flow volume, mixture composition, water content and slope angle at such a large scale (Turnbull et al., 2014), whereas on a smaller scale, it is comparatively easy to alter boundary conditions and to reconfigure the flume e.g. alter bed slope and shape. However, Iverson (2015) states that reduced-scale experiments show disproportionately large effects of viscous shear resistance and cohesion, and disproportionately small effects of excess pore-fluid pressure, affecting the dynamics of the flow, so suggests that flume modelling of debris flows should be undertaken at the *'largest scale possible'* to reduce these effects. This is demonstrated by Equations 1.3 to 1.5 and discussed in more detail below.

Therefore, whilst small-scale flume models are unlikely to achieve full dynamic similarity which refers to the geometric and kinematic similarity of a flow where boundary conditions are the same for flows of different scales (Iverson et al., 2010), they reproduce the primary characteristics (such as grain-size segregation and levee formation (Savage and Iverson, 2003)) of natural debris flows (Paola et

al., 2009). Johnson (1970) also asserts that as similar features are observed in debris-flow deposits of all sizes, the same processes are also likely to occur over a range of scales, meaning that it may be viable to model debris flows at small scales. Indeed, Davies (1994) suggests that small-scale modelling is possible where high-viscosity water (water and wall-paper paste) and coal particles are used to represent the fluid and solid phases respectively. However, channel length was a limitation of Davies' (1994) research, and so recirculating channels have been used to eliminate the need for long channels (Chow, 1959). The debate surrounding scale, which is an important theme in experimental debris-flow research (examples: Davies, 1994; Silbert et al., 2001; Iverson et al., 2010; Sheidl et al., 2013; Turbull et al., 2014; Iverson, 2015) is the focus of this research.

This chapter will provide an overview of debris-flow scaling, and the issue presented for small-scale modelling. The need for scaling is presented in the following section, followed by an overview of the key dimensionless numbers used in the development of scaling relationships between debris flows of different scales, and some examples of their use. This is followed by an introduction to experimental modelling of debris flows.

Figure 1.2. Photograph of the large-scale (95 m length) USGS debris flow flume used for debris flow experiments (From Iverson et al., 2011).

1.2. Scaling

Scaling between debris-flow flume experiments and natural debris flows is a major issue in debris-flow research, as in order to reduce the scale of such large geomorphic systems, there is a necessity for dimensions and ratios (which determine the behaviour of the processes) to be distorted (Iverson and LaHusen, 1993; Sheidl et al., 2013; Bennett et al., 2015; Iverson, 2015). These distortions typically affect the depth of the flow and in the size and density of sediment in the flow, which are important factors in determining debris-flow behaviour (Bennett et al., 2015).

Iverson (2015) asserts that macroscopic details cannot be analysed in small-scale experimental debris flows due to the time-scale separation of macroscopic gravity-driven motion and grain-scale stress generation due to the shallow flow-depth in small-scale experiments, and only some behavioural characteristics can therefore be studied in small-scale models. De Haas (2016) recognises the development of levees in small-scale debris-flow flume experiments, and suggests that the exaggeration of intermolecular forces at a small scale (Iverson and Logan, 2002; Iverson, 2015) is to be expected due to the shallow flow depth, high velocities, and large characteristic grain-size to flow depth ratio. However, the lack of development of levees in other experimental debris flows has led Iverson (2015) to argue that small-scale flume experiments are not appropriate for studying the macroscopic details of debris flow behaviour as levees are a key geomorphic characteristic of natural debris flows. Therefore, the differences between debris flows of different scales create a requirement for scaling relationships to be defined. Scaling between experimental and natural

debris flows require scaling on the length-scale, and on the grain-scale (Iverson et al., 2010), and can be addressed by dimensional analysis or by normalisation of differential equations, using dimensionless scaling numbers.

1.3. Dimensionless Scaling Numbers

Dimensionless numbers are used in scaling between experimental and natural debris flows (Iverson, 1997; Iverson and Denlinger, 2001; Iverson et al., 2010; Iverson, 2015; de Haas, 2016), and allow for quantitative comparison of different scales of debris flow. For a debris flow to occur, driving forces must exceed resisting forces. There are three forces that offer resistance to debris-flow motion; collisional forces, frictional forces, and viscous forces. Furthermore, there are three dimensionless parameters that describe the relationships between these forces (de Haas, 2016), and are therefore useful in scaling up from small-scale experimental debris flows to the typical scale of natural debris flows (Table 1.3.1). These are the Bagnold number, the Savage number, and the Friction number. The use of the Bagnold, Savage and Friction numbers in debris-flow scaling, as well as other dimensionless numbers which are used in the literature in debris-flow scaling are summarised in Table 1. 2.

Table 1. 2. Dimensionless numbers, their physical meanings, the equations for their calculation, and typical values observed in natural debris flows. (Iverson, 1997; Iverson, 2010; Haas, 2016). Where: δ is mean grainsize (m), v_s is volumetric solids fraction, γ is flow shear rate (s^{-1}), H is flow depth (m), L is length of the flow (m), g is gravitational acceleration (m s^{-2}), k is permeability (m^2), μ is interstitial fluid viscosity (Pa.s), ρ_f is mass density of the interstitial fluid (kg m^{-3}), ρ_s is mass density of the solid phase (kg m^{-3}), v is velocity (m s^{-1}). P_0 is a reference value of ρ such as the value at static, limiting equilibrium, and D is a pore pressure diffusion term (m^2 s^{-1}).

Dimensionless number	Significance and physical meaning	Equation	Typical values of prototype	Example of use
Bagnold number, N_B	Ratio of collisional forces to viscous forces	$N_B = \frac{v_s \rho_s \delta^2 \gamma}{(1 - v_s)\mu}$	10^0-10^8	Martino and Davies, 2003
Savage number, N_S	Ratio of collisional forces to frictional forces	$N_S = \frac{\rho_s \delta^2 \gamma^2}{(\rho_s - \rho_f) g H \tan \varphi}$	10^{-7}-10^0	Iverson, 1997
Friction number, N_F	Ratio of frictional forces to viscous forces	$N_F = \frac{v_s (\rho_s - \rho_f) g H \tan \varphi}{(1 - v_s)\gamma \mu}$	10^0-10^5	De Haas, 2016
Mass number, N_M	Ratio of solid inertia to fluid inertia	$N_M = \frac{v_s \rho_s}{(1 - v_s)\rho_f}$	1-10	Iverson et al., 2010
Darcy number, N_D	The ability of pore fluid pressure to mediate grain-grain interactions	$N_D = \frac{\mu}{v_s \rho_s \gamma k}$	10^4-10^8	Iverson, 1997
Grain Reynolds number, N_{Rg}	Ratio between solid inertial stress and the fluid viscous shearing stress	$N_{Rg} = \frac{N_B}{N_M} = \frac{\rho_f \gamma \delta^2}{\mu}$	0.01-2	De Haas, 2016
Reynolds number, N_R	Measure of the influence of viscous effects relative to flow size	$N_R = \frac{\rho_0 H \sqrt{gL}}{\mu}$	<2000	De Haas, 2016
Geometrical ratio, ε	Ratio between debris flow thickness and length	$\varepsilon = \frac{H}{L}$	<<1	Iverson et al., 2010
Pore pressure number, N_P	Ratio of timescales for debris flow motion and pore pressure diffusion	$N_P = \frac{\sqrt{L/g}}{H^2/D}$	10^{-6}-10^{-1}	Iverson and Denlinger, 2001
Froude Number, Fr	Used to characterise flows where gravity is important	$Fr = \frac{v^2}{gL}$	0-2	De Haas, 2016

The calculation of dimensionless numbers often requires a range of assumptions, as some of the parameters included in the equations cannot be easily measured in the laboratory. One such parameter is shear rate (1/s), which cannot be measured in small-scale debris-flow flume experiments. Therefore, flow shear rate is estimated by dividing average flow velocity over the average depth of the flow (Kaitna et al., 2014). This must be taken into consideration when assessing the methodological limitations of this research, as although this is considered a reasonable estimate, as evidenced by its use in many small-scale experimental studies (Kaitna and Rickenmann, 2007; D'Agostino et al., 2012; Kaitna et al., 2014), and by its use in debris-flow scaling (Savage and Hutter, 1989; Iverson, 1997), it may affect the accuracy and interpretation of the results.

1.4. Experimental Debris-Flow Scaling Issues

Comparison of Bagnold, Savage and Friction numbers between the large-scale USGS debris-flow flume experiments and smaller scale studies (using secondary data from flume experiments (Fairfield, 2011; D'Agostino et al., 2012; Haas, 2016)) is shown in Table 1.3. This shows that the dimensionless numbers calculated based on the smaller scale flume experiments are, in most cases, high in comparison to those in large-scale experiments (and in natural debris flows). However, this is to be expected due to the shallow flow depths resulting in high shear rates, and due to the large grain size:flow depth ratio in small-scale debris flows (de Haas, 2016), as theoretically, based upon normalised model equations and dimensional analysis, the divergence from expected behaviour should grow in proportion to the thickness of the mass cubed (Iverson, 2015). There is no consistent trend shown in this data, indicating that there are considerable differences in debris-flow behaviour for these different scales considered.

Table 1.3. Dimensionless numbers used in developing scaling relationships between different sized experimental debris flows, showing a range of debris flow flume lengths. (Data from Parsons et al., 2001; Fairfield, 2011; Bettella et al., 2012; de Haas, 2016)

Flume Length (m)	**Study**	**Bagnold number**			**Savage number**			**Friction number**		
		Mean	Min	Max	Mean	Min	Max	Mean	Min	Max
1.5	D'Agostino et al., 2012	50300	600	100000	100	0.6	200	1000	800	1200
2	De Haas, 2016	813	37	1589	1.21	2.25	0.17	1450	141	2760
8	Fairfield, 2011	26799	7113	94496	2.62	0.9	10.8	117538	6358	431769
10	Parsons et al., 2001	0.135	0.002	1.672	0.0005	0.000007	0.0027	201	43	1870
95	USGS	400	-	-	0.2	-	-	2000	-	-

The key characteristics of debris flows should be replicated at a reduced scale. Natural debris flows exhibit a distinctive morphology, with a high-friction, coarse grained snout, followed by a saturated tail. This arises due to kinetic sieving, which results in coarse grains rising to the surface of the flow, which are then moved to the front of the flow by shear (Johnson et al., 2012) to make a high-friction snout (Ancey, 2013). The high-friction snout behaves as a granular flow, followed by a saturated tail. The saturated tail pushes aside the snout to form lateral levees (Haas, 2016); a distinctive geomorphological signature of debris flows (Savage and Iverson, 2003). The process of kinetic sieving, along with buoyancy effects and squeeze expulsion (whereby the percolation of fine particles facilitates the upward motion of larger particles) also results in grain-size segregation. This is another distinctive characteristic of natural debris flows, with most deposits coarsening upwards (Johnson et al., 2012). These characteristics are important to note, as they should be replicated in small-scale debris-flow experiments if they are fully representative of the natural process. As such, the grain-size segregation will be a key criterion in assessing how representative of natural debris flows the small-scale debris flow experiments produced in this research are.

However, not all previous small-scale debris flow experimental studies have replicated the key characteristics observed in natural debris flows, which is problematic for ensuring small-scale debris flows are representative of natural flows. Indeed, in many small-scale debris-flow flume experiments, laterally graded levees, which are a characteristic feature of natural debris-flow deposits (Turnbull et al., 2015) were undeveloped or did not form in small-scale deposits (Van Steijn and Coutard, 1989; Liu, 1996; D'Agostino et al., 2010; Bettella et al., 2012; D'Agostino et al., 2013). In addition, Iverson (2015) states that even where

deposits generated using small-scale laboratory modeling resemble natural deposits, the processes under which they formed are not necessarily similar, as geometric similarity does not necessarily imply dynamic similarity (Massey, 1989).Therefore, this discrepancy between form and process will be considered when analyzing the results of small-scale experiments in this research.

1.5. Dimensional Analysis

Dimensional analysis is based upon the principle of dimensional homogeneity, meaning that the dimensions on one side of a physical equation must be balanced with those on the other side (Iverson et al., 2015), and is a valuable tool in scaling (Cheng and Cheng, 2004) as it allows the number of important system parameters to be reduced, enabling small-scale modelling (Bolster et al., 2011). Dimensional analysis aims to provide information about the relationship between different parameters involved in a particular phenomenon (Bridgman, 1922).

In relation to debris flows, dimensional analysis is used to make inferences about the dimensionless parameters which describe the evolving downslope velocity of the debris flow (Iverson et al., 2015). Dynamic similarity - which implies geometric and kinematic similarity, such that the ratio of the magnitudes of forces at fixed points are fixed (Massey, 1989) – requires three primary quantities (length, time, and mass) to be measured using constant units (Young, 1989). Theoretically, measurements of the primary quantities should change inversely with the size of the debris flow (Bridgman, 1922). These primary quantities mean that any mechanical quantity, a, will be a function of length, L, time, T, and mass, M where the function takes the form of a power product:

$$[a] = L^{\alpha} T^{\beta} M^{\gamma} \qquad [1.1]$$

Here, α is a dimensionless number if one or more of the numerical values of the exponents, $\alpha, \beta,$ and γ, is not zero (Yalin, 1971). Such dimensionless variables are known as π groups. Dimensional analysis can be completed through the derivation of π groups, allowing physical relationships to be considered independently of units prescribed by humans onto natural processes which occur independently of such constraints (Iverson, 2015).

In order for dimensional analysis to be carried out, firstly, a list of independent variables should be devised and the independent dimensions of these variables identified. Dimensionless quantities and the relationships between them should then be established (Cheng and Cheng, 2004). Iverson et al. (2015) describes the specific methodology for carrying out dimensional analysis in debris-flow scaling. The 2-Dimensional equations used for analysis of scaling relationships in this study are summarised here.

Firstly, a list of parameters which are considered to be important to debris-flow behaviour, and therefore to the evolution of the debris flow velocity, $\bar{u}$, is devised:

$$\bar{u} = f\left(g, L, H, \rho_0, \rho_s, \rho_f, \sigma, \theta, \phi, \mu_f, c_f, E_f, E, k, m, t\right) \qquad [1.2]$$

This list of parameters considers the case of a fluid-filled debris flow, and allows for macroscopic dimensional analysis. Here, f is an unknown function, g is acceleration due to gravity (m s^{-2}), L is length (m), H is thickness (m), ρ_0 is the bulk density of the mixture (kg m^{-3}), ρ_s is the density of the solid grains (kg m^{-3}), ρ_f is interstitial fluid density (kg m^{-3}), σ is a stress component (Pa), θ is slope angle, ϕ is the internal friction angle, μ_f is the viscosity of the fluid phase (Pa s), and c_f is the cohesive shear strength of the fluid phase (Pa) and is important where the fluid contains suspended mud (as is often the case in debris flows). E_f is the elastic bulk

modulus of the fluid phase (Pa), E is the mixture bulk modulus (Pa), k represents the Darcian pore-fluid permeability of the granular solid aggregate (m^2), m is the solid volume fraction of the granular mass (m^3), and finally, t is time (s).

This list of important parameters can be reduced through dimensional analysis to the following relationship:

$$\frac{\bar{u}}{(gL)^{1/2}} = f_5\left(\frac{H}{L}, \frac{\sigma}{\rho g H}, \frac{t}{(L/g)^{1/2}}, \theta, \phi, m, \frac{\rho_s}{\rho_0}, \frac{\rho_f}{\rho_0}, \frac{c_f}{\rho_0 g H}, \frac{E_f}{\rho_0 g H}, \frac{E}{\rho_0 g H}, \frac{(L/g)^{1/2}}{\mu_f H^2/kE}, \frac{\rho_0 H (gL)^{1/2}}{\mu_f}\right) \quad [1.3]$$

This relationship is used in this study to compare between the large-scale USGS flume experiments described by Iverson et al. (2010), and small-scale experimental debris flows. It is the inclusion of the final two grouped terms in Equation 1.3 which Iverson (2015) uses to argue that small-scale debris flow experiments are not representative of natural debris flows. This is due to the presence of $\mu_f H^2$ in the denominator of one group, and μ_f/H in the denominator of the other group, as

$$\frac{\rho_0 H (gL)^{1/2}}{\mu_f} \quad [1.4]$$

can be rewritten as

$$\frac{\rho_0 (gL)^{1/2}}{(\mu_f/H)} \quad [1.5]$$

As such, because water viscosity remains constant at different scales, μ_f will be kept constant whilst H is reduced to laboratory scale, resulting in disproportionately large viscous shear resistance, and disproportionately small pore pressure diffusion at a small scale. However, this can be compensated for by adjusting the viscosity of the mixture (Davies, 1994). In this study, the clay-content

of the debris flow mixture will be altered to effectively alter the fluid viscosity of the mixture.

In this study, the dimensionless parameters introduced in Table 1.2 will be used to demonstrate scaling relationships between the small-scale debris flows in this study, and the large-scale debris flows described by Iverson et al. (2010). However, the use of dimensional analysis for debris-flow scaling has some limitations: such analysis must assume idealised kinematic behaviour in a debris flow, and so variations in energy conversion and dissipation which occur at flow boundaries are ignored. The large variations in grain-size in natural debris flows and the unsteady, non-uniform behaviour of a natural debris flow (Iverson, 1997) are also not accounted for, although dimensional analysis does not have a requirement for uniform, steady flows.

1.6 Normalisation of Differential Equations

Normalisation of differential equations is a more precise method of scaling than dimensional analysis. In the case of debris-flow scaling, a depth-integrated model can be used (Figure 1.3). Iverson and George (2014) provide a detailed methodology for the derivation of dimensional model equations, which can then be used for scaling. The following expression is used to quantitatively assess scaling relationships between small-scale and large-scale experimental debris flows (Iverson, 2015):

$$D^* = \varepsilon^{1/2} \frac{\rho_0 g H}{E} \left(\frac{(L/g)^{1/2}}{(\mu_f H^2/kE)} \right) \left[p^* - \frac{\rho_f}{\rho_0} \frac{g_z}{g} h^* \right] \qquad [1.6]$$

The terms which are different to those defined in Equation 1.3 are defined as follows: $\frac{g_z}{g}$ refers to gravitational acceleration where the effect of local slope

angle and orientation is taken into account, and the terms with asterisks are dimensionless quantities in the equation:

$$D^* = D/(gH)^{1/2} \quad [1.7]$$

where D is the depth-integrated debris dilation rate (m s^{-1}).

$$p^* = p_b/\rho_0 gH \quad [1.8]$$

where p_b is basal pore-fluid pressure.

$$h^* = h/H \quad [1.9]$$

where h is the local thickness of the moving mass.

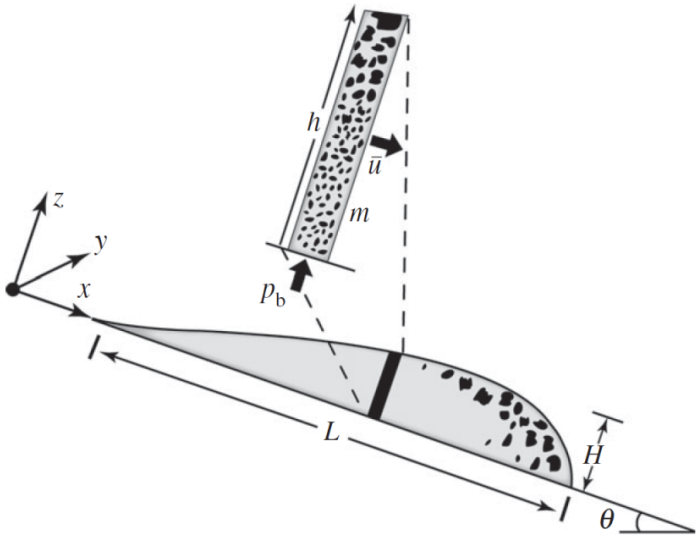

Figure 1.3. Diagram of a debris flow cross-section used to demonstrate a depth-averaged model for debris-flow evolution, showing some of the key parameters from equations used for scaling using both dimensional analysis and normalisation of differential equations. (From Iverson and George, 2014).

Equation 1.6 contains many of the same dimensionless parameters as in Equation 1.3. Iverson (2015) asserts that this equation holds the same implications for debris-flow scaling as Equation 1.3, whereby small-scale experiments are expected to diverge considerably from expected behaviour due to the reduction in

thickness, while fluid viscosity remains constant. Again though, this issue can be overcome by adjusting the clay content in the debris-flow mixture to alter viscosity. As with the dimensional analysis, measured and calculated values of the important debris-flow parameters (Table 1.2) from the debris-flow experiments from this study and from Iverson et al. (2010) will be compared to consider the scaling relationships between small-scale, large-scale, and natural debris flows.

1.7. Debris Flow Flume Modelling

In order to simulate debris flows in an experimental setting, three attributes of the experiments are important: sediment composition or mixture, initial bed conditions and channel slope. Although the first two of these attributes are affected by scaling the latter is not but is nevertheless extremely important in experimental studies as debris-flow dynamics are particularly sensitive to small changes in slope (Liu, 1996) but this is something that is not always tested in experiments due to fixed slope conditions.

1.7.1. Sediment Mixture

The composition of natural debris flows is highly variable, which impacts directly upon the velocity, and therefore upon the behaviour of the flow (Takahashi, 1981). Typically grain sizes range from silt and clay, to boulders exceeding 3 m in diameter (Sharp and Nobles, 1953). The composition of the sediment mixture in debris flows is important as it influences the dynamics of the flow. Sosio and Crosta (2009) found that an increase in particle size changes the rheological behaviour of a debris flow from shear thinning to shear thickening, and the percentage of sand in the flow influences the frictional character by increasing the friction in the snout when the percentage of sand is increased (Parsons et al., 2001). Indeed Pierson (1985) observed an increase in velocity where debris flows

had greater proportions of sediment compared with more dilute flows due to reduced flow resistance as a result of dampened turbulence. The sediment mixture in experimental debris flows must, therefore, be adjusted with respect to the flume model scale so that it reproduces behaviour observed in natural debris flows.

Iverson et al. (2010) demonstrate through large-scale debris-flow experiments that experimental debris flows with significant clay content and a rough bed most accurately represent the behaviour of natural debris flows. In past experimental studies, reconstituted debris-flow material from the deposits of natural flows has been used to make the material representative of the prototype (Hubl and Steinwendtner, 2000). However, given the large range of debris-flow compositions (Takahashi, 1981), such a study cannot be considered representative of all debris flows. Alternatively, natural materials such as clay, sand and gravel are commonly used in debris-flow flume experiments (Van Steijn and Coutard, 1989; Major, 1997; Iverson et al., 2010; Iverson et al., 2011; Haas, 2016). This allows sediment composition to be varied, allowing the behaviour of the flow to be altered (Parsons et al., 2001; Iverson et al., 2010; Fairfield, 2011).

The water content of the debris-flow mixture is also important as it influences both the behaviour of the flow and the stability of the bed (Weber and Rickenmann, 1999). Indeed, debris-flow rheology is determined by the interaction of the solid and fluid phases of the flow, which sets them apart from other types of mass movement events (Costa, 1988; Iverson, 1997 Berti et al., 1999; Savage and Iverson, 2003; Procter, 2011; Haas, 2016). Rheology refers to the observable mechanical effects of physical laws that operate on scales too small to be resolvable at a macroscopic scale (Iverson, 2003). The rheology of debris flows is

an important consideration for this thesis, as there are scale-dependent interactions between the solid and fluid phases of debris flows (Sheidl et al., 2013) which determine the rheology and therefore the behaviour of the flows. Iverson (2003) states that the rheology of a debris flow evolves over time due to the variable interactions of solid and fluid phases, such that a single approximation of debris-flow rheology cannot be made. As such, the scaling of the sediment mixture used in debris-flow experiments is vital in determining behaviour of the flow.

However, it is not possible to achieve full dynamic similarity between small-scale experimental debris flows and natural debris flows as the viscosity of water remains constant over both scales, and so scaling-ratios become distorted as both Froude and Reynolds similitudes cannot be satisfied simultaneously (Felder and Chanson, 2009). However, Henderson (1966) asserted, that Froude scaling (Table 1.3.1) can be used to ensure representativeness, if not full dynamic similarity. This is important for the design of flume experiments, as the desired Froude number can be achieved by altering the bed roughness, typically by roughening the bed with sand (Sheidl et al., 2013). As such, dynamic scaling parameters (Table1.3.1) are used in this study, not only to determine scaling relationships between small- and large-scale experimental debris flows (through a comparison with Iverson et al. (2010)), but also to ensure that a representative flow mixture and bed roughness are used.

Alternatively, Davies (1994) uses high-viscosity water in place of the fluid phase of the debris flow in a small-scale flume experiment. This accounts for the increased viscosity in the fluid phase of natural debris flows caused by the van der Waals' forces between clay particles in the water (Coussot, 1995) and produces

small-scale debris flows comparable to natural flows. Glycerol (Turnbull et al., 2015), wall paper paste (Martino and Davies, 2003), and thixotropic fluid (Chanson et al., 2004) have also been used in place of the fluid phase of debris flows to mimic the high viscosity of interstitial fluid in debris flows. As such, there are many alternative ways of scaling debris-flow mixtures, but the importance of scaling the mixture to the size of the flume is great in all cases, as the interactions between the solid and fluid phase of the debris flow determine the flow behaviour (Sheidl et al., 2013).

1.7.2. Bed Conditions

Bed conditions are an important consideration in the design of flume experiments due to the control on natural debris-flow dynamics: Smooth beds reduce resistance to flow, so debris flows on smooth beds are approximately 30% faster than on rough beds (Iverson et al., 2010). However, the enhanced friction on rough beds and channel walls provides resistance to flow and encourages the growth of lateral levees which channelize the debris flows, and therefore rough beds do not decrease the runout of the flow (Johnson et al., 2012). Iverson et al. (2010) propose that a rough bed produces debris-flow characteristics most representative of a natural flow. There are many methods of roughening beds in debris-flow flumes, which are used extensively in the literature as smooth beds are unlikely to be representative of natural debris flows. These include using sandpaper to roughen the bed (Haas, 2016), and gluing sand to the channel (Major and Pierson, 1992). However, the relative size of the bed sediment and the sediment that comprises the debris-flow mixture is also important. In natural debris flows, where both the mixture and bed sediment sizes are equal, the bed will be eroded, but if the mixture sediment size is increased beyond the size of the bed sediment, the debris flow behaves as though it were moving over a rigid bed

(Papa et al., 2004). This is important as the entrainment of bed sediment impacts upon the behaviour of a debris flow, as the volume of a debris flow is increased (Liu, 1996), hence giving it greater destructive power.

The wetness of the debris flow bed is also important for debris-flow characteristics, as this alters pore-pressure and therefore alters the friction on the bed, influencing the velocity of the flow (Iverson et al., 2011). However, it is also suggested that pore water pressure is not present in continuously deforming sediments, and so may not play a key role in debris-flow dynamics (Deangeli, 2009). However, as water is a requirement for debris flows to occur, regardless of the debate surrounding pore pressure and its role in debris-flow behaviour, bed conditions need to be taken into consideration when designing experimental debris flows. Water content of the bed also influences bed stability: The angle of stability remains constant up to a critical water content, which then causes a decrease in stability (Weber and Rickenmann, 1999). As such, water is important in debris-flow initiation as well as debris flow dynamics.

1.7.3. Slope

In order for debris flows to be initiated, there must be a sufficient slope angle (Milne et al., 2012). Whilst some debris flows, such as bentonite debris flows, can occur on slopes as low as 5° (Anderson et al., 1969), most debris flows occur on slopes around 30° (Iverson et al., 2011). As such, bed slope must be considered important as a high slope angle is generally required for debris-flow initiation.

Debris-flow behaviour is sensitive to variation in both bed slope (Lorenzini and Mazza, 2004; Guthrie et al., 2010; Fairfield, 2011; Pudasaini, 2011), and lateral variation in slope (Iverson et al., 2010). Debris flows on steep slopes tend to have greater velocities than those on lower slopes. For example, typical debris

flow velocities range between 0.5 m s^{-1} and 20 m s^{-1}, and these variations were attributed to variations in flow composition and slope geometry (Lorenzini and Mazza, 2004). Slope has an impact on the volume, and depositional area of the flow, which is important for hazard mapping, as faster flows are likely to entrain more material from the bed. Therefore, the steeper the slope of the bed, the larger the depositional area of a debris flow is likely to be. As such, the slope of the main channel affects the depositional area indirectly by increasing the volume of sediment due to greater entrainment on steeper slopes due to greater velocities (Liu, 1996). Indeed, a limiting topographic method can be used to estimate runout distances based on slope angle (D'Agostino et al., 2010), whereby debris flow continues on slopes >10˚, stops on slopes of 4˚, and between 4 and 10˚, stops when the following condition defined by Burton and Bathurst (1998) is met:

$$\begin{pmatrix} Distance\ travelled\ on \\ slopes\ between\ 4°and\ 10° \end{pmatrix} > 0.4(Elevation\ lost\ on\ slopes > 10°) \qquad [1.10]$$

Overall, bed slope has a major influence over debris-flow behaviour, and so a consideration of the impacts of varying slope angle will form the basis the experiments conducted in this research.

1.8. Aims and Objectives

Whilst it has been shown theoretically that there are potential scaling issues with small-scale experimental debris flows, (Iverson et al., 2010), the significance of this in terms of the use of such studies in debris flow management and prediction has not been quantified experimentally. This thesis aims to document for the first time a quantitative analysis of the scaling relationships between small-scale debris-flow experiments and large-scale experiments and natural debris flows. The aim of this thesis is to replicate experiments carried out in the USGS debris-flow flume (Iverson et al., 2010) on a smaller scale (approximately 1/10 of

the size of the USGS flume). This will allow for the development of scaling relationships between small-scale experimental debris flows and larger scale experimental and natural debris flow counterparts.

The objectives of this research are:

1) *To replicate at approximately 1:10 scale the USGS debris-flow flume experiments as documented by Iverson et al. (2010), and to provide a direct comparison of large- and small-scale experiment results.*

2) *To quantify scaling differences between small-scale debris-flow flumes and large-scale debris-flow flumes / natural debris flows, with reference to dimensionless scaling numbers and geometric analysis of the morphology of runout deposits.*

3) *To demonstrate the utility of flexible small-scale debris-flow flume experiments compared to larger, more restrictive models, in which initial boundary conditions are fixed. This will be achieved by varying the slope angle in the small-scale flume relative to the fixed 31˚ in the large-scale USGS debris-flow flume, varying the mixture composition to alter mixture viscosity, and replicating the experiments ten times for each set of boundary conditions.*

Chapter 2 will present the methodologies of this study, introducing the debris-flow flume facility which was used to conduct this research. Chapter 3 will present the results of the flume experiments, which will be later analysed and discussed (Chapter 4), and compared with natural debris flows and the large-scale debris-flow flume experiments conducted by Iverson et al. (2010) to facilitate consideration of scaling issues in small-scale experiments. Finally, Chapter 5 summarises the main findings of the research.

2. Methodology

2.1. Background

The initial conditions of the debris-flow experiments in this study were designed around those used in the large-scale USGS flume described in Iverson et al. (2010) (Table 2.1), and replicated at a reduced scale in the small-scale flume. This was purposeful, in order to:

(1) demonstrate the utility of small-scale experimental debris flows in comparison to large-scale ones by mimicking the experimental conditions as closely as possible; and

(2) carry out additional experiments where slope angles were varied around 31˚ (Iverson et al., 2010), to demonstrate the important influence of small variations of slope on debris-flow behaviour. An attribute which cannot be easily modelled in large-scale facilities where the initial boundary conditions of debris-flow experiments cannot be easily altered e.g. slope in the large-scale USGS flume (Turnbull et al., 2014).

The data collected in this research was directly compared with secondary data from Iverson et al. (2010), and with data previously collected from experiments conducted in the same flume and in flumes of even smaller scales (Fairfield, 2011 (8 m long flume and 2 m long flume); Procter, 2011 (8 m long flume); de Haas, 2016 (2 m long flume)) in order to quantify empirical scaling relationships. The experiment properties are reported in Table 2.1.

There is a scaling ratio of 10:1 for the large-scale USGS flume experiments and the small-scale flume used for the experiments in this research.

Table 2.1. Properties of sediment used in experiments conducted by Iverson et al. (2010), which this study aims to replicate. SGM refers to a mixture of sand and gravel with significant mud proportions, and SG refers to a mixture of sand and gravel. (From Iverson et al., 2010). Where measurements were not available, N/A is shown.

Property	**USGS Experiment Subset**			**Small-scale Experiments**
	SGM Rough Bed	SG Rough Bed	SG Smooth Bed	
Initial sediment volume behind headgate, including pore space (m^3)	9.73±0.45	9.80±0.33	9.72±0.44	0.0089
Initial sediment water content, weight percent (water weight / dry sediment weight) x100	8.0±2.8	6.6±2.0	6.1±1.5	20.5
Net water added to sediment prior to flow release (m^3)	2.05±0.29	2.20±0.52	2.22±0.31	0.00306
Total water (initial + added) in sediment at time of flow release (m^3)	3.34±0.45	3.30±0.22	3.17±0.23	0.00306
Mean sediment porosity, before water application	0.39	0.37	0.36	0.32
Mean pore volume before/after 2% compaction caused by water application (m^3)	3.8/3.6	3.6/3.4	3.5/3.3	N/A
Mean saturation of pore space at flow release (%)	93	97	96	N/A
Mean wet bulk density of sediment at flow release (kg m^{-3})	2010	2060	2070	2020
Wet bulk density of slurry deposits after flow has ceased	2100±110	2070±90	2070±90	N/A

2.2. Debris flow flume experiments

The debris-flow flume used in this research (Figure 2.1) was 8 m in length, 0.2 m in width, and 0.12 m in depth, and encased in a 1 m wide box frame. The board at the base of the flume channel which the experimental debris flows runout onto was painted white for greater contrast between the board and the deposit for better visualization of the deposit and morphology, and was painted with a 4 cm × 4 cm grid for scale. In contrast to the large-scale USGS flume which has a fixed slope of 31° for the majority of its length (Iverson and LaHusen, 1993), the slope of the flume used in these reduced scale experiments is uniform over its full length, but the overall bed slope can be varied between 10° and 50°. This is a major benefit of small-scale flumes. However, as the aim of this research is to replicate the initial conditions of the USGS experiments as closely as possible, the set-up of the reduced scale flume was similar (Figure 2.2). Experiments were carried out at 31˚ with a rigid bed in order to replicate the USGS experiments, and further experiments were carried out at 29˚ and 30˚. Varying the slope angle over a small range allowed the sensitivity of debris-flow behaviour and variability in debris-flow characteristics with just a small change in initial conditions to be assessed and so demonstrates the utility of the small-scale flume compared to large-scale flumes. Varying slope angle over a small range is therefore useful.

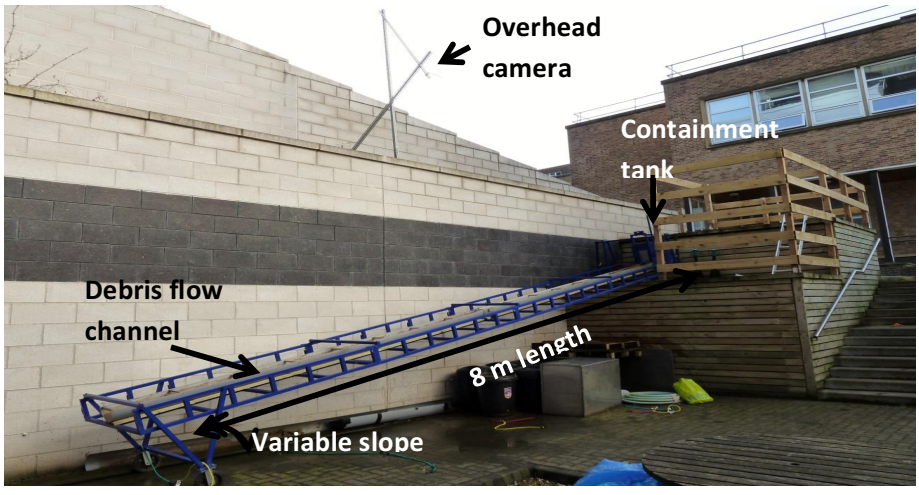

Figure 2.1. Small-scale debris flow flume apparatus used for this study

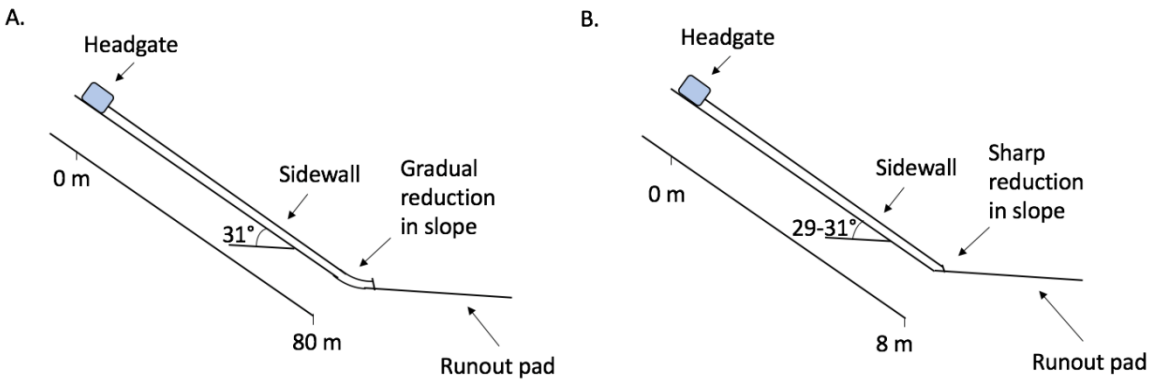

Figure 2.2. USGS debris flow flume initial set-up conditions (A) which were replicated at a reduced scale in this study (B).

In order to make the bed rough to replicate the USGS experiments (Iverson et al., 2010), the channel of the flume had 2 mm sand glued onto it (Parsons et al., 2001; Rombi et al., 2006; Fairfield, 2011; Procter, 2011; Sheidl et al., 2013; Sheidl et al., 2015). The debris-flow flume facility has a containment hopper (Figure 2.3) from which 18kg of sediment mixture is released in a dam-break- style initiation whereby the release gate is opened using a lever to initiate the flow. The size of the head gate was unimportant given that the debris-flow mixture was released en masse. Despite a dam-break release not replicating exactly the conditions in nature, whereby debris flows tend to be initiated by a small force imbalance as opposed to a catastrophic one, this initiation mechanism is widely used in debris-flow experiments as it is easily replicated (Iverson, 2015), and is the same as the mechanism used in the USGS experiments (Iverson et al., 2010), so its use is justified here.

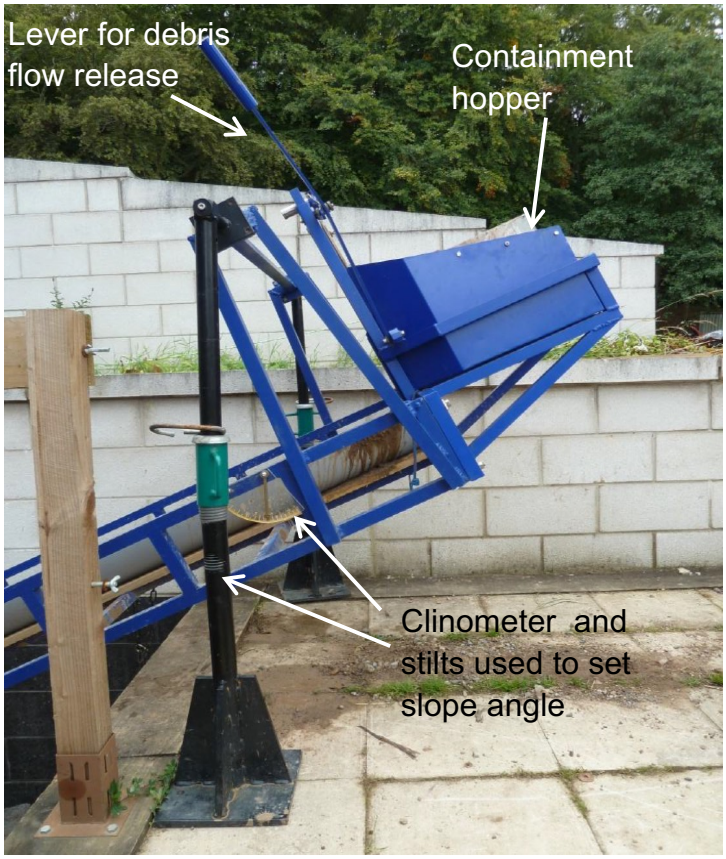

Figure 2.3. Debris flow flume containment tank for input of sediment mixture.

For the experiments designed to replicate the USGS experiments, the bed of the debris-flow flume channel was rigid and non-deformable. In debris flows flowing over rigid beds, debris-flow dynamics are dependent on slope, sediment discharge rate, and friction angle. On deformable beds, debris-flow dynamics are governed by the condition that the driving force must be equal to yield stress at the bed surface (Egashira et al., 2001) and by feedbacks from the bed, particularly if the bed sediment is wet (Iverson, 2015). As such, feedbacks from the bed which govern the evolution of natural debris flows will be overlooked in the rigid bed experiments conducted in this study.

Figure 2.4 shows the experiments which were carried out in this study, whereby initial conditions were varied around the USGS experiments, in addition to experiments where the slope and the bed conditions of the channel were varied. Ten repeats of the experiments based on the USGS experiments were carried out to ensure repeatability and to ensure that the results were accurate and therefore appropriate to use for the validation of numerical models (Turnbull et al., 2014). The experiment repeats were also used to demonstrate the inherent variability of debris-flow dynamics (Warburton and Davies, 1994; De Haas et al., 2015) which is expected due to spontaneous breakdown of the flow into surges. This intrinsic variability will be considered through analysis of the debris-flow deposits and flow characteristics. This is a clear advantage of small-scale experiments, as due to time- and cost- restraints, it is not possible to conduct as many repeat experiments in large-scale experimental debris flows.

Further experiments were carried out to consider the effects of interstitial fluid viscosity on debris-flow behaviour. Viscosity can be varied through changing the temperature or though adjusting the volume of clay in the debris-flow experiments (Equation 2.1). Given that temperature could not be controlled in this experiments, viscosity was adjusted through changing the clay content. Interstitial fluid viscosities of 0.001, 0.002, 0.0025 (standard mixture used in the experiments used to test the influence of slope), 0.004, and 0.005 were compared.

$$\mu/\mu_w = 1 + 2.5v_{fines} + 10.5v^2{}_{fines} + 0.00273\exp(16.6v_{fines}) \quad [2.1]$$

Where μ is the interstitial fluid viscosity, μ_w is the dynamic viscosity of water (0.001002 Pa.s), and v_{fines} is the volume fraction of the interstitial fluid occupied by fines.

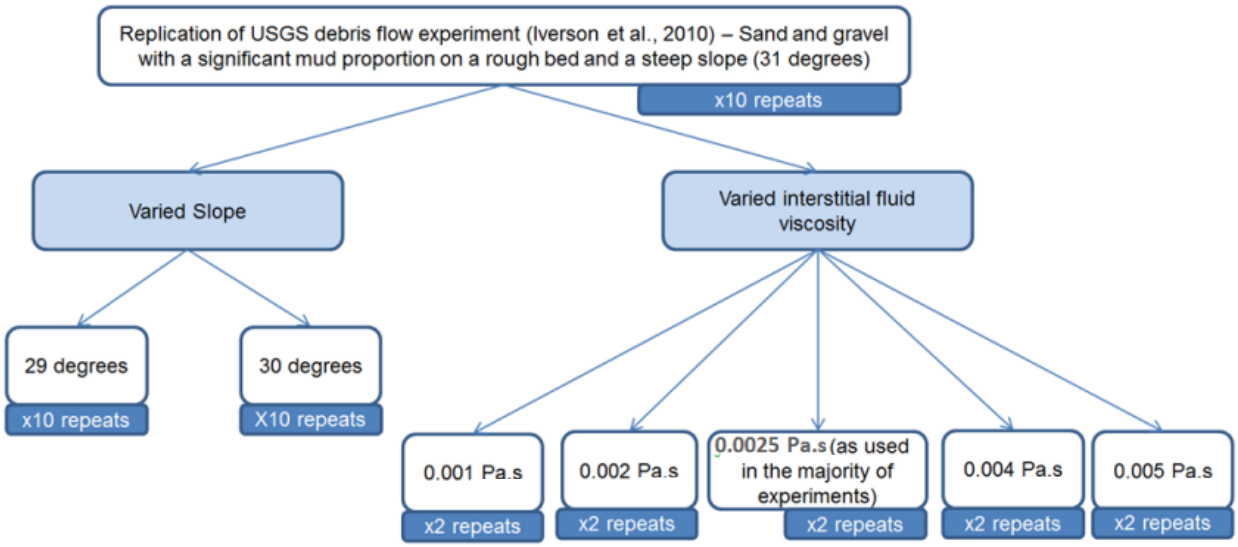

Figure 2.4. Experiments completed using the small-scale flume. All experiments were varied around the conditions of the USGS experiments, with slope or mixture composition being altered, and other conditions kept constant.

2.3. Testing the Composition of sediments used in the experiments

Given that Iverson et al. (2010) found that the sand and gravel mixture with a significant mud proportion and a rough bed generated results most similar to natural debris flows, a mixture of a similar composition, scaled to the size of the small-scale flume was used for the experiments in this research (Table 2.2). This was completed by initially maintaining the proportions of the USGS mixtures, however, a series of initial experiments demonstrated that the proportion of water in the sediment mixture needed to be increased in comparison to that used in the USGS flume in order for the debris-flow mixture to flow down the channel without stopping before it reached the runout board (Table 2.3). This is likely to be due to the increased effects of viscous shear and cohesion where the same fluid viscosity is used in a smaller-scale experiment, as identified by Iverson, 2015. Therefore, a

mixture was developed using a similar composition to that used in previous debris-flow experiments using the same flume as used in this research (Procter, 2011) (Table 2.2).

As such, the mixture composition used in the debris flows in the experiments carried out in this research are not scaled directly in relation to the USGS mixture. However, the composition is a reasonable approximation of natural debris flows, with bulk-density and water content values being within the ranges expected for natural debris flows (Webb et al., 1999; McCoy et al., 2010). However, the differences in flow composition may impact the dynamics of the flow. For example, there is a greater proportion of gravel in the mixtures used in these experiments compared to that of the USGS experiments, and as there is already likely to be a reduced grain-size to flow depth ratio in small-scale flows (de Haas, 2016), the effects of this are likely to be amplified. There is also a greater volumetric fraction of interstitial fluid in these experiments, which will affect flow dynamics as debris-flow behaviour is extremely sensitive to small changes in water content (Pierson and Scott, 1985). However, given the similarities of this mixture to previous experimental mixtures (Procter, 2011), it was deemed a suitable composition.

Table 2.2. Mixture compositions used in debris flow flume experiments in the large USGS debris-flow experiments, and the experiments completed in this research.

Material	**USGS Composition**		**Composition used in this study**	
	Percentage weight (%)	Weight (kg) (scaled to 18kg equivalent)	Percentage weight (%)	Weight (kg)
10 mm Gravel	22	3.96	34	6.12
Sand	60	10.8	38.5	6.93
Clay	6	1.08	10.5	1.89
Water	12	2.16	17	3.06

Table 2.3. Summary of initial debris-flow experiments used to determine the appropriate sediment mixtures for use in the experiments. Sediment Mixture 1 refers to the proportions used by Iverson et al. (2010), and where (silica) is shown, silica sand was used, rather than yellow sand which was used for the majority of the experiments to test the effects of using different materials. Sediment Mixture 2 refers to that developed from Procter (2011). Where (N/A) appears in the Deposit length column, the debris flow did not reach the runout board.

Run	Sediment mixture used	Additional Water (kg)	Runout Distance in channel (m)	Deposit length (if applicable) (m)
1	1 (silica)	0.30	4.3	N/A
2	1	0.50	5.2	N/A
3	1	0.60	8.0	1.12
4	1	0.60	7.2	N/A
5	1 (partial silica)	0.60	8.0	1.14
6	1 (silica)	0.60	2.0	N/A
7	1	0.84	3.4	N/A
8	1	1.25	6.8	N/A
9	2	0.00	8.0	1.04
10	2	0.00	8.0	1.20

The inclusion of the term ‘debris’ in ‘debris-flow’ suggests that a range of grain sizes are present (Iverson and George, 2014). Therefore, a combination of different grain-sized natural sediments was used: Once mixed, clay made up part of the fluid phase of the debris flow, and ensured that the mixture was representative of natural debris flows by increasing the viscosity of the fluid phase (Davies, 1994; Ashworth et al., 1996). Fine kiln dried sand made up part of the solid phase, and finally, gravel was used to represent the coarsest fraction of the solid phase. Each component of the mixture was weighed in the same quantity for

each experiment, and the mixture was mixed thoroughly for five minutes each with an electric hand-mixer to ensure that the sediments were completely mixed and no large clay lumps were left in the mixtures. This procedure was kept constant to allow for comparison between experiment runs.

Given that the grain-size distribution of debris flows affects the rheology, and therefore the overall behaviour of the flows (Sosio and Crosta, 2009), particle size analysis was carried out on the debris-flow mixtures in order to determine the grain-size distributions. In the experiments, the composition of the debris-flow material was kept constant, using the same quantities of each size fraction (gravel, sand, and clay), however within these fractions, there is some variability.

The range of particle sizes making up the mixture composition in each experiment was determined using Particle Size Analysis. Firstly an approximately 0.2 kg subsample of each debris-flow mixture was dried at 105 ˚C and weighed to determine the water content. Water was then added to the samples, and phi sieves (11.31 mm, 8 mm, 5.66 mm, 4 mm, 2.83 mm, and 2 mm) were used to separate particles by grain size. The separated particles were then dried again and weighed. All particles smaller than 2 mm in diameter were then further analysed: Firstly, a smaller sub-sample was obtained using a riffle box to remove bias from the sub-sampling. The sub-samples were then analysed in the Beckman Coulter LS13 320 Laser Diffraction Particle Size Analyser machine, and the composition determined using laser diffraction to measure particles between 0.4 and 2000 μm (Blott and Pye, 2006).

Bulk density was calculated by dividing the mass (kg) by the volume (m^3), yielding an average wet bulk density of 2020±41 kg m^{-3}. This is within the range recorded for natural debris flows - typically between 1400 and 2500 kg m^{-3} (McCoy et al., 2010) - and so is considered representative. The volumetric water content

averaged 36%, suggesting that the mixture is representative as debris flows typically contain less than 40% water by volume (Webb et al., 1999), albeit at the wetter end of this range.

The debris-flow mixture also needed to be representative of the large-scale USGS experiments to allow for comparison. One criteria for comparison is whether the debris-flow deposit geometry generated using the composition described in Table 2.2 is similar in geometry to those generated by USGS debris-flow flume experiments (Major, 1997). This is similar to the rheology tests carried out when comparing concrete using a dollop test (Iskender, 2016). Given the ratio of channel length (m) to deposit length (m) is approximately 8.3:1.3 for the USGS experiments (Major, 1997) and 8:1.2 in the experiments conducted in this study, the debris-flow morphology was considered approximately comparable.

2.5. Data Acquisition

The small-scale flume described in section 2.2 was used as the main means of data collection in this study. The debris-flow experiments were recorded using a 16 MP Panasonic Lumix DMC-F5 digital camera, mounted vertically above the flow (Figure 2.1). This footage was used to determine flow velocity using frame-by-frame analysis using Quicktime Player. The videos were analyzed at 25 frames per second, yielding an error of 0.25 m s^{-1} in flow velocities of 6.25 m s^{-1}. The flow was recorded from 6 m down-channel owing to restrictions in the field of view of the camera, and across the full length of the runout board. Qualitative data on the dynamics of the flow was also recorded using a GoPro (Hero 4) camera positioned at the end of the flume, recording the flow obliquely. Flow depth was estimated using mass balance considerations based upon the known volume of sediment, and the measured runout area, coupled to observations from the video footage.

Debris-flow models, including experimental models such as the one used here, should produce morphological characteristics similar to that of the prototype if the flow dynamics were representative of natural debris flows. The debris-flow deposits from the small-scale flume experiments conducted in this research should display key features of natural debris flows such as levees, coarse-grained flow fronts and saturated tails, and surge-type behaviour. As such, photographs of the deposits were taken to produce 3D models of the runout deposits which could then be analyzed to create a topographic model of the deposits. The imagery of the debris-flow deposit was collected by taking a minimum of 30 photographs of each flow deposit, using a 5 MP ipad camera which allowed for clear images to be taken without the need for re-sizing the photographs which would reduce image quality (as for cameras with higher resolutions) (Westoby et al., 2012). The photographs were taken from as many angles as possible in order to capture every part of the deposit.

2.5. Structure from Motion (SfM)

Structure from Motion (SfM) refers to the use of photographs taken of a single object, or in this case a single land form (runout deposit), from multiple angles in order to develop a dense point cloud, which can then be georeferenced and scaled for analysis (Smith and Vericat, 2015). In this study, this analysis involved the creation of digital elevation models (DEM) of the experimental debris-flow deposits to calculate volumes and to characterise the morphology of the deposits to quantitatively compare these deposits to both the large-scale USGS deposits (Iverson et al., 2010) and natural debris-flow deposits. Data from Iverson et al. (2010) will be used for comparison with large-scale experiments, and data from natural debris flows summarised by de Haas (2016) will be used for comparison with natural debris flows.

Agisoft Photoscan was used to generate a 3D pointcloud of photographs taken of the debris-flow deposits and channels generated in the flume experiments using the workflow shown in Figure 2.5. Figure 2.6 shows an example of a 3D point cloud generated from photographs taken of a debris-flow deposit resulting from an experiment carried out in the small-scale flume. Following the construction of such point clouds, Digital Elevation Models (DEMs) were produced and imported into ArcMap to generate data about the morphology of the debris-flow deposits, including width, length, area, volume, and to generate cross-profiles to demonstrate the topography of the deposits. The use of SfM in this research is justified as it is a less cost- and time-intensive alternative to methods such as Terrestrial Laser Scanning Scanning (Smith et al., 2015; Carrivick et al., 2016), and at scales <10 m^2, produces data comparable to such methods (Smith and Vericat, 2015).

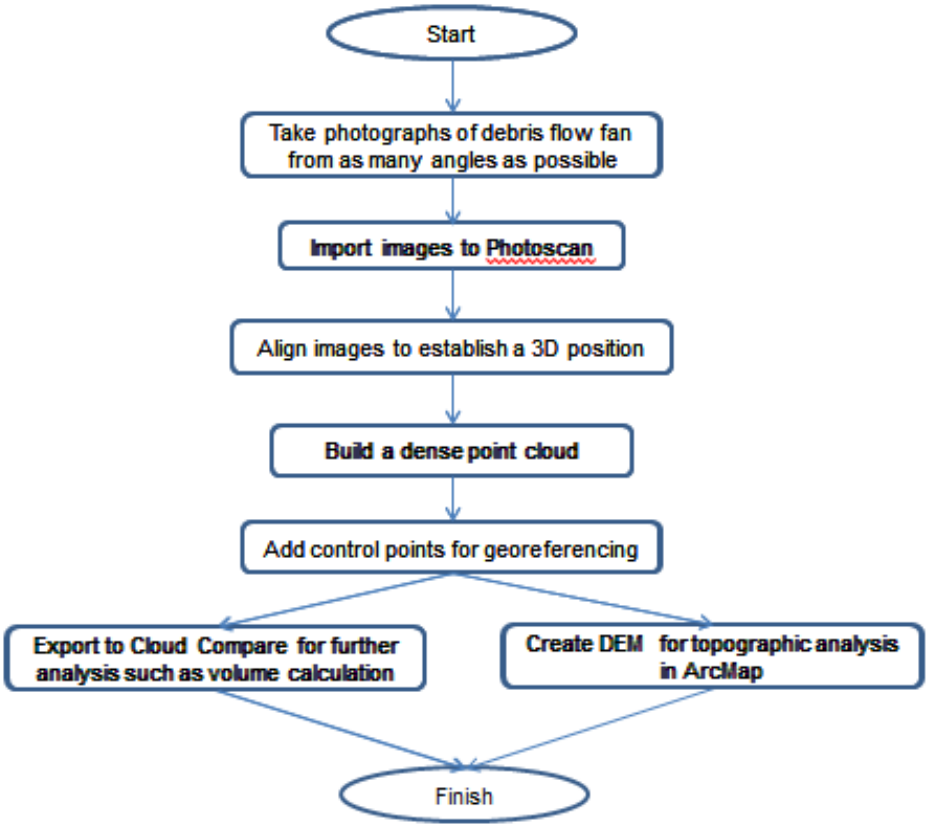

Figure 2.5. Methodology used in Photoscan to generate a 3D pointcloud from photos of a debris flow fan.

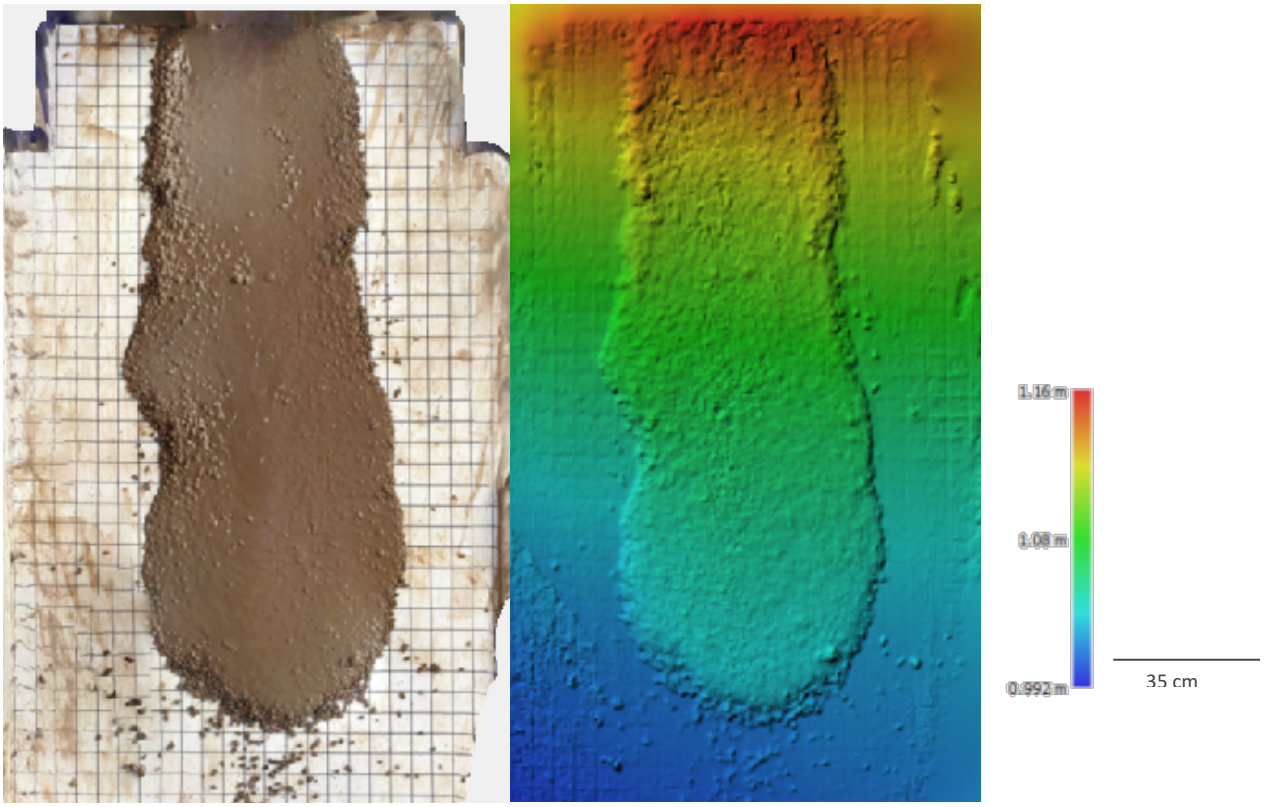

Figure 2.6. Output from Photoscan, showing a screenshot of the 3D point cloud generated from photographs of an experimental debris-flow deposit, and a DEM produced from this. The outputs of the SfM have an error of 0.032 m.

2.6. Debris Flow Scaling

Debris flow scaling is necessary if small-scale experiments are to be useful in hazard management of natural debris flows. Scaling laws are theoretical constraints of self-similarity of a phenomenon, such as a debris flow (Barenblatt, 1996). As Iverson (2015) states, debris-flow scaling can be addressed either using dimensional analysis, or by normalising differential equations. In this study, dimensionless parameters identified in the debris-flow flume experiments were used to compare between small and large scale experimental debris flows. The results of the analysis were compared directly to results of an experiment from the

large-scale USGS debris-flow flume facility (Iverson et al., 2010), to provide a quantitative analysis of debris-flow scaling.

However, as previously mentioned (Chapter 1), the inability to measure properties such as shear rate in small-scale experiments poses a limitation to the methodology. As such, values for some of the parameters needed for calculating dimensionless numbers for scaling between large and small-scale debris flows were estimated, which must be taken into account when considering the validity of the results.

2.7. Summary

Small-scale flume debris-flow experiments are carried out using an 8 m long, 0.2 m wide, open channel flume facility. The initial conditions of these experiments were designed around the USGS large-scale debris-flow flume experiments Iverson et al. (2010), but at reduced scale. Experiments were run on a roughened bed using a sediment mixture which best emulates natural debris-flow dynamics. This approximately followed the rationale of Iverson et al. (2010), although the mixture was scaled appropriately to the size of the flume facility used in this study. Taking advantage of the flexibility of the reduced scale flume, experiments were run in multiple replication and using a range of bed slope angles to assess the importance of this in controlling flow processes.

Data generated by the flume experiments enabled analysis for debris-flow scaling relationships to be developed. 3D photography was used to allow the morphology of the experimental debris flows to be compared to that expected in the prototype. Finally, dimensional analysis and normalisation of differential equations that describe debris-flow behaviour were used to quantitatively assess debris-flow scaling relationships, as is the overall aim of this research.

3. Results

This chapter provides a detailed description of the results of the small-scale open channel debris flow flume experiments and subsequent data processing. In order to scale the experiments from small-scale debris flows, key dimensionless parameters discussed in previous chapters are considered. The results are considered alongside the results from Iverson et al.'s (2010) large-scale USGS flume experiments, providing a direct comparison of small-scale and large-scale experiments.

The results from the debris flow experiments carried out in this research are summarized in Table 3.1.

Table 3.1. Summary of results from the small-scale debris flow experiments, showing the mean values and standard deviation.

Slope angle (°)	**Viscosity of interstitial fluid (Pa.s)**	**Number of Samples in Subset**	**Mean Maximum Length of deposit (cm)**	**Mean Maximum width of deposit (cm)**	**Mean depth of flow (cm)**	**Mean Area of deposit (cm^2)**	**Mean velocity of flow ($m\ s^{-1}$)**
29	0.0025	10	127.50 ± 11.72	48.30 ± 4.98	1.98 ± 0.62	4312 ± 695	1.68 ± 0.45
30	0.0025	10	162.20 ± 65.41	51.60 ± 2.46	1.92 ± 0.35	6020 ± 3140	4.07 ± 1.29
31	0.0025	12	161.20 ± 35.11	50.45 ± 5.96	1.80 ± 0.69	6438 ± 1316	4.02 ± 0.59
31	0.001	2	250.00 ± 0.00	55.00 ± 5.00	2.88 ± 0.13	12992 ± 448	5.37 ± 0.68
31	0.002	2	170.50 ± 9.50	48.50 ± 1.50	3.25 ± 0.25	7328 ± 1088	4.48 ± 0.20
31	0.004	2	41.50 ± 22.50	29.00 ± 7.00	1.75 ± 0.25	1048 ± 712	1.04 ± 0.39
31	0.005	2	N/A*	N/A*	2.50 ± 0.00	N/A*	1.35 ± 0.00

*Debris-flow did not reach runout board, so no deposit could be measured

3.1. Debris-Flow Composition

Whilst the debris-flow mixtures were kept constant for all the experiments investigating the variability of slope angle, there were some small natural variations in the measured size fractions of the sampled debris-flow mixtures. The results of the particle size analysis are shown in Figure 3.1. For each debris-flow run, three samples were analysed, so each plot shown is comprised of 30 samples. The composition of the mixtures used in the USGS experiments (Iverson et al., 2010) is shown for comparison.

The grain-size distribution of each of the debris-flow experiments were very similar, so there was little variation in mixture composition across the experiments. Whilst the particle size distributions in these experiments differ considerable from the USGS particle size distributions, in general, the composition of the sediment mixture shows a bimodal grain-size distribution, similar to that used in the USGS debris-flow mixture. Therefore, the relative size compositions used here were similar to the USGS mixtures despite being scaled down. This bimodal grain-size distribution is also common in natural debris flows (Scott, 1988; Vallance and Scott, 1997; Saucedo et al., 2008), so the mixtures used in the small-scale experiments in this research can be considered similar in overall form to prototype flows.

However, the fine-grained fraction of the mixtures was greater than that of the USGS debris-flow mixture due to adjustments made to the mixture to ensure that the debris flows reached the runout board (see Section 2.3). This is important as it may influence the microscopic nature of the flows (Iverson, 2015). The impact of the clay content on debris-flow behaviour is therefore considered further in Section 3.5.3.

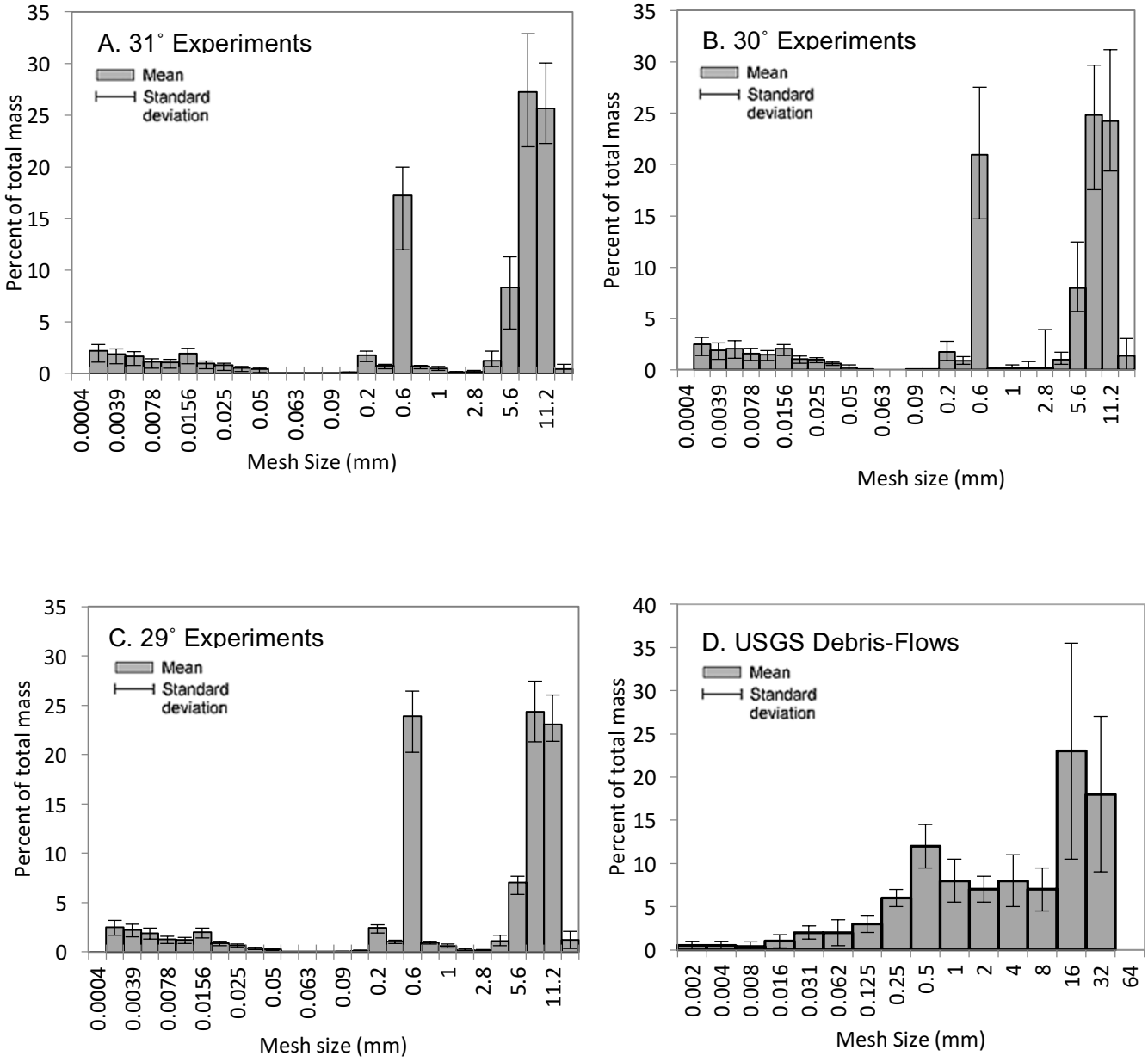

Figure 3.1. Grain-size distributions of the sediment mixtures used in the flume experiments. The histogram bars show the mean percent of total mass for each size class and the error bars show the standard deviation. (A) shows the distributions for the mixtures used for the 31˚ slope experiments, (B) shows the distributions for the mixtures used for the 30˚ experiments, and (C) shows the distributions for the mixtures used for the 29˚ slope experiments. (D) is the grain-size distribution of the mixture used in the USGS experiment replicated on a smaller scale here (From Iverson et al., 2010).

In the experiments designed to consider the effect of mixture composition on debris-flow behaviour, the viscosity of the mixture was varied (0.001 Pa.s, 0.002 Pa.s, 0.0025 Pa.s (the same mixture as used for the slope angle experiments), 0.004 Pa.s, and 0.005 Pa.s). This was achieved by altering the volumetric fraction of clay in the interstitial fluid (Figure 3.2). The larger grain-size fraction of the mixture was held constant so the mixture retained the bimodal grain-size distribution typical of debris flows. However, as the viscosity was increased, there was a greater percentage of clay-sized particles (<0.0625 mm (Iverson et al., 2010)) in each mixture, ranging from 1.7% in the 0.001 Pa.s mixture to 3.42% in the 0.005 Pa.s mixture as a fraction of the total solid volume.

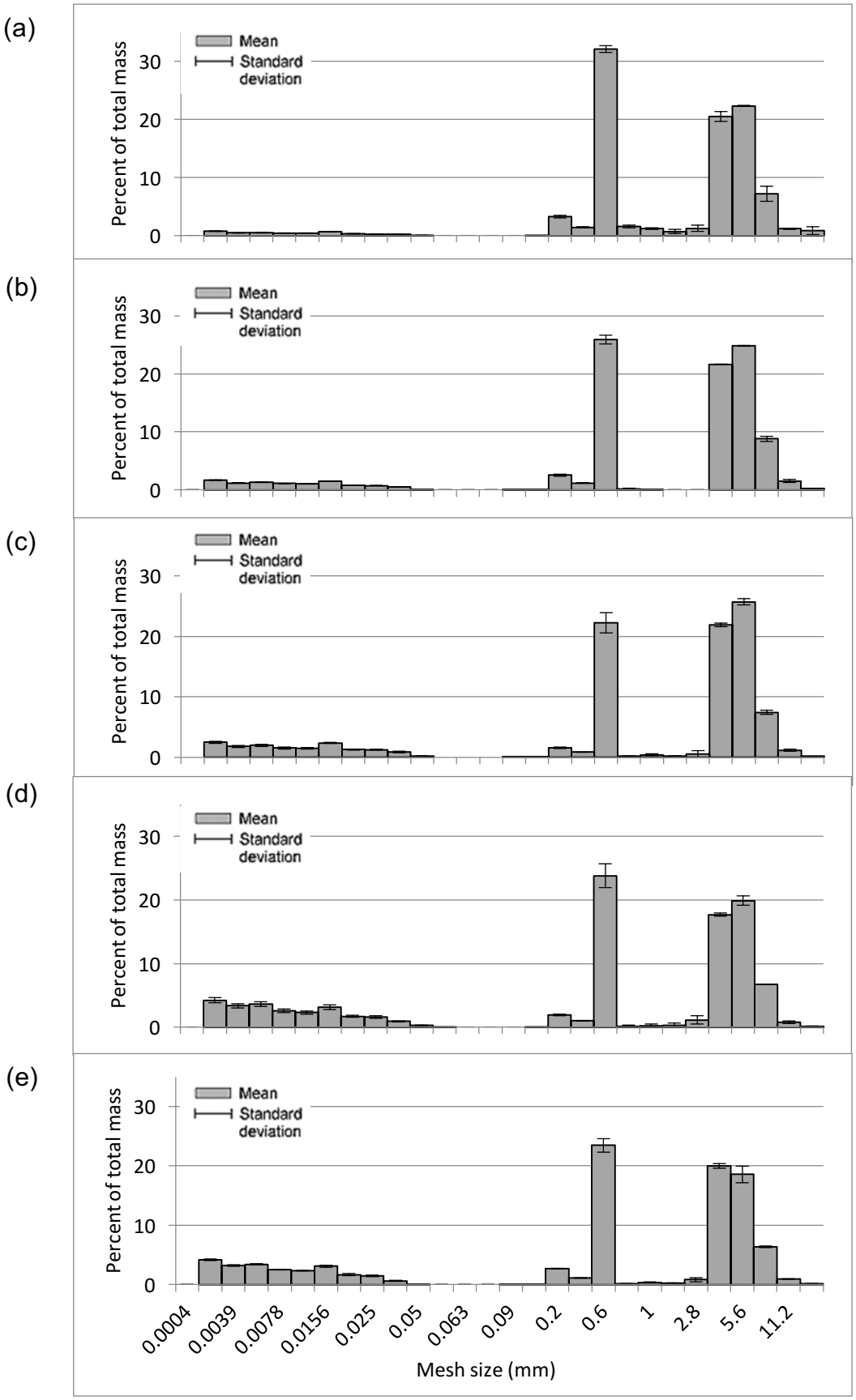

Figure 3.2. Grain-size distribution of the sediment mixtures of varying viscosities: (a) 0.001 Pa.s, (b) 0.002 Pa.s, (c) 0.0025 Pa.s, (d) 0.004 Pa.s, (e) 0.005 Pa.s. The histogram bars show the mean percent of total mass for each size class and the error bars show the standard deviation from the six samples analysed to make each plot.

3.2. Flow Front Positions and Speeds

The position of the debris flow front was measured sequentially (every 0.25 m) for each experiment, both within the lower part of the channel, and on the runout board. The flow in the lower part of the channel, from 6 m to the termination of the flow between 8.2 and 10.5 m, was measured in a single field of view from the overhead video camera. Figure 3.3 summarises the position of the flow front over time for the experiments which were carried out with the aim designed to consider the effects of bed slope angle on debris-flow behaviour. The mean flow front positions for each experiment are also shown in Figure 3.3. The graphs show considerable variation between debris flows with the same initial starting conditions, emphasising the intrinsic variability in debris-flow behaviour.

Differences between experiments conducted at different slope angles were also noted. Experiments carried out at higher slope angles reached maximum runout length more quickly (greater velocity) than experiments carried out at lower slope angles, with experiments reaching their maximum runout lengths by an average of 5.65 s, 6.55 s, and 8 s after the sediment gate being opened, at slope angles of 31°, 30°, and 29° respectively (excluding slow creep of the debris flow after the main flow had stopped). There was also variability between runs within each experiment set. In the 29° and 30° runs, Run 1 was slower to reach the maximum runout position, and had a shorter maximum runout length than other runs because the channel was dry, and so pore pressure from the flow dissipated, resulting in greater net frictional resistance to flow than for debris-flows on a wet bed (Reid et al., 2011). There was greater variability between the experiments carried out at higher slope angles: maximum runout length varied by 1.4 m, 1.52 m, and 0.28 m for slopes of 31°, 30°, and 29° respectively.

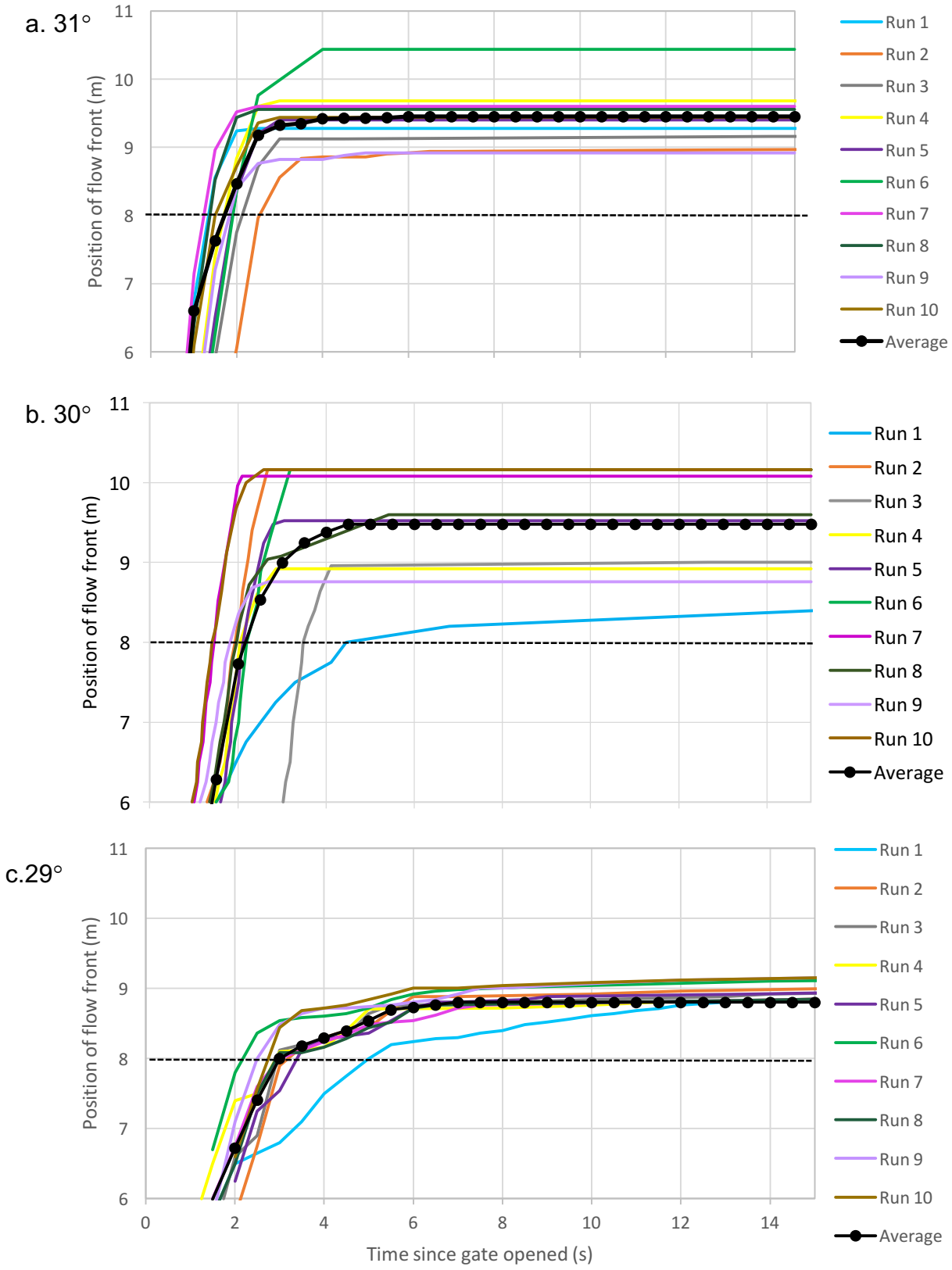

Figure 3.3. Position of flow fronts as a function of time, including flow on the runout board. The black dashed line shows the point at which the flow enters the runout board. The coloured lines show the position of the flow fronts measured in each individual experiment, and the black lines with markers depict the average flow front position over time for each experiment subset. (a) shows the experiments conducted at a 31˚ slope; (b) shows the experiments conducted at a 30˚ slope, and (c) shows the experiments conducted at a 29˚ slope.

There is also an impact of mixture viscosity on the evolution of the flow front position over time. Figure 3.4 shows the average position of the flow front over time for the experiments conducted using the different mixture viscosities. The flow front position evolution of '*Run 2, 0.005 Pa.s'* is not included in Figure 3.4 as the debris flow was deposited in the channel (maximum extent of 5.54 m from the headgate - out of the field of view of the video camera) and did not reach the runout pad. The maximum measurable runout length (10.5 m) was restricted by the length of the runout board in the case of the 0.001 Pa.s debris flows, as the debris flow would have extended beyond the runout board if it had not been intercepted by the toe wall of the board.

Figure 3.4 shows that the debris flows with lower viscosities reached their maximum runout distances more quickly than the more viscous debris flows: For example, in the 0.001 Pa.s flows, the maximum runout time was 3.36 s compared with 37.01 s for the 0.005 Pa.s runs. The runout distances were also much greater for less viscous debris flows: The average runout distance was 10.00 m (although this was restricted by the length of the runout board), 9.60 m, 9.28 m, 8.28 m, and 6.42 m for interstitial fluid viscosities of 0.001, 0.002, 0.0025, 0.004, and 0.005 Pa. s respectively.

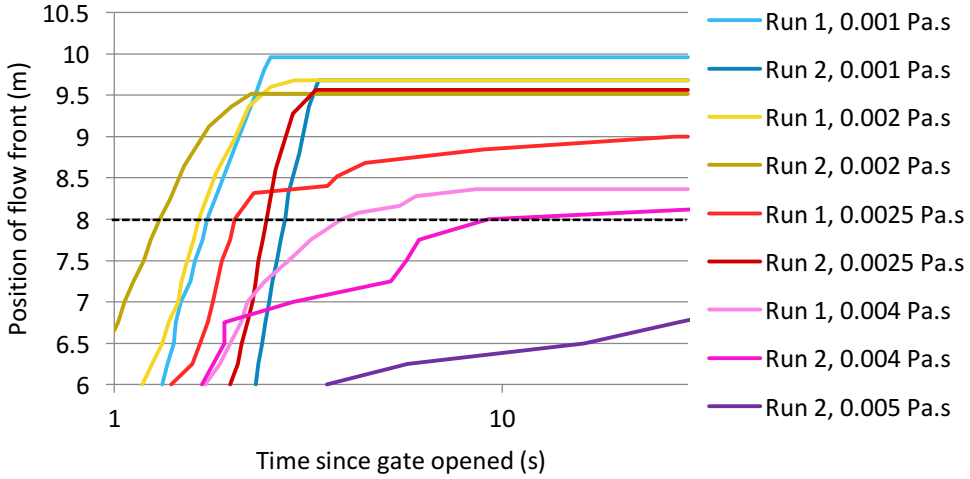

Figure 3.4. Position of flow fronts of the debris flows as a function of time, including flow on the runout board, where flows reached the runout board. The black dashed line shows the point at which the flow enters the runout board (8 m). The coloured lines each represent a single debris flow experiment.

3.3. Velocity

The impact of channel slope on flow velocity can be clearly seen in Figure 3.5, which shows the flow velocities measured at 0.25 m intervals along the flume channel, starting from 6 m from the headgate. Consistent with results from previous research, the average velocity of the debris flows increased as slope angle was increased (Lorenzini and Mazza, 2004; Procter, 2012; Stancanelli et al., 2015; Cao et al., 2017). The average debris flow velocity for the experiments carried out at 31° was 4.02 m s^{-1}, the average velocity for debris flows at 30° was 3.28 m s^{-1}, and the average velocity of the flow fronts for the experiments carried out at 29° was 1.68 m s^{-1}. The break in slope at 8 m down-slope, where the flume reached the runout board and the slope angle is reduced from 29°-31° to 5°, resulted in rapid deceleration of the flow in all experiment subsets. For the 31° runs, the average velocity of the flow front dropped from 4.84 m s^{-1} to 0.87 m s^{-1} after 8 m, for the 30° runs, the average velocity of the flow front dropped from 4.07 m s^{-1} to 1.89 m s^{-1} after 8 m, and finally, for the 29° runs, the average velocity of the flow front dropped from 2.72 m s^{-1} to 0.08 m s^{-1} after 8 m. This change in velocity with slope is non-linear, suggesting that slope is not the only control on debris flow velocity.

The magnitude of the scatter between velocities of individual runs appears to be controlled, at least in part, by slope angle. The variation in debris-flow velocity between debris flows within each experiment set (where initial boundary conditions were the same) was most pronounced in the experiments which were conducted at higher slope angles (Figure 3.6). In the experiments conducted at 29˚, average velocity of the flows ranged between 0.60 and 2.53 m s^{-1}, whereas in the 30˚ experiments, there was increased scatter, with average velocity ranging

from 3.42 to 5.47 m s^{-1}, if the anomalously slow first run is excluded. In the 30˚ experiments this increased further, with average velocity ranging from 3.15 to 6.25 m s^{-1}.

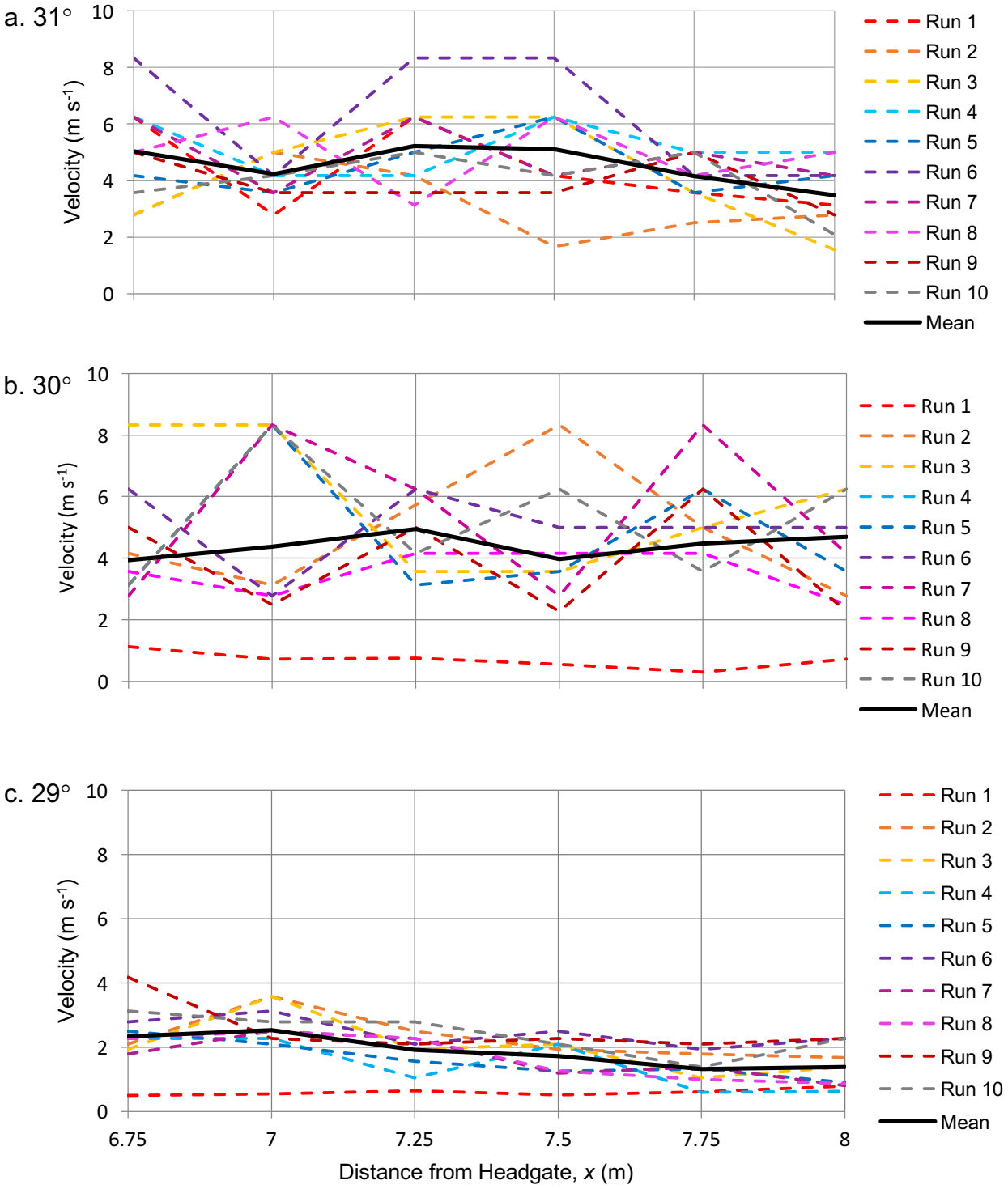

Figure 3.5. Flow velocities at intervals along the flume channel. (a), (b), and (c) are the experiments carried out at 31˚, 30˚, and 29˚ slope angles respectively. The black lines show the average velocity at each point along the channel for each experiment set.

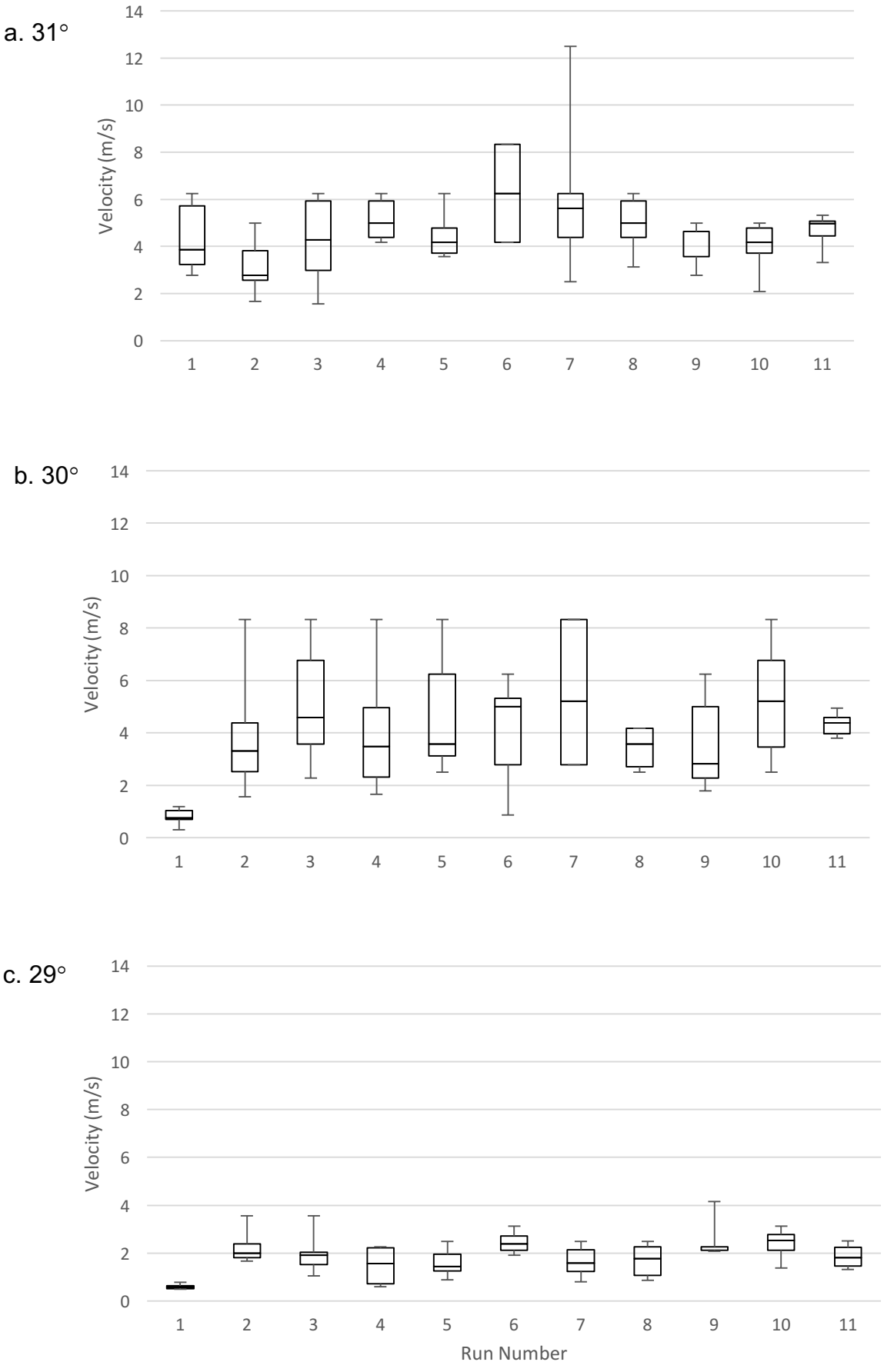

Figure 3.6. Boxplots of debris-flow velocity (between 6 and 8 m downslope) for different slope angles: (a) 31°, (b) 30°, and (c) 29°, with 11 replicate experiments.

Viscosity also has a significant impact on flow velocity, as demonstrated by Figure 3.7. The velocity of the debris flows with higher viscosities was lower than that of the debris flows with lower viscosities: The average velocity of the debris flows was 4.57 m s^{-1}, 3.45 m s^{-1}, 3.45 m s^{-1}, 1.29 m s^{-1}, and 1.35 m s^{-1} for viscosities of 0.001 Pa.s, 0.002 Pa.s, 0.003 Pa.s, 0.004 Pa.s, and 0.005 Pa.s respectively. The velocity of the debris flows increases over distance at low viscosities (with the exception of the lowest viscosity), and decreases over distance at higher viscosities. The variation in the velocity was greatest for the debris flows with the lowest viscosities (Figure 3.8).

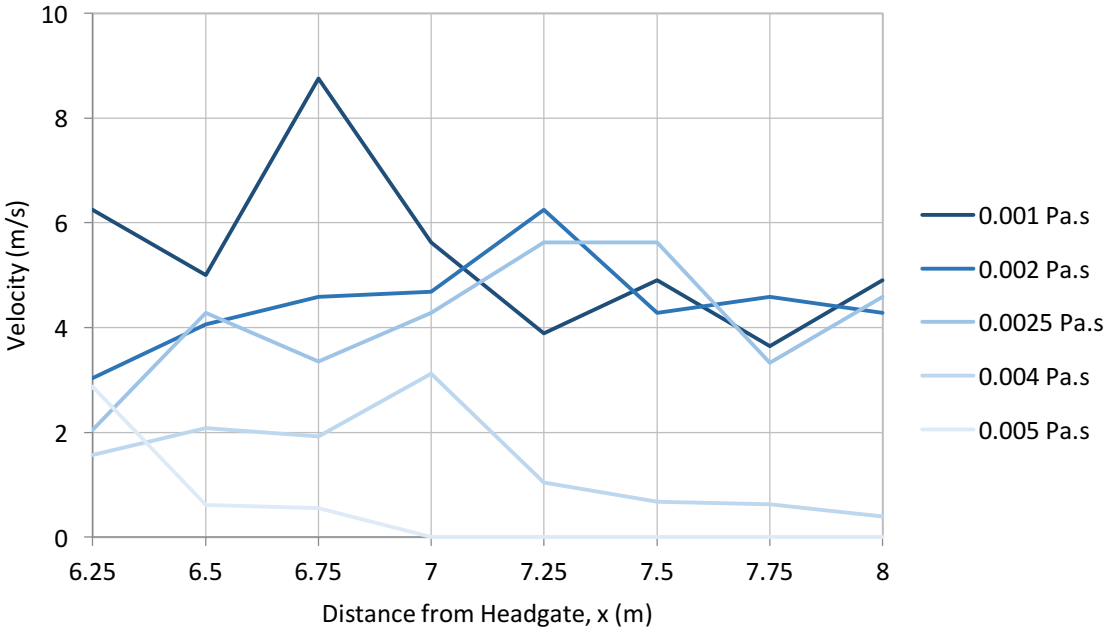

Figure 3.7. Average flow velocities at intervals along the flume channel for debris flows of different viscosities.

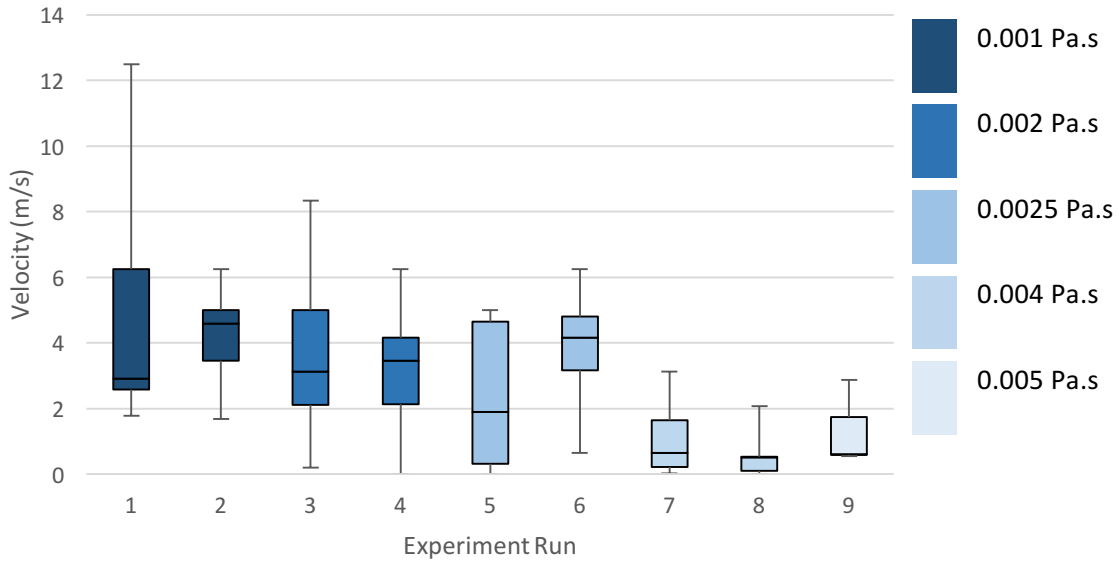

Figure 3.8. Variation in velocity for debris flows of different viscosities.

3.3. Roll Waves

There was considerable variability in the number of roll waves observed between debris flows conducted at different slope angles, and conducted at the same slope angle. Several debris flows exhibited surge behaviour, whereby the debris flow occurs as a series of roll waves, as is often observed in nature (Davies 1990). Such surges, or roll waves, are often characterised by an increase in flow depth and velocity, which is significant due to the increased destructive power that this results in (Zanuttigh and Lamberti, 2007). Roll waves indicated unsteady flow, described by Froude number (Table 1.2), typical of natural debris flows.

Roll waves occurred in all of the debris-flow experiments. This evidence includes video footage of the debris flows, whereby roll waves were identified by surges of higher velocity, and in the morphology of the debris-flow deposit (Johnson and Rodine, 1984) (Figure 3.9). The presence of roll waves may suggest dynamics similar to those observed in natural debris flows, although this is not

necessarily the case, as different processes can give rise to the formation of similar features via equifinality.

a. b.

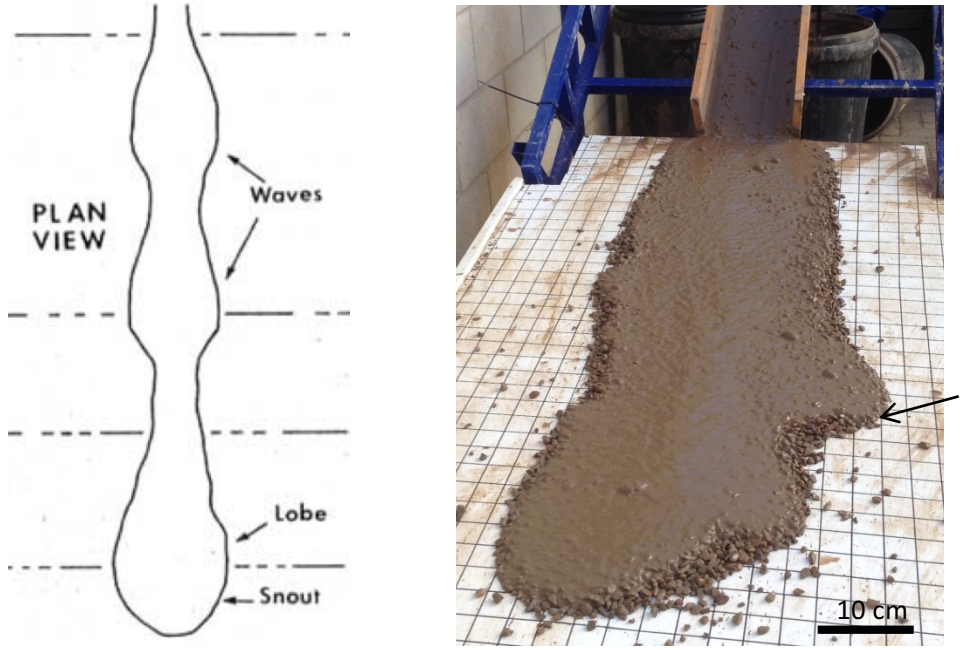

Figure 3.9. Morphological characteristics of debris-flow deposits which are indicative of surge behaviour. (a) is a schematic diagram of a debris-flow deposit formed through surging behaviour (From Johnson and Rodine, 1984), and (b) is a debris-flow deposit (from experiment run 9, 29˚ slope) showing evidence of surge behaviour in this research.

3.4. Runout Deposit Morphology

The debris-flow deposit morphology was assessed using measurements taken during the experiments, including length and width data. Area, perimeter, and shape data was gathered based upon the photos taken of the debris-flow deposits.

The lengths of the debris-flow runout deposits varied considerably, both between and within experiment subsets. Across all experiments carried out on different slope angles, there was a mean deposit length of 150.30 ± 44.96 cm. Within experiment subsets there was also considerable variation, particularly at

higher slope angles: the mean deposit length for experiments conducted at 29˚, 30˚, and 31˚ was 127.50 ± 11.72 cm, 162.20 ± 65.41 cm, and 161.20 ± 35.11 cm respectively. As such, the experiments conducted at 29˚ showed the least variation about the mean, compared to the experiments conducted at 30˚ which showed the most variation.

There was less variation in the maximum width of deposits. The mean maximum width of the deposits across all three slope angles tested was 50.10 ± 4.86 cm. The variation within each experiment subset was also small: the mean maximum deposit width for experiments conducted at 29˚, 30˚, and 31˚ was 48.30 ± 4.98 cm, 51.60 ± 2.46 cm, and 50.45 ± 5.96 cm, respectively. This may suggest that slope was not important in determining width, as there was little variation between experiment subsets. The variation in width with interstitial fluid viscosity, however, is more apparent, with width decreasing as viscosity increases, highlighting the influence of viscosity on the lateral spreading of the deposit.

The area of the deposits increased with slope angle (Table 3.1), however, as with debris-flow velocity, the increase in area did not increase linearly with slope angle. There was also variation within experiment subsets due to the intrinsic variability of debris-flow behaviour. This variation was greater for debris-flows which occurred at higher slope angles. The area of the deposits also increased as the interstitial fluid viscosity of the debris-flow mixture was decreased.

Observations were also made about the shapes of the debris flow deposits. As demonstrated in Figure 3.9, the shape of many of the deposits was indicative of roll wave occurrence. There was, however, considerable variation in deposit shape, as shown in Figure 3.10. These considerable variations in deposit form

(particularly in length, area, and shape) demonstrate the intrinsic variability of debris flow behaviour and highlight the importance of repeatability in debris-flow experiments which is a major benefit of using small-scale flumes.

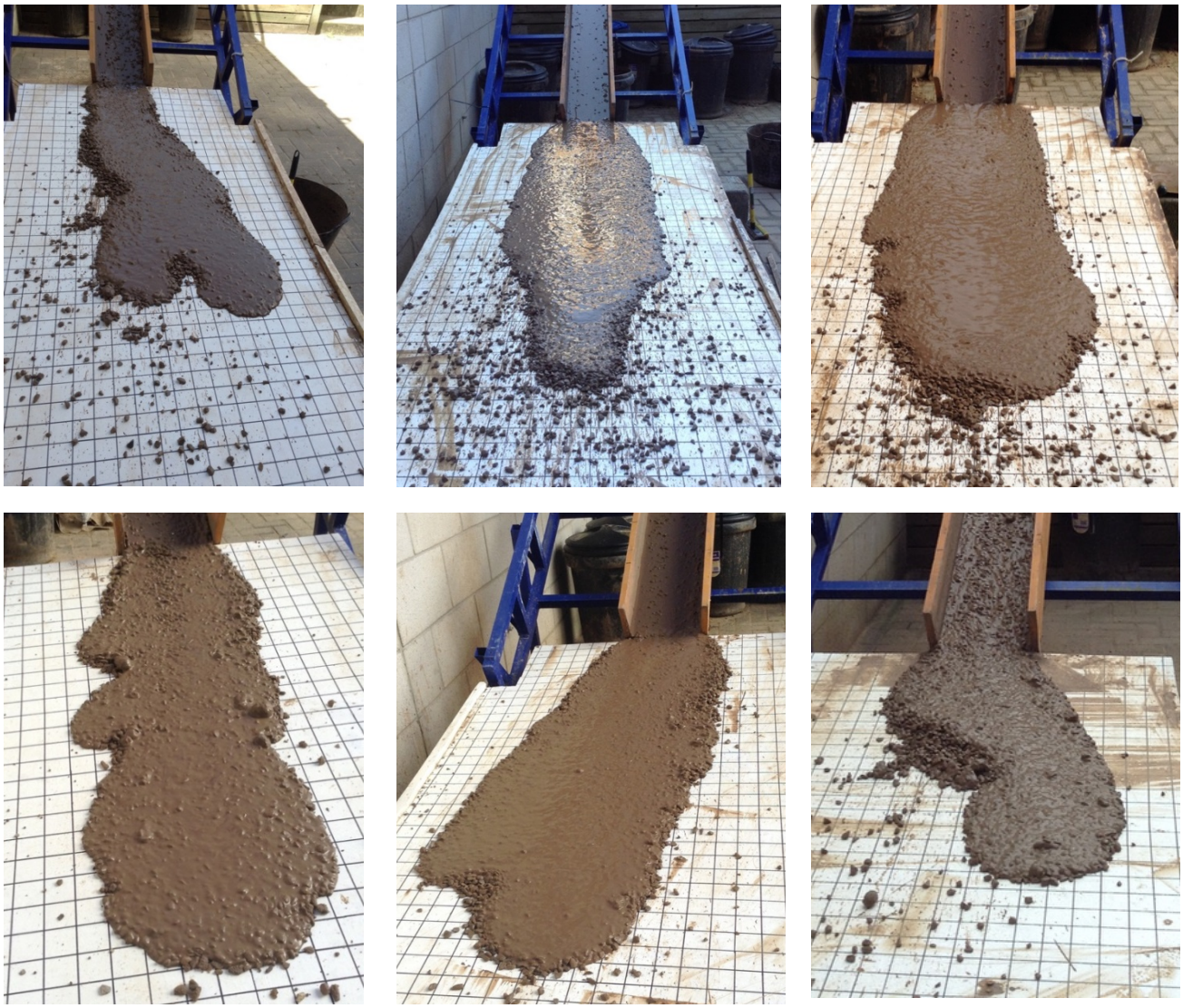

Figure 3.10. Examples of debris flow deposits, showing the varied deposit shapes produced.

Figure 3.11 shows the volumes of the deposits generated during these small-scale experiments. There is considerable variation between the volumes of the deposits. This is due to differential deposition within the channel of the flume, as all of the debris flow mixtures were of equal starting volumes. The volume of the deposits increases with increasing slope angle. The volume of the deposits decreased with increasing viscosity, due to greater deposition within the channel

at higher viscosities. Indeed, at a viscosity if 0.005 Pa.s, the debris-flow was deposited in the channel and did not reach the runout board.

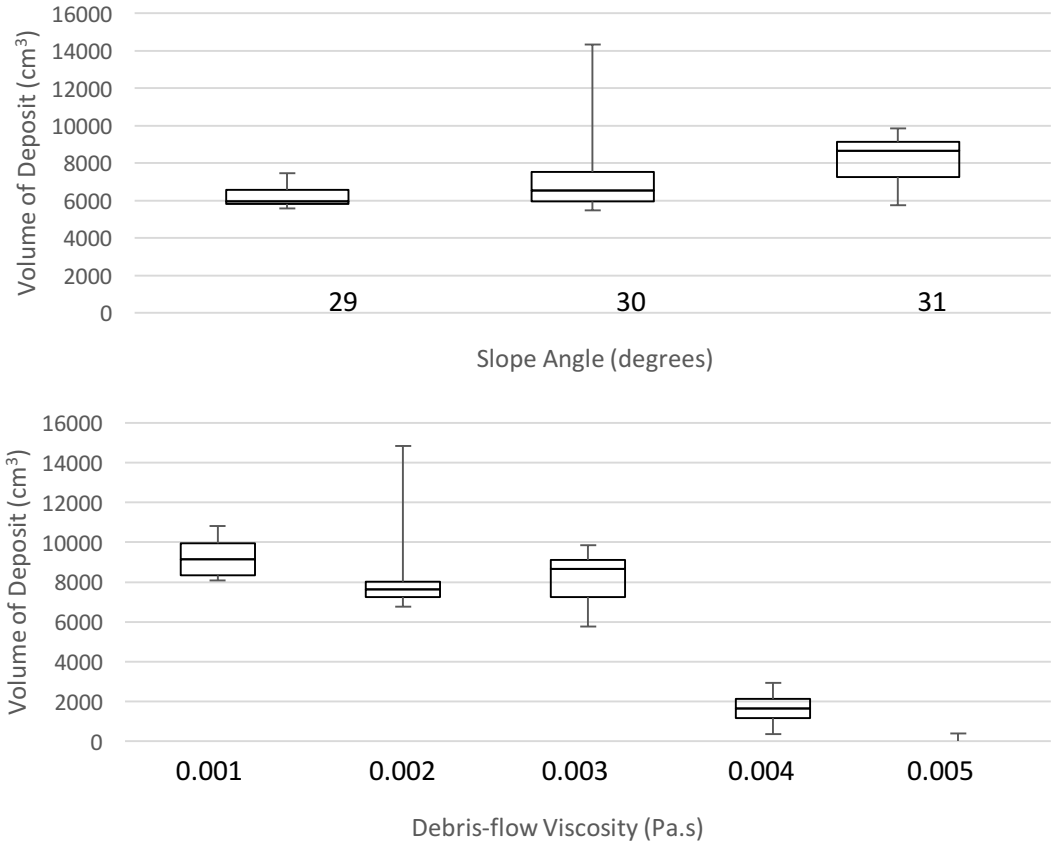

Figure 3.11. Volumes of debris flow deposits for debris flows which occurred at different slope angles (A) and at with different mixture viscosities (B).

As in previous small-scale debris-flow experiments (de Haas, 2016), the morphology of the debris-flow deposits generated during the experiments in this study tended to be consistent with the characteristic morphology of natural debris flows, with steep, coarse grained snouts and lateral levees, and finer, saturated tails. This is demonstrated by the results of the Structure from Motion. Figure 3.12 shows the cross-sectional topography of a debris flow deposit produced in this research, demonstrating the presence of lateral levees, which are a key characteristic identified in Chapter 1 as being needed to demonstrate that small-

scale experimental debris-flows can be representative of natural debris-flows. As such, the majority of the experiments were representative of natural debris flows.

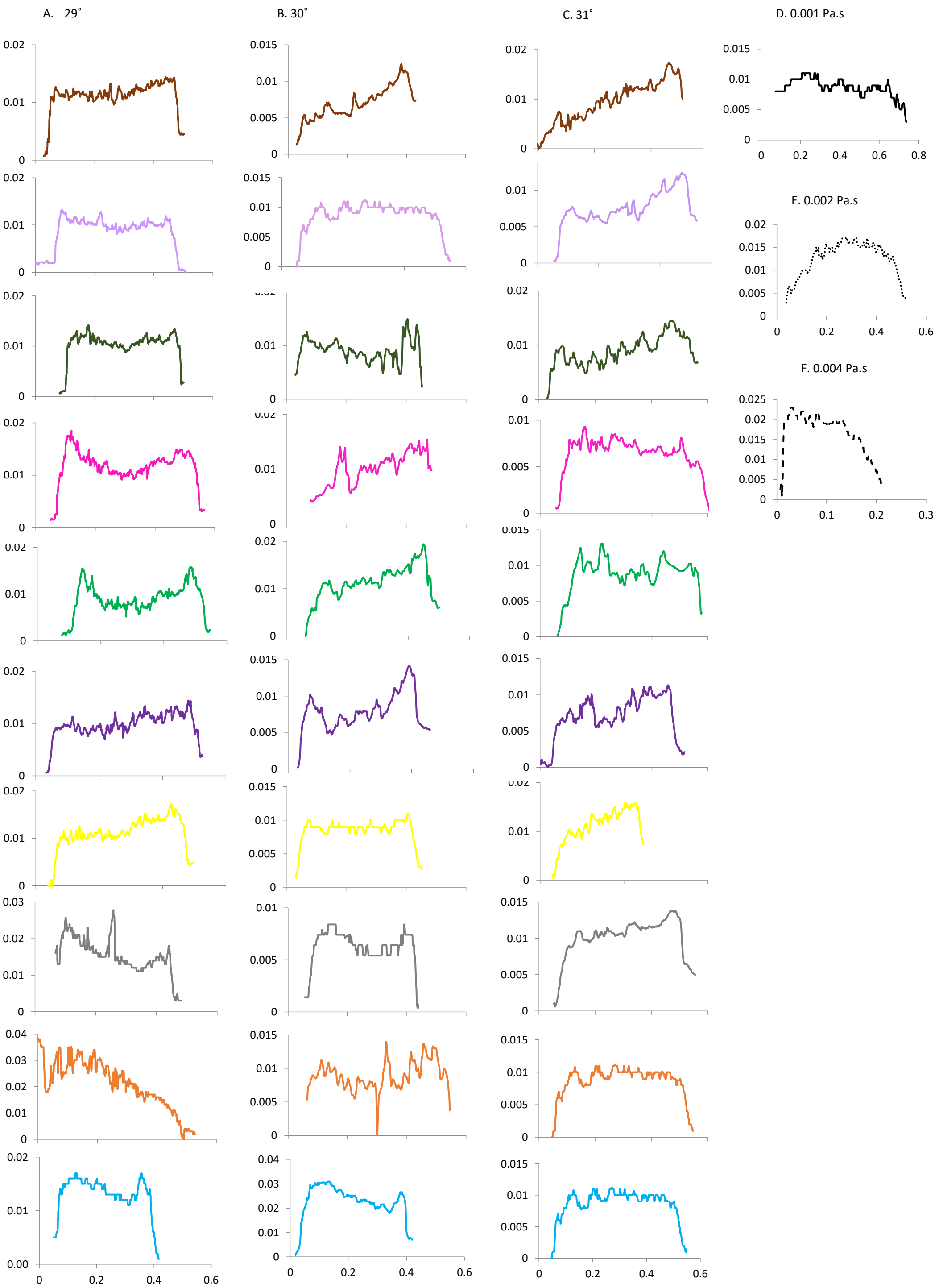

Figure 3.12. Cross-transects of the debris-flow deposits from flows at different slope angles (with viscosities of 0.0025 Pa.s): (a) 29˚, (b) 30˚, and (c) 31˚, and at different viscosities: (d) 0.001 Pa.s, (e) 0.002 Pa.s, and (f) 0.004 Pa.s.

In addition to the variations in debris flow deposits formed under the same initial conditions, as shown in Figure 3.12, there was also variation in the morphology of the deposits formed from debris-flows which occurred at different slope angles (Figure 3.13). The DEMs show the topography of the debris-flow deposits.

There were also differences in the topography of deposits in the experiments designed to demonstrate the effects of differing interstitial fluid viscosities on debris-flow behaviour. Figure 3.14 shows some DEMs of deposits generated from sediment mixtures of different viscosities for comparison. The surface roughness of the deposits appears to increase with increasing debris-flow viscosity, indicating a greater degree of sorting in these flows. No DEM is shown for the debris-flows with viscosities of 0.005 Pa.s, as the debris flows didn't reach the runout board. The debris flows at particularly low viscosities (0.001 Pa.s) are not representative of the majority of natural debris-flow deposits, as there was no grain-size segregation, so deposits lack the coarse-grained snout and fine tails.

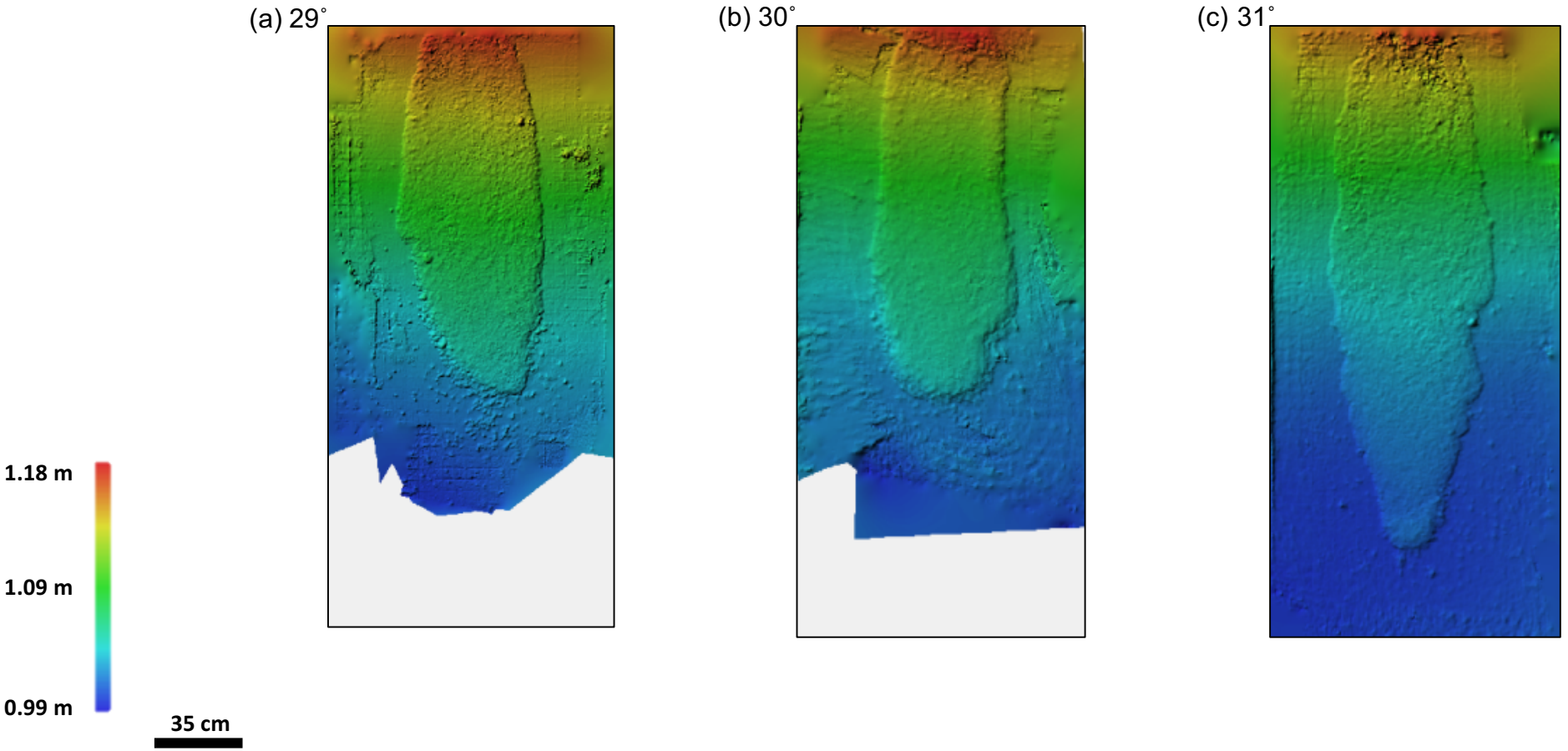

Figure 3.13. Examples of DEMs produced for debris-flow deposits produced at different slope angles: (a) 29°, (b) 30°, and (c) 31°.

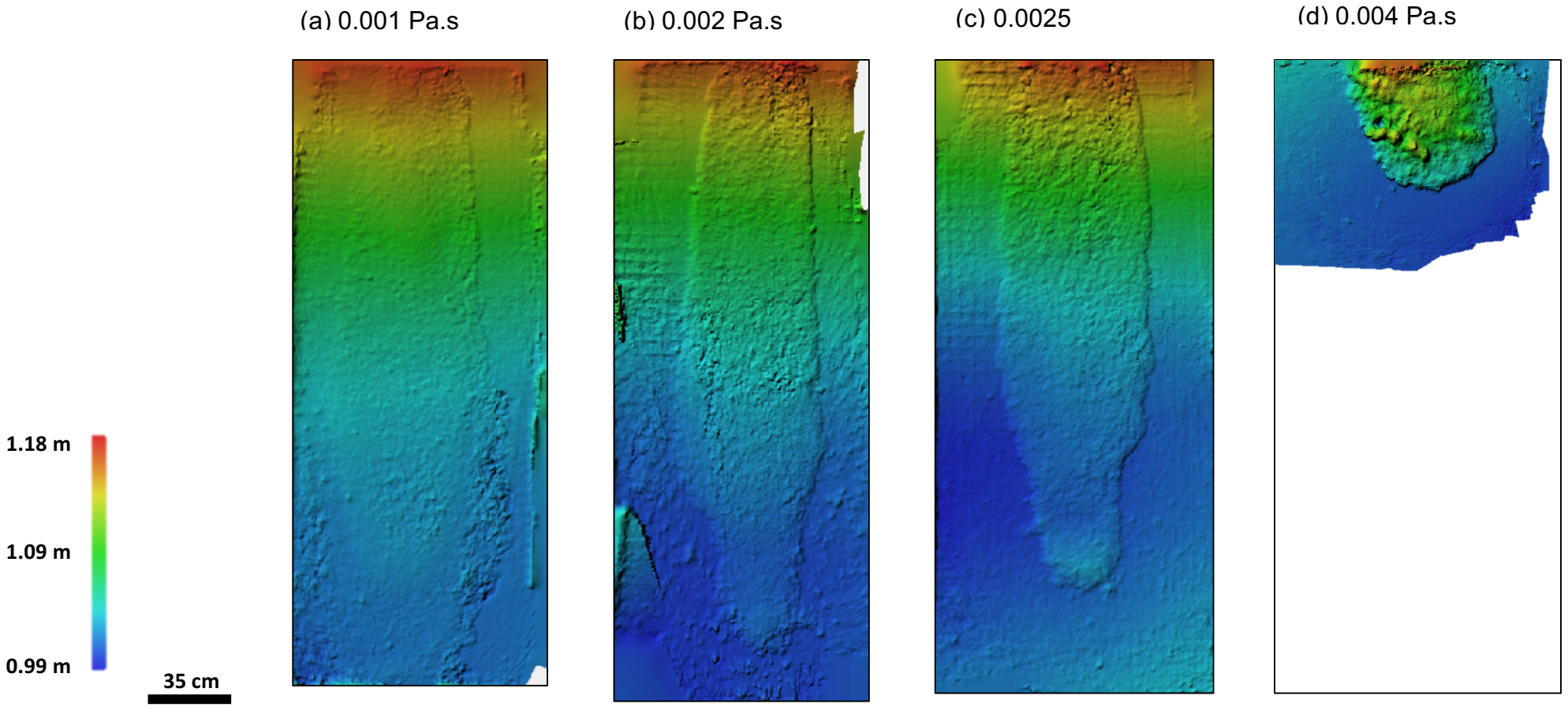

Figure 3.14. Examples of DEMs produced for debris-flow deposits produced at different mixture viscosities: (a) 0.001 Pa.s, (b) 0.002 Pa.s, (c) 0.0025 Pa.s, (d) 0.004 Pa.s.

3.5. Effect of Initial Conditions on Debris-Flow Dynamics

3.5.1. Effects of Slope Angle

As debris-flow experiments were conducted using a variety of slope angles (29˚, 30˚ and 31˚), an analysis of the effect of slope angle on key debris-flow behavioural characteristics was undertaken. Figure 3.15 shows the relationship between average velocity within the channel and maximum deposit length. There are notable differences between the debris-flow experiments conducted at different slope angles. In general, increased slope angle tended to result in greater velocities and longer run-out distances, and the greater the velocity, the greater the maximum deposit length. However, there were also considerable differences within experiment sets, as shown by the considerable scatter in the data, particularly at higher slope angles.

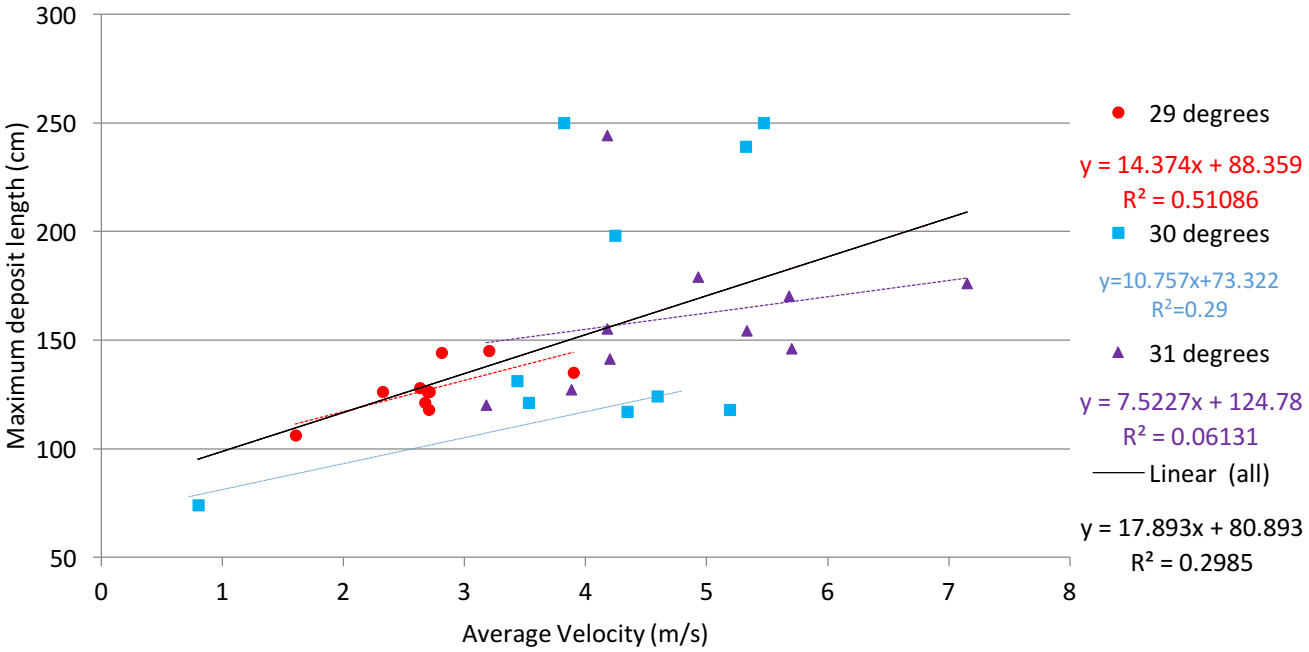

Figure 3.15. Relationship between average velocity of each debris-flow experiment and the maximum deposit length. The different experiment sets are shown with a different marker. The trendline for the whole dataset is shown in black, and the trendlines for the experiment sub-sets are shown by the coloured lines.

The experiments carried out at 31˚ show a greater variation in maximum deposit length than those carried out at 30˚ and 29˚, with R^2 values of 0.06, 0.29, and 0.51 respectively. The slopes of the relationships show that the 31˚ slope angle has the lowest rate of change of deposit length as velocity increases, and where the anomalously high runout lengths are excluded for the 30˚ runs, the 29˚ experiments saw the greatest rate of change. Therefore, the influence of debris-flow velocity on maximum deposit length is more important for debris flows which occur on lower slope angles than for debris flows which occur on steeper slopes. However, overall, the relationship between average velocity and maximum runout length is statistically significant, with a p-value of 0.002, which is far less than the common alpha level of 0.05.

Flow depth does not appear to correlate with slope angle or maximum deposit length: A p-value of 0.79 for the relationship between flow depth and maximum deposit length, signifies the relationship is not significant (a = 0.05). There is also no obvious difference between the debris flows which occurred at different slope angles, so it is unlikely that debris flow depth was a major direct control on debris-flow behaviour in these experiments. Indeed, the p-value of the relationship between flow depth and slope angle is 0.57, well above the common alpha level of 0.05 for which relationships are considered significant.

3.5.2. Effects of Bed Conditions

As described in Chapter 2, the channel used for the debris-flow flume experiments in this study was rigid and non-erodible. Based on previous experiments carried out by other researchers in a small-scale flume with a non-erodible bed (2 m long, and 0.12 m wide), it was expected that due to the bed preventing erosion and infiltration, the debris-flow deposit will not display grain-size segregation, and that there will be no distinction between the debris-flow

channel and the lobe (De Haas et al., 2015). This is due to the influence of bed erodibility on debris-flow dynamics (Egashira et al., 2001).

However, in the experiments reported here there was grain-size segregation in the majority of flows, with many deposits showing coarse-grained snouts and saturated tails typical of natural debris flows (Figure 3.16). Therefore, given that the presence of grain-size segregation in debris-flow deposits was identified in Chapter 1 as a key criteria for judging the use of small-scale flumes in modelling debris flows, it can be asserted that the debris flows produced in this research do show similar form to that expected in natural debris flows. However, even where initial boundary conditions were the same, not all of the flows developed clear lateral levees, demonstrating the natural variability of debris-flow behaviour.

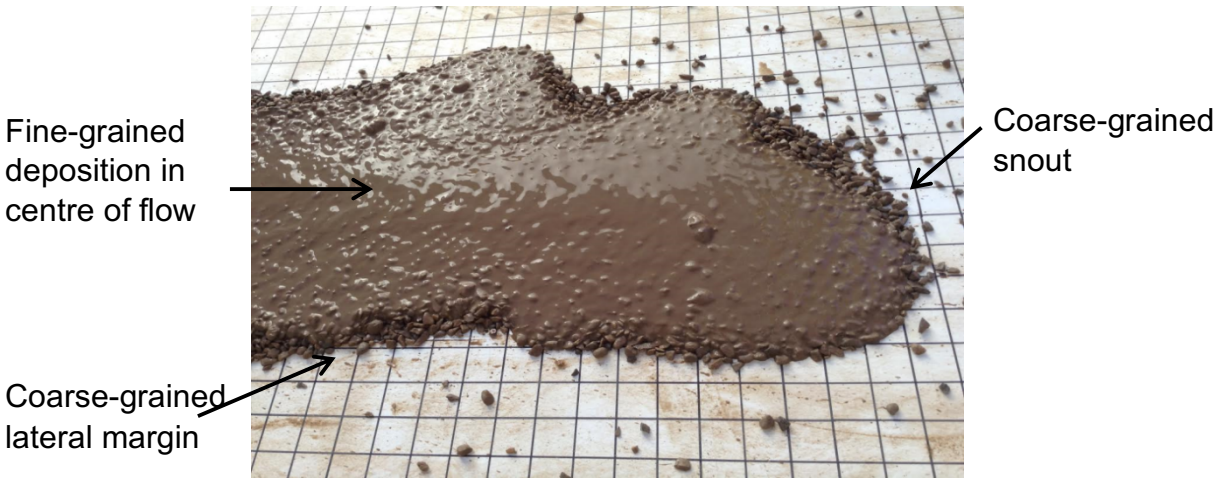

Figure 3.16. Image of a debris flow deposit generated during a rigid-bed experiment, demonstrating some key characteristics of natural debris-flow deposits.

3.5.3. Effects of Debris-Flow Composition

Despite the fact that the mixture compositions were kept constant for all the variable slope experiments, there were differences in the final mixtures due to natural variations in the materials used (Figure 3.7). Therefore, the effect that this variation had on debris-flow behaviour must be considered in order that the results can be compared. Table 3.2 shows the p-values of the relationships between the clay-sized fraction (<0.0625 mm (Iverson et al., 2010)) content of the debris-flow mixtures as a percentage of the total mixture, and some key indicators of debris-flow behaviour.

Table 3.2. P-values for relationships between the clay-sized fractions (% of total solid volume) of mixtures of experiments conducted at different slope angles and maximum deposit length, maximum deposit width, and average velocity. P-values below 0.05 indicate statistical significance, and are underlined. 10 samples were used in each relationship.

P- Values	**Maximum deposit length (cm)**	**Maximum deposit width (cm)**	**Average flow velocity (m s^{-1})**
Clay content in experiments conducted at 29˚ (9.24-15.20% clay)	0.16	0.15	0.11
Clay content in experiments conducted at 30˚ (8.47-17.98% clay)	<u>0.04</u>	<u>0.003</u>	0.32
Clay content in experiments conducted at 31˚ (9.38-19.46% clay)	0.17	0.93	0.75

With the exception of the experiments carried out at 30˚, there is no statistically significant correlation between debris-flow behaviour and the quantity of clay-sized grains used in these experiments as the p-values for the relationships

between clay content (%) and average velocity, maximum deposit length, and maximum deposit width are generally greater than 0.05 (Table 3.1.). Therefore, the small variations in mixture composition were not significant in influencing the debris-flow behaviour, and so reasonable comparisons between the experiments can be made.

There was also variability in the total volumetric fraction of the coarser grains in the debris-flow mixtures. Given the increased importance of individual grains in small debris flows compared to large-scale debris flows (de Haas, 2016), it is useful to consider the impact that these differences may have had on debris-flow dynamics. Given that the greatest differences in the large-fractions were for grains ranging from 5.6 - 16 mm, these grains were considered for comparison. Figure 3.17 shows the relationships between the % of grains ranging from 5.6 – 16 mm and some key debris-flow behavioural indicators.

The relationships between the proportion of coarse grain fractions and the debris-flow characteristics are clearer than those between the mud-sized fractions of the debris-flow mixture and the debris-flow characteristics. Whilst the R^2 values are rather low, all three relationships shown in Figure 3.17 are statistically significant, with p-values of 1.26×10^{-7}, 0.025, and 8.55×10^{-5} for deposit length, deposit width, and flow velocity respectively, all considerably lower than the 0.05 threshold for statistical significance. Overall, the proportion of coarse-grains in a debris flow mixture can be considered to be important in influencing the dynamics of debris-flow deposition

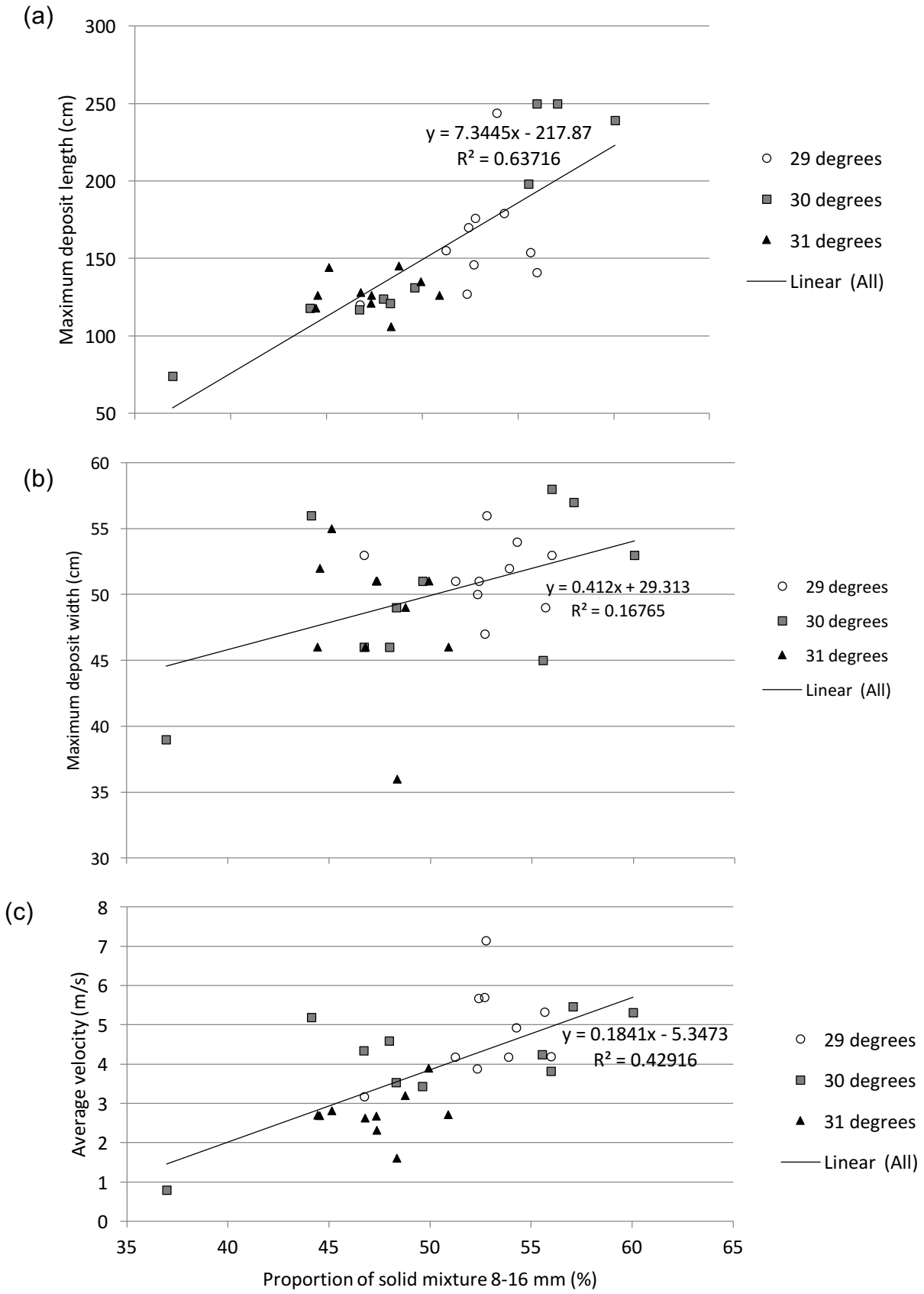

Figure 3.17. Relationships between the proportion of the total debris-flow mixture which is made up of coarse grains (8 mm -16 mm) and some key indicators of debris-flow behaviour: (a) Maximum deposit length (cm), (b) maximum deposit width (cm), and (c) average debris-flow velocity (m s^{-1}). Experiments carried out at different slope angles are indicated by different markers.

In addition to considering the natural variability of the materials used within the standard mixtures where grain-size fractions were kept constant, the importance of mixture composition was also considered by directly varying clay content (Takahashi, 1981). By altering clay content the viscosity of interstitial fluid of the debris-flow mixture was varied. Given the range of variability in clay content in these experiments relative to the standard mixtures (3.78% - 26.29%), a greater impact on debris-flow behaviour was expected.

Figure 3.18 shows the relationships between mixture viscosity and deposit length, deposit width, and debris-flow velocity, all of which are considered to be key indicators of debris-flow behaviour (Fannin and Wise, 2001; Hürlimann et al., 2008). Maximum deposit length includes the 8m of the channel, given that not all debris flows reached the runout board. There is only one data point for 0.005 Pa.s in the velocity graph as the debris flow in one experiment was deposited in the channel outside of the field of view of the video camera so velocity could not be calculated.

There is a strong correlation between interstitial fluid viscosity and the maximum runout length of the debris flows, with runout length decreasing with increasing viscosity. This relationship has an R^2 value of 0.84, and a p-value of 0.00019, so is highly statistically significant (a=0.05). The relationship between viscosity and deposit width is also statistically significant, with a p-value of 3.29×10^{-5}, and viscosity accounts for 90% of the variance in deposit width, based on the R^2 value, which reflects the importance of viscosity in influencing the lateral spreading of the flow. The relationship between in-channel velocity (from 6 to 8 m down-flume) is also statistically significant, with a p-value of 0.0003. There is some scatter about the trendline, but with an R^2 value of 0.86, viscosity can be said to control the majority of the variation in average velocity for these experiments.

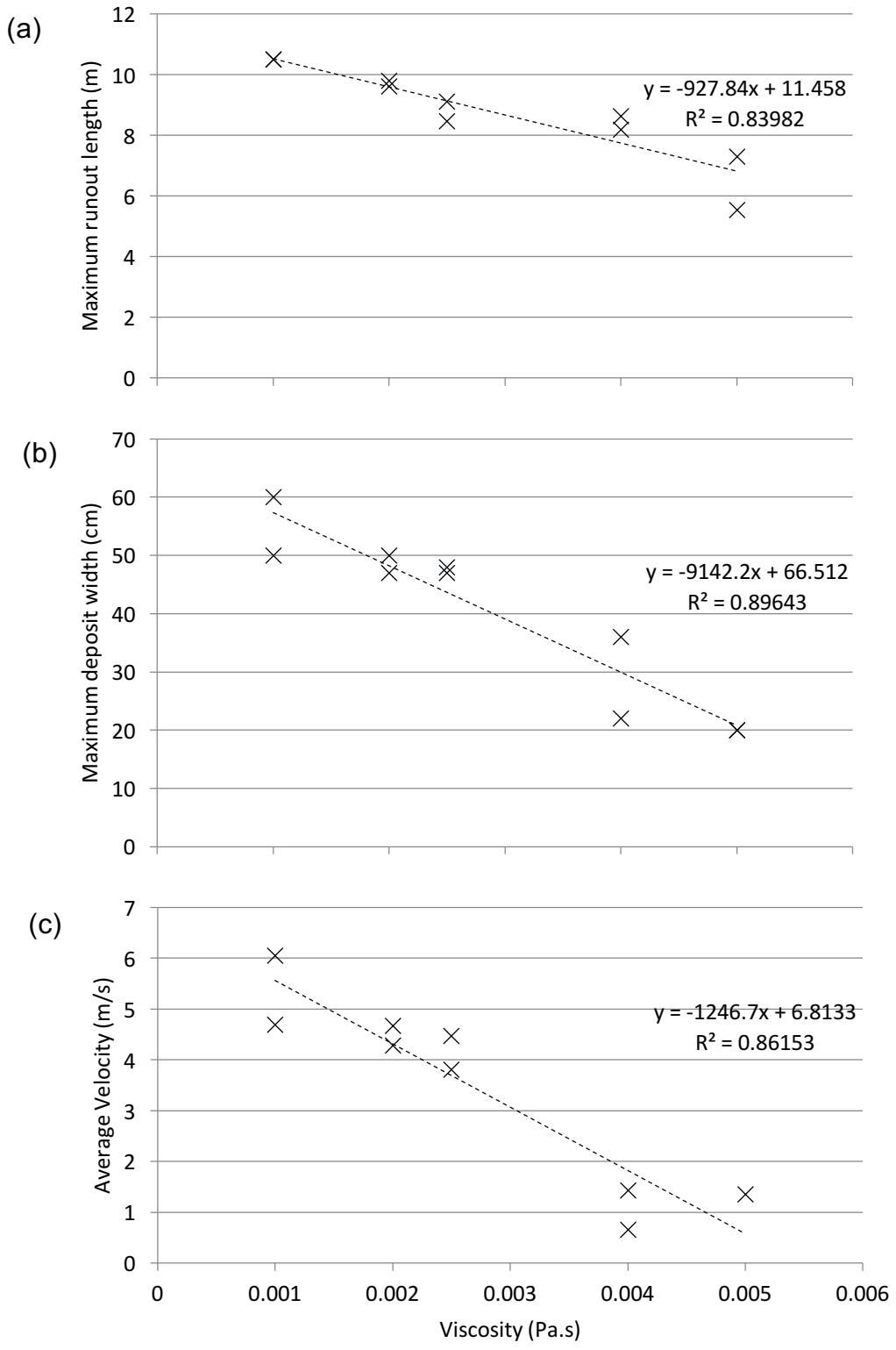

Figure 3.18. Relationships between debris-flow mixture viscosity and (a) maximum runout length, including the channel length, (b) maximum deposit width, and (c) average in-channel velocity between 6 and 8 m down-flume. Linear trend lines are shown by the black dashed lines.

3.6. Debris Flow Scaling

Here, a comparison of results of this study is made with larger-scale experimental flows (Iverson et al., 2010), and smaller-scale flows (de Haas, 2016). In addition to the assessment of morphological and behavioural similarities of these small-scale debris flows to large-scale flows described earlier in this Chapter, a comparison of dimensionless numbers was used to provide a quantitative analysis of debris-flow scaling relationships.

Table 3.2. shows the physical and dimensionless parameters typically used for scaling between small-scale experimental debris flows and debris flows of different scales. This includes a comparison between the values obtained from Haas' (2016) experiments, which were conducted at a miniature scale (2 m flume), the small-scale experimental values from this study (8 m flume), the large-scale experimental values from the USGS flume (90 m flume), and values typical of natural debris flows (de Haas, 2016). Table 3.3 shows that the values of the main dimensionless numbers typically used in scaling (Bagnold, Savage, and Friction numbers, which explain the ratios of forces acting to determine debris-flow behaviour (Table 1.2)) are generally within the range of values expected for natural debris flows for the experimental debris flows carried out on the small-scale flume. However, the Savage number was higher than expected in some cases: This tended to be where shear rate was particularly high due to high flow velocities and shallow flow depths, and where the grain—size: flow-depth ratio was high.

Whilst slope had a statistically significant relationship with the Bagnold and Friction numbers of the debris flows carried out in this research (p-values of 0.014 and 0.02 respectively), the relationship between slope and the Savage number

was less significant, with a p-value of 0.14. These results are similar to those produced in a 1.5 m flume by Bettella et al. (2012) where Savage number was also much higher than that typically observed in natural debris-flows (Table 1.3). The Savage numbers are likely to be larger than expected due to the nature of the calculation (Table 1.2). This is due to the larger grain-size to flow-depth ratio (δ/H) in these small-scale experiments compared to natural debris flows and compared to the large-scale USGS experiments. Indeed, where the grain-size: flow-depth ratio was over 0.4, a particularly high Savage number was produced in these experiments (Figure 3.19). As Table 3.3 shows, grain-size: flow-depth ratios in the USGS debris-flow experiments are much smaller than those produced here, and so this explains why the Savage numbers were higher than expected in the experiments conducted in this research. If Ns > 0.1 at typical depths, grain collision stresses may affect flow dynamics significantly (Savage and Hutter, 1989).

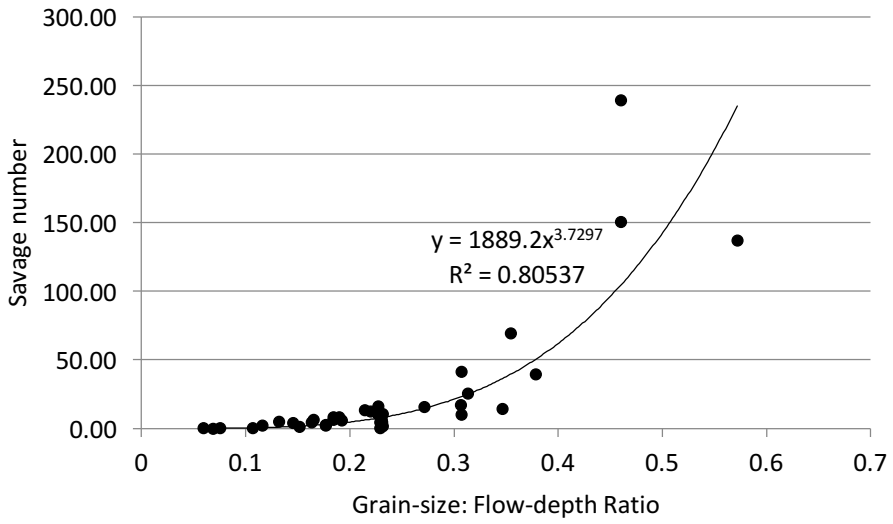

Figure 3.19. Relationship between the grain-size: flow-depth ratio and Savage number.

Table 3.3. Physical and dimensionless parameters of small-scale and natural debris flows. Adapted from de Haas (2016), with data from Iverson (1997), Major (2000), Iverson and Delinger (2001), Iverson et al. (2010), Zhou and Ng (2010) and this study.

Parameter	Symbol (Unit)	De Haas (2016) Debris Flow (Very Small Scale)	Debris Flows From This Study (Small-Scale)	USGS Flume Debris Flow (Large-Scale)	Typical Range Natural Debris Flows
			Physical Parameters		
Typical grain diameter	δ (m)	0.0005 – 0.002	0.002 – 0.005	0.001	10^{-5} – 10
Flow depth	H (m)	0.005 – 0.018	0.008 – 0.03	0.1	0.1 – 10
Grain-size:depth ratio	δ/H	0.1	0.06-0.625	0.01	
Flow velocity	u (m/s)	0.9 – 2.9	0.68 – 5.13	10	0.1 – 20
Flow shear rate	γ (1/s)	105 – 371	34 -248	100	1 – 100
Solid density	ρ_s (kg/m^3)	~2650	~2650	2700	2500 – 3000
Fluid density	ρ_f (kg/m^3)	1000 – 1533	1290	1100	1000 – 2200
Solid volume fraction	v_s (-)	0.35 – 0.59	0.56	0.6	0.4 – 0.8
Fluid volume fraction	v_f (-)	0.65 – 0.41	0.44	0.4	0.2 – 0.6
Fluid viscosity	μ (Pa.s)	0.001 – 0.0035	0.0025	0.001	0.001 – 0.1
Friction angle	ϕ (deg)	~42	~42	40	25 – 45
Hydraulic permeability	k (m_2)	$1.1x10^{-16}$ – $2.1x10^{-13}$	10^{-11}*	10^{-11}	10^{-13} – 10^{-9}
Hydraulic diffusivity	D (m^2/s)	$5.8x10^{-9}$ – $1.2x10^{-1}$	-	10^{-4}	10^{-8} – 10^{-2}
			Dimensionless Parameters		
Savage number	N_S	0.17 – 2.25	0.02 - 239.15	0.2	10^{-7} – 10^{0}
Bagnold number	N_B	37 – 1589	73 - 19134	400	10^{0} – 10^{8}
Friction number	N_F	141 – 2760	80 - 4678	$2x10^3$	10^{0} – 10^{5}
Mass number	N_M	1.2 – 3.63	2.24 – 2.99	4	1 – 10
Darcy number	N_D	$3.2x10^4$ – $5.9x10^7$	$2.4x10^2$ – $1.3x10^4$	$6x10^2$	10^4 – 10^8
Grain Reynolds number	N_{Rg}	31 – 504	31 - 7820	100	0.01 – 2
Reynolds number	N_R	$2.3x10^4$ – $1.4x10^5$	$6.2x10^4$ – $5.1x10^5$	$3x10^3$	$<10^5$
Pore pressure number	N_P	0.003 - 200	-	$6x10^{-3}$-0.008	10^{-6} – 10^{-1}

*Estimated based on data from Iverson (1997)

As slope has a major influence on velocity (Figure 3.3), the relationships between velocity and key dimensionless parameters are shown in Figure 3.20. Average flow velocity has a positive correlation with Bagnold number and Savage number, an inversely proportional correlation with Friction number. These relationships are as expected, based on the calculations of the key dimensionless numbers (Table 1.2), as velocity is included in the numerator of the equation for calculating Bagnold number and Savage number, and in the denominator of the equation used to calculate Friction number. All of these relationships are statistically significant, with p-values of 1.03×10^{-6}, 6.71×10^{-4}, and 6.14×10^{-5} respectively. As such, velocity, and therefore slope angle, has a major influence on debris flow behaviour, as the dimensionless numbers provide insight into the debris-flow dynamics as they describe the relationships between the forces acting on the flow. This highlights the importance of slope angle on debris-flow dynamics, as flow behaviour was highly sensitive to slope angle over just a small variation in slope (2˚).

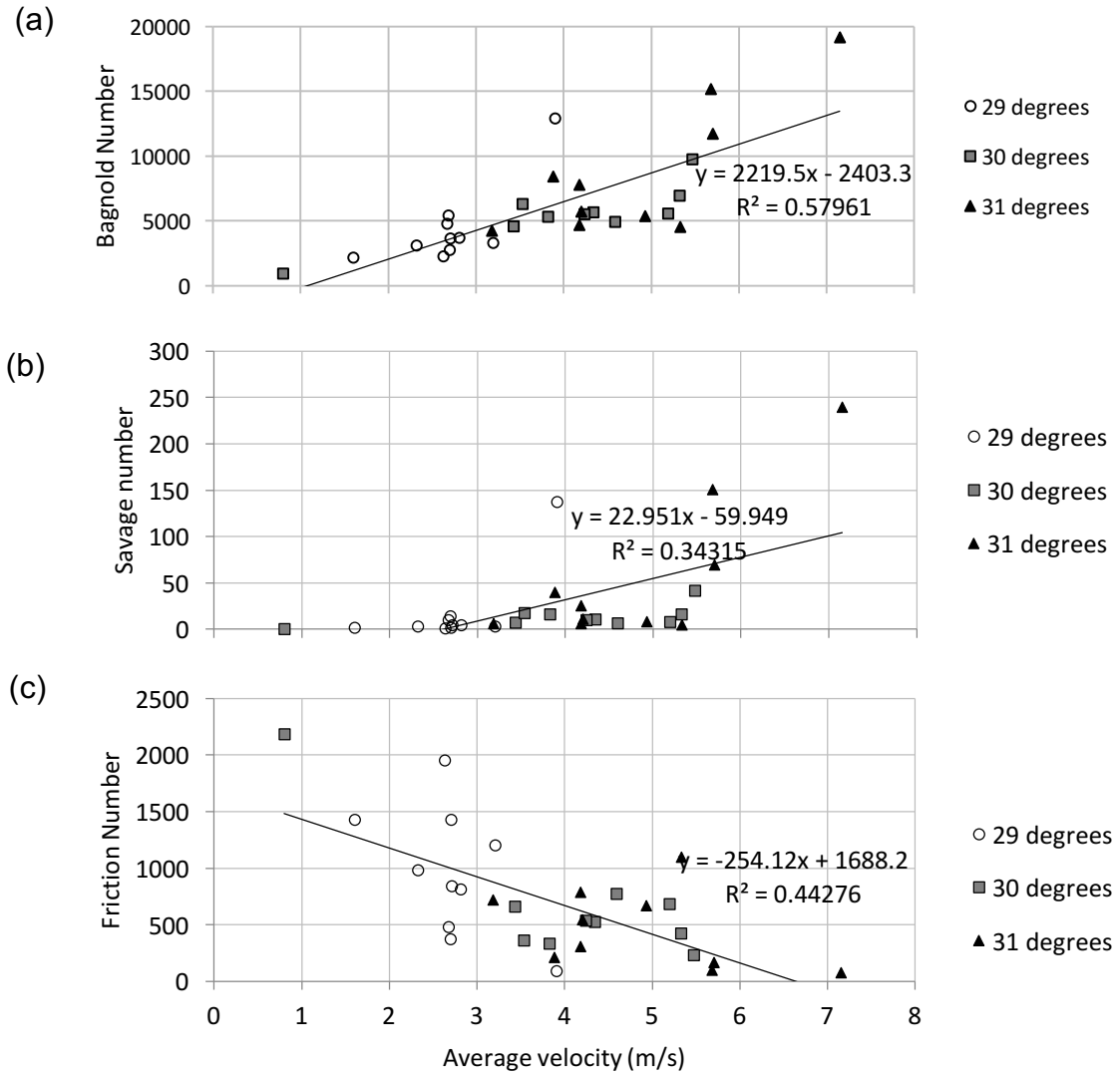

Figure 3.20. Relationship between average flow velocity and (a) Bagnold Number, (b) Savage number, and (c) Friction number.

Figure 3.21 shows the influence of interstitial fluid viscosity on the dimensionless numbers used in debris flow scaling. There is a statistically significant inversely proportional relationship between interstitial fluid viscosity and Bagnold number (p-value=0.013), and a positive correlation between interstitial fluid viscosity and Friction number (p-value=0.015). However, a similar relationship is not seen with Savage number (p-value of 0.62). This is because viscous forces are only considered in Bagnold and Friction numbers (Table 1.2).

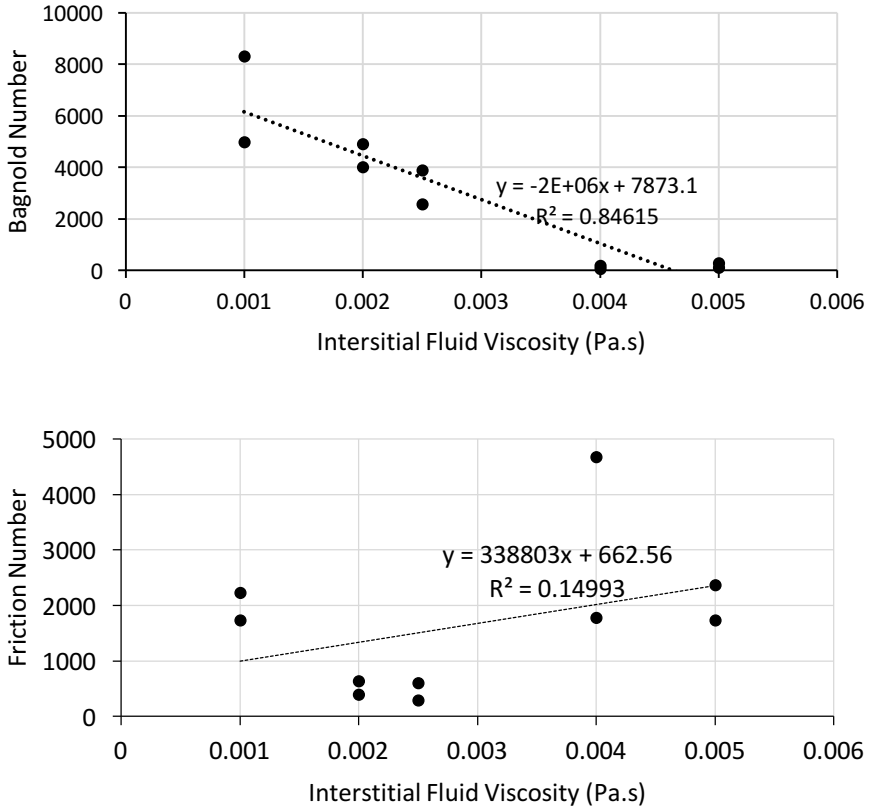

Figure 3.21. Relationship between interstitial fluid viscosity and (a) Bagnold Number, and (b) Friction number.

Flow depth also appears to exert significant control on the dimensionless parameters used in debris-flow scaling (Figure 3.22). Indeed, the inversely proportional relationship between flow depth and Bagnold Number has a p-value of 6.3×10^{-7}, well below the value of 0.05 for 5% significance. Similarly, there is an inversely proportional relationship between flow depth and Savage number (p-value = 4.2×10^{-5}). There is a positive correlation between flow depth and Friction number (p-value=3.1×10^{-7}).

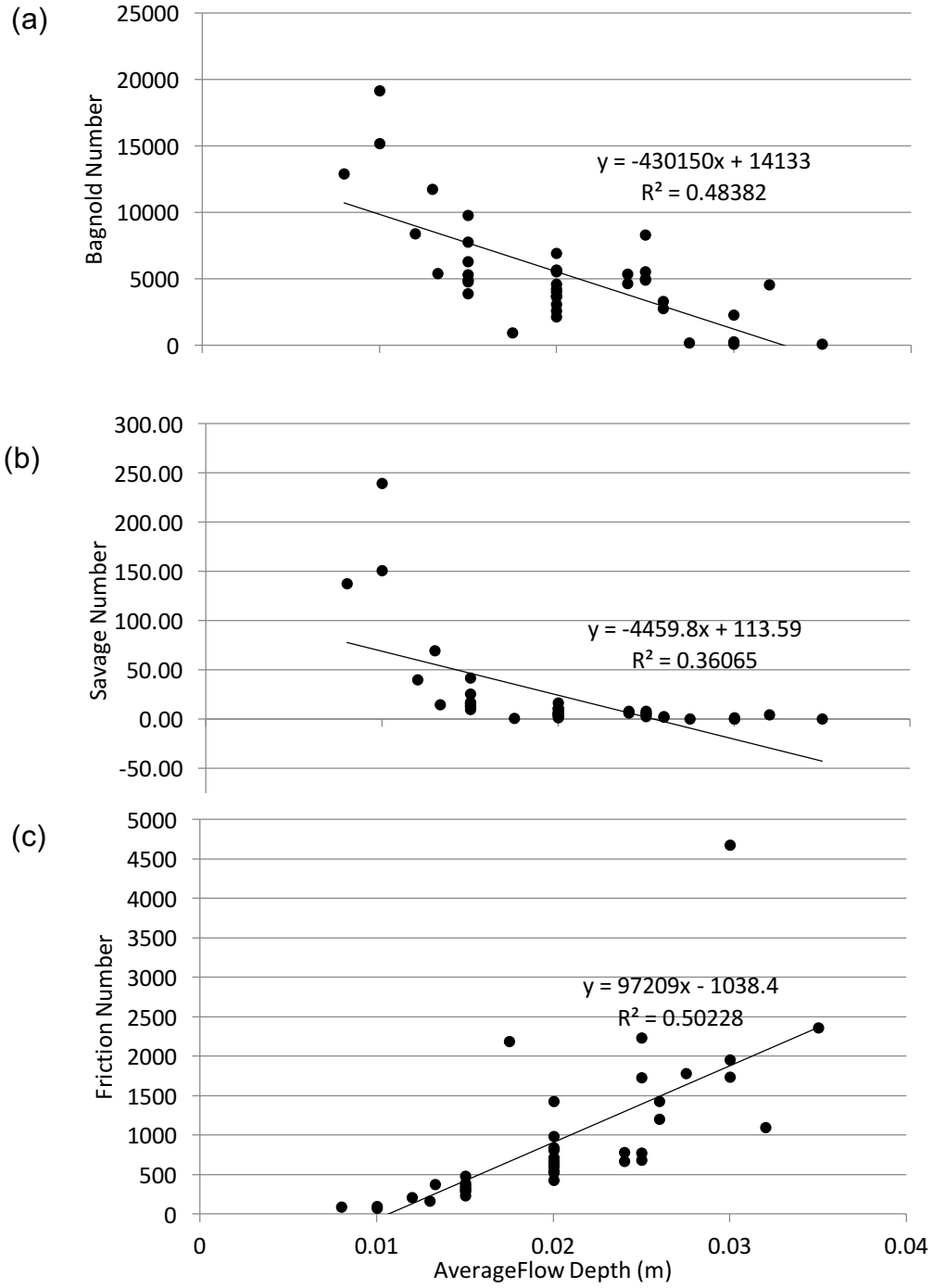

Figure 3.22. Relationship between average flow depth and (a) Bagnold Number, (b) Savage Number, and (c) Friction Number.

Iverson and Denlinger (2001), Savage and Iverson (2003), and Iverson et al. (2010) state that the Reynolds number (shown in Table 3.3) can be used to demonstrate the potentially problematic scale-dependent aspects of debris-flow behaviour which make small-scale experiments unsuitable for modelling debris flows. This is due to the amplification of viscous effects in small-scale debris flows compared to large ones where dynamic viscosity remains the same. However, the values for Reynolds number in these experiments are within the range of those considered typical of natural debris flows, and in fact, are closer to the prototype values than the values derived from large-scale USGS debris flows are.

Furthermore, the values for dynamic viscosity can be altered through varying the volumetric fraction of clay used in the interstitial fluid. Here, where experiments were carried out using dynamic viscosities greater than that of the standard mixture (Table 2.2), Reynolds number decreased, and where dynamic viscosity was lower than that of the standard mixture, Reynolds number increased (average Reynold's numbers of 3.4×10^5 and 1.2×10^5 respectively, compared to an average Reynolds number of 1.5×10^5 for the standard mixture). This demonstrates the influence of viscosity on debris flow dynamics, as viscous effects are less important in low-viscosity mixtures. As the same is true for debris flows with a large value for $H\sqrt{gL}$ (see Table 1.2) (de Haas, 2016), using lower-viscosity mixtures may reduce the divergence of scale-dependent behaviour from the behaviour of natural and large-scale experimental debris flows when conducting small-scale experiments.

The Savage number is particularly important to consider in this study, as the small-scale debris-flow experiments produced flows savage numbers 2 orders of magnitude higher than that expected of natural debris flows (Table 3.3). Therefore, this will have a significant impact on the dynamics of the debris-flows

produced in these experiments. Given that Savage number describes the ratio of collisional to frictional forces in a flow (Table 1.2), the Savage number was particularly high in these experiments due to a greater influence of friction in these small-scale debris-flows compared with natural debris-flows. This is likely to be due to the increased friction from the walls of the channel in a small-scale flow, in addition to the basal friction from the channel bed, as the small channel width meant that the debris flows were constrained by the walls of the channel.

3.7. Summary

The results from the small-scale flume experimental debris flows have been presented. The experimental results were assessed in terms of behavioural and process similarities, morphological similarities, and a comparison of dimensionless numbers in order to provide an analysis of scaling relationships in channelized debris flows. The key results from this research are summarised below:

- Where the mixture composition was kept the same, the small variations in clay content were too small to have a significant impact on debris-flow behaviour, so the results of the experiments produced in this study can be reasonably compared.
- The morphology of debris-flow deposits produced using the small-scale flume was more significantly influenced by small variations in the proportion of coarse grains in the debris flow mixture than by small changes in clay content, contrary to the expectations on Iverson (2015) for small-scale debris flows.
- Debris-flow dynamics are highly sensitive to small changes in slope angle (2°) and small changes in interstitial fluid viscosity (0.001-0.005 Pa.s).

- There is considerable intrinsic variability in debris-flow behaviour, even where initial conditions are kept constant, as evidenced by the variation in key debris-flow characteristics including velocity, runout distance and deposit morphology, which highlights the need for repeat experiments in debris-flow research. Here, 10 repeats of each subset were used; this would be recommended as a minimum number of repeats given the great variability in form produced.
- Despite the small-scale flume experiments conducted in this research being carried out over a rigid bed, the morphological characteristics of the debris-flow deposits were consistent with those expected of natural debris-flows.
- The key dimensionless numbers typically used in debris-flow scaling (Bagnold, Savage, and Friction numbers) of the debris-flows produced in these small-scale experiments are generally within the ranges of the values expected for natural debris flows, with the exception of Savage number in some instances where the grain-size: flow-depth ratio was particularly large (>0.4).
- The Reynold's numbers of the small-scale experimental debris-flows produced here were closer to the values expected of natural debris flows than the USGS values were, despite Reynold's number being a key indicator of the scale-dependent behaviour of debris-flows.

4. Discussion

This chapter discusses the results presented in Chapter 3, and provides a comparison of the key results to the large-scale USGS flume experiments (Iverson et al., 2010). The scaling relationships between small- and large-scale debris flow experiments, and ultimately, natural debris flows are discussed in relation to the main aims and objectives of the work (Chapter 1).

4.1. General characteristics of small-scale debris-flow experiments

The experimental debris flows studied in this research, as with many other small-scale and large-scale experimental debris flows (Haas, 2016; Iverson et al., 2010), produced many characteristics which were similar to natural debris flows. The debris flows consistently produced coarse-grained snouts and saturated tails, and produced flow behaviour such as roll waves (Figure 3.9) which are characteristic of natural debris flows. As such, despite the differences which are expected to occur on a macroscopic scale (Iverson, 2015), small-scale debris flow experiments can be used to replicate some of the key characteristics of natural debris flows.

4.1.1. Initial Sediment Release

In common with the large-scale experiments documented by Iverson et al. (2010), the debris flows produced in this research were initiated in a dam-break-style release, which inevitably impacted upon the initial flow, as the majority of natural debris flows on steep slopes tend to initiate from landslides (Brayshaw and Hassan, 2009), from the infiltration of overland flow into loose material which becomes fluidised (Coe et al., 2008; Zhuang et al., 2013), or from an increase in pore-water pressure as a result of rising groundwater levels (Imaizumi et al.,

2016). However, as Iverson et al. (2010) state, a dam-break initiation was necessary in order to allow for repeatability of the experiments, so this is not a draw-back associated exclusively with small-scale experiments. Further, Zhuang et al. (2013) state that dam-break-style initiations do occur in some circumstances, although these tend to be on lower angled slopes than those tested here (typically 10 ± 2°). Dam-break style initiations result in rapid acceleration of the mass initially, compared with slower onsets which occur in most natural debris flows (Iverson et al., 2010). Given that the type of initiation affects debris-flow dynamics (Zhuang et al., 2013), it is suggested that the type of initiation of debris flows should be used to inform hazard management practices. The influence of different types of initiation may therefore limit the use of experiments such as the ones conducted in this research, and in the large USGS flume as only a single release mechanism is considered. Here though, the delivery channel of the flume used in the experiments in this research is sufficiently long for the debris flow to become channelized and well-mixed prior to reaching the runout pad, so the impact of the release mechanism on the flow is minimized.

4.1.2. Rigid Bed

Iverson et al. (2010) also note that the use of a rigid bed in the large-scale debris-flow experiments was the most notable difference between the experimental and natural debris flows impacting upon the flow dynamics, as many of natural debris flows occur over erodible beds (King, 1996; Bovis and Jakob, 1999; Hungr et al., 2005; Han et al., 2016). The experiments conducted in this research were also conducted on a rigid bed, and whilst this does impact upon flow behaviour as the volume of the debris flows decrease as they travel down-slope as opposed to entraining bed-sediment and increasing in volume (Papa et al., 2004; Schürch et al., 2011), again, this is not a challenge unique to small-scale

experimental debris flows. Further, in the small-scale flume used here, a deformable bed can be used, allowing for conditions closer to that of a natural eroding slope to be replicated (Davies, 2017).

4.1.3. Repeatability and Duration

Over the course of six months, 80 experiments were completed using the small-scale flume (50 for this study, including 10 initial experiments to determine an appropriate mixture composition, 30 at 3 different slope angles (29˚, 30˚, and 31˚), and 10 at different viscosities), compared to just 28 experiments over 11 years in the large-scale USGS flume which provided the basis for Iverson et al. (2010)'s discussion of large-scale flume modelling. Therefore, this demonstrates the advantage of small-scale flume debris-flow experiments due to the relatively short amount of time in which a large quantity of data can be collected. This means hypotheses can be rapidly tested, intrinsic variability evaluated in detail and research can be conducted at a pace impossible at larger scales.

4.2. Sensitivity of Flow to Debris-Flow Composition

The debris-flow materials used for the experiments varied due to inherent variability of the composition, despite the same measured quantities of each material (gravel, sand, and clay) being used for each experiment (Figure 3.1). Iverson et al. (2010) found that increasing the proportion of clay in the large-scale USGS experiments resulted in thicker, shorter deposits being formed. However, in the small-scale experiments carried out in this research, small variations in the clay proportion of the mixture (<0.0625 mm (Iverson et al., 2010)) did not have a statistically significant effect on debris flow characteristics (Table 3.1). Where the mixture composition was kept the same (clay content varied between 8.47 and 19.48% clay content as a proportion of the solid mass), the lack of correlation

between clay proportion of the mixtures and the debris-flow velocity and deposit morphology (length and width) (Table 3.1.) suggests that the variations in mixture composition in these small-scale experiments were insufficient to alter pore-water pressure and therefore insufficient to influence debris-flow behaviour (Kaitna et al., 2016). Therefore, despite the proportion of the material <0.0625 mm varying, the flow composition variations between experiments conducted in this research were not important in determining debris-flow characteristics and the experiments can be reliably compared.

However, the coarse-grained fraction of the sediment mixture varied more greatly than the fine-grained fraction (average coarse-grained content of 51.4 ± 4.8% compared with 13.6 ± 2.6% for the fine-grained fraction). This may be important for debris flow behaviour, as in small debris-flows such as the ones carried out in this research, the dynamics of the flow are more sensitive to individual grains than in large debris flows (Davies, 1993) due to the increased grain-size to flow-depth ratio (δ/H) (Table 3.2). Indeed, the relationships between the proportion of coarse grains (which were classified as grains between 8 and 16 mm for the purpose of this analysis) and debris-flow velocity and runout distance were statistically significant (Figure 3.17). Therefore, in these small-scale experiments, coarse grains can be considered important in determining debris-flow behaviour. This has implications for the repeatability of such experiments, however, as small changes in mixture composition can have large impacts on debris-flow behaviour. This highlights a difference between the small-scale experiments conducted here, and large-scale experiments, as the influence of the coarsest fractions of the flow mixture were not seen as strongly in the large-scale USGS experiments. Indeed, the effects of coarse-grains on debris-flow behaviour were not modelled in the USGS experiments, and the grain-size to flow-depth ratio

of the flows in the USGS experiments deviated further from the ranges typical of natural debris-flows than the small-scale experiments produced here did (Table 3.2).

The importance of the proportion of coarse grains in determining with debris-flow behaviour may be related to the rheology of the flow: In the experiments conducted in this research, the average proportion of particles ranging from 8 mm to 16 mm range from 44.45% to 54.98%. This crosses the critical value for the proportion of coarse-grained particles in a debris flow of 50%, above which, the Coulomb friction stress (the denominator of the Savage number equation (Table 1.2)) becomes more important in influencing debris flow rheology (Schürch, 2011), and a debris flow of quasi-static motion develops (Takahashi, 2007). This explains why a small change in the proportion of coarse grains (8 mm – 16 mm) in these experiments had a greater impact on debris-flow behaviour than a small change in the proportion of clay-sized grains.

Overall, the greater influence of coarse-grains on debris-flow behaviour compared to clay-sized grains in these experiments is important as Iverson (2015) argues that the fine-grained fraction of the debris-flow mixture is most likely to affect the behaviour of small scale debris flows but in fact, the results of these small-scale experimental debris flows actually show that the morphology of debris-flow deposits (in terms of length and width (Figure 3.17)) is more influenced by the coarse fraction of the flow. However, given the potential discrepancy between form and process whereby similar deposits do not necessarily imply similar processes (Massey, 1989; Iverson, 2015), whilst the coarse-grained proportion of the flow appears to be dominant in influencing debris-flow deposition, the fine-grained proportion of the flow may still be important in influencing dynamics of the flow.

The bimodal distribution of grain sizes used in the experimental debris-flow mixture is significant as it is similar to that used in the USGS experiments (Iverson et al., 2010), and also to grain-size distributions observed in natural debris flows (Phillips and Davies, 1991; Lowe and Guy, 2000). The bimodality index developed by Wilcock (1993) is used as a measure of the degree of bimodality of fluvial gravels, B. Although not directly related to debris-flow composition, it can be used as a general index of the bimodality of the sediment mixture here:

$$B = \left(D_c/D_f\right)^{1/2}\left(F_c + F_f\right) \quad [4.1]$$

Where D_c and D_f are the grain-sizes of the coarse and fine fractions respectively (mm), and F_c and F_f are the proportions of the coarse and fine fractions respectively. A high value of B indicates greater bimodality of the sediment mixture. Here, B = 1.79, based upon the composition of the mixture (Figure 3.1). This is comparable to the bimodality of the USGS experimental mixture where B=2.09. The similarity of the small-scale experimental mixtures and the USGS mixture justifies the comparison between the two sets of experiments. The USGS mixture was slightly more bimodal than the mixture used in this research, as although there is a greater proportion of coarse grains in the mixture used here, the total fine grain proportion is greater in the USGS mixtures. Both mixtures are representative of natural debris-flow mixtures which are typically bimodal, such as the debris-flow deposits on the South Dolomite alluvial fan, California (Kim and Lowe, 2004).

However, as these calculations are based upon the pre-flow compositions, this is not necessarily representative of natural debris flows, as grain-size distribution analyses tend to be completed on the debris-flow deposit, and the grains are thought to be modified during the flow (Caballero et al., 2014), and additional material is entrained from the bed (Berti et al., 1999). However, given

that the length of the debris-flow flume was short, grain modification in transport will have been limited and so the composition of the debris flow deposits produced in these experiments will have been similar to the original mixture, therefore producing deposits of similar compositions to natural debris flows in that they have bimodal grain-size distributions. In addition, due to grain-size segregation during debris-flow motion, the grain-size composition of the deposits varies spatially, with coarse grains accumulating at the snout of the deposit, and fine grains making up the tail.

4.3. Flow Front Positions and Speeds

There was considerable variation between debris-flow velocities between flows in individual experiment sets (Figures 3.6 and 3.8). This highlights the intrinsic variability of debris-flow behaviour, as each experiment within the subsets had the same initial conditions. This emphasises the importance of repeat experiments in experimental debris-flow research. The first runs in each experiment subset tended to have lower average velocities than the later runs. This is because the bed of the flume was dry initially, so the pore pressure from the debris-flow mixture was transferred to the bed, increasing the effective friction on the flow, and therefore reducing the velocity of the flow (Rickenmann et al., 2003; Iverson et al., 2011). The bed was made wet by the previous debris flows for later runs in the experiment sets, which increased the pore-water pressure and therefore reduced the effective friction acting on the flow. This is in support of the findings of studies completed on natural debris flows whereby initial debris flows had slower flow velocities than subsequent ones (Doyle et al., 2011). Thus, the behaviour of the small-scale debris flows conducted here can be considered to be representative of natural debris flows but it should also be recognised that bed-conditioning is an important process controlling debris-flow dynamics.

The greater runout distances and greater velocities of debris-flow experiments carried out at higher slope angles (Figure 3.5; Figure 3.15) demonstrate the sensitivity of debris-flow behaviour to small changes in slope angle (29 to 31°), which emphasises the importance of modelling debris flows at different slope angles as the length of the runout is an important consideration for hazard management (Hubl and Steinwedtner, 2000); with every 1 degree change in slope angle, the in-channel velocity of the flow increased by an average of 1.06 m s^{-1} and the runout distance increased by an average of 16.35 cm. In natural debris flows, this increase in runout distance with an increase in slope is often due to the greater incorporation of bed sediment in the debris flow at steeper slope angles, as there is a power-law relationship between debris-flow volume and runout distance (D'Agostino et al., 2010). This results in a positive feedback effect, whereby an increase in flow velocity results in greater erosive potential, thereby increasing volume, which again results in greater erosive potential. Entrainment of bed material is therefore increased, which increases the volume (and runout distance) further. However, as the bed was rigid for the experiments conducted in this research, this effect was absent, and the increased runout distance was likely to be due to the increased velocities at steeper slope angles, as observed in previous studies (Prochaska et al., 2008; Xiao-quing et al., 2014; De Haas et al., 2015).

This highlights the importance of bed conditions in influencing debris-flow behaviour. Indeed, based on experiments carried out using the same mixture composition, and the same flume as was used in this study, the average velocity of the debris flows over a deformable bed in the same flume was approximately 32% greater than the average velocity of debris flows over a rigid bed in this study at the same slope angle (Davies, 2017). Given that velocity impacts upon the flow

dynamics due to its impact on dimensionless parameters which dictate the force-balance of the flow (as seen in Figure 3.20), the lack of a deformable bed in the experiments presented in this research may be problematic in terms of scaling to natural debris flows which mainly occur on deformable beds. However, this cannot be seen to be a draw-back of small-scale experimental debris flows exclusively, as the USGS experiments were also carried out on a rigid bed (Iverson et al., 2010) Furthermore, as demonstrated by the comparison of dimensionless scaling numbers in Table 3.3, the small-scale experiments produced results similar to both the USGS large-scale flume experiments and natural debris flows, so this issue did not impact upon the flow dynamics to such an extent that it made the experiments unrepresentative of larger-scale flows.

4.4. Roll Waves

Roll waves are a key characteristic of debris-flow behaviour often observed in natural debris flows, and so the manifestation of roll waves in the debris flows in this research suggests that the small-scale experiments are representative of natural debris flows, which typically exhibit unsteady, surging behaviour (Hungr, 1999). Roll waves occur where the Froude number reaches a critical value determined by the Reynolds number of the flow (Table 1.2) and the cross-sectional shape of the channel (Edwards, 2014). Froude number is determined as follows:

$$Fr = \frac{v^2}{gL} \qquad [4.2]$$

where v is flow velocity (m s^{-1}), g is gravitational acceleration (m s^{-2}), and L is the length of the flow (m). In general, in the small-scale experiments conducted here, the Froude numbers of the flows were subcritical (Pierson, 1981), and increased with slope angle (F= 0.030 for 29˚ experiments, F=0.043 for 30˚

experiments, and F=0.051 for 31˚ experiments). However, disturbances to the flow can result in roll-wave instabilities, resulting in the critical Froude number being exceeded, and therefore resulting in surge behaviour (Edwards, 2014), hence the presence of roll waves in this research. This is in support of previous studies, which also find roll waves developing in subcritical flows (Julien and Hartley, 1986). The development of roll waves has implications for hazard predictions as surges pose great destructive potential due to the increased impact forces associated with them (Hübl et al., 2009).

Whilst surge behaviour was observed in the experiments (Figure 3.9), even on long flumes, there is often insufficient distance for roll waves to fully develop (Davies, 1990), so the development of roll waves in these experiments may not have been as extensive as in natural debris flows. It should also be noted that the data on roll wave occurrence in this study is from qualitative observations, and to determine the cause of the development of roll-wave instabilities, further research would be needed.

However, Munachen (2006) states that under current understanding of debris-flow behaviour, the aerial extent of debris-flow deposits cannot be related to the geotechnical attributes of surge behaviour. As such, the disparities in roll-wave behaviour between natural debris flows and those observed in these experiments are not necessarily problematic as there does not appear to be a clear relationship with debris-flow deposits (which are indicative of debris-flow dynamics (Iverson et al., 2010)). This is an area that warrants further quantitative investigation.

4.5. Runout Deposit Morphology

The deposit morphology of the debris flows in these experiments exhibited characteristics typical of natural debris flows; these included coarse-grained

snouts and lateral margins, saturated tails, and channel-length to deposit-length ratios similar to those measured in large-scale experimental debris flows which are thought to be representative of natural debris flows (Figures 3.10 and 3.13) (Iverson, 2015).

The debris-flow deposits produced in the experiments designed to mimic those carried out in the large-scale USGS flume had similar proportions to the USGS deposits in relation to the width-length relationships of the deposits, and in relation to the relative lengths of the flumes (the small-scale debris flows and USGS debris flows had an average flume length to deposit length ratio (m) of approximately 8:1.2 and 8.3:1.3, respectively). This is demonstrated in Figure 4.1 below, whereby the proportions of the deposits are similar, and both show evidence of surging. Therefore, as scaling down the debris flow experiments produced debris-flow deposits of similar proportions, it can be asserted that on the full-deposit scale, there were no obvious drawbacks to modelling on a smaller scale.

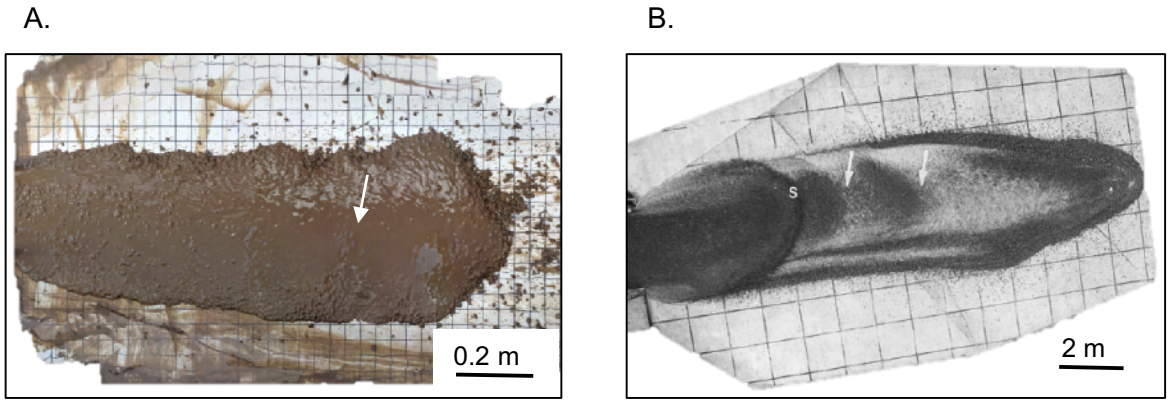

Figure 4.1. Comparison between (A) a debris-flow deposit from the small-scale experiments completed in this study, and (B) a debris-flow deposit from the USGS flume (From Major, 1996). Surging is indicated by the white arrows.

The morphology of the debris-flow deposits, as shown by the outputs from the morphological analysis (Section 3.4), demonstrates the similarities between small-scale experimental debris flows and natural debris flows. Figure 3.12 demonstrates the presence of lateral levees in the majority of the debris-flow deposits (with the exception of deposits formed by the different viscosity mixtures), formed by the shouldering apart of the coarse flow front by the saturated debris-flow tail (Iverson, 2003). Given that lateral levees are a key characteristic of natural debris flows identified in Chapter 1, and debris-flow deposits are indicative of behaviour in the channel (Iverson et al., 2010), this suggests that the small-scale experimental debris flows produced here produce deposits representative of natural debris-flow deposits.

However, not all debris flows produced in this research formed lateral levees. For example, the low-viscosity mixtures formed debris-flow deposits which appear to lack clear grain-size segregation, and are not representative of natural debris-flow deposits (Figure 3.12; Figure 3.14). This is due to a change in the rheology of the flow as viscosity is changed (Ilstad et al., 2004). The dimensionless numbers used in debris-flow scaling demonstrate the influence of viscosity on debris-flow behaviour: Due to the inclusion of viscosity parameters in the calculations for Savage number and Bagnold number (Table 1.2), the viscosity of the debris-flow mixture was statistically significant in determining the values for these numbers (Figure 3.21), and as these numbers describe the flow dynamics, it is expected that variations in viscosity should result in variations in debris-flow behaviour and, as a result of this, in variations in deposit morphology. This highlights the sensitivity of debris-flow behaviour to small changes in mixture viscosity, as small changes resulted in considerable differences in debris-flow

deposit characteristics (Figures 3.12 and 3.14) and in debris-flow behaviour (Table 1.2, and Figure 3.21).

4.6. Influence of Slope Angle on Runout

The slope angle at which debris flows occur has been shown to have important implications for debris-flow behaviour: This is shown in Figure 3.15 where an increase in slope angle results in higher velocities and greater maximum deposit lengths. This behaviour is expected as it emulates behaviour observed in research on natural debris flows (D'Agostino et al., 2010). Here, the full range of influence of slope angle on debris-flow behaviour cannot be compared to the large-scale USGS experiments as in those experiments, slope angle was kept constant (at 31˚) due to limitations in controlling initial boundary conditions. Therefore it is only the results of the experiments conducted at 31˚ in the small-scale flume that can be used for comparison.

The runout distances recorded for debris-flow experiments in this study have a positive correlation with slope angle (Figure 3.3). This relationship is expected, as slope angle has previously been used as a predictor of debris-flow runout lengths, which can then be applied in hazard management (Benda and Cundy, 1990; Shieh and Jiang, 1992; Prochaska et al., 2008). For example, based upon observations of natural debris flows in Utah, Vandre (1985) found that runout distance was around 35 – 45% of the elevation difference between the head of the flow and the head of the deposition fan, thus making slope the controlling factor on debris flow runout distances. As previously discussed, this relationship is likely to be due to the increased velocity associated with the increased slope in these experiments due to the presence of a rigid bed, whereas on natural slopes,

entrainment from the bed is likely to influence the behaviour and runout of the flow (Prochaska et al., 2008).

Nevertheless, when compared with predictions of runout previously reported, the runout distances recorded in the rigid-bed experiments correspond well with predicted runout distances in natural debris flows based upon slope angle (Figure 4.3). As in Procashka et al. (2008), two parameters used to relate runout distance average slope angle – α (which is the angle between a line drawn from the midway point of the slope and the maximum runout length of the debris-flow deposit, and the horizontal) and β (which is the angle of the slope measured from the midway point of the slope and is equivalent to the slope angle in this case, seeing as the slope was uniform) - were calculated using trigonometry based upon the flume length, flume slope, runout length, and runout slope (Figure 4.2) in order to compare between the small-scale experiments produced in this research, and large-scale experiments and natural debris flows.

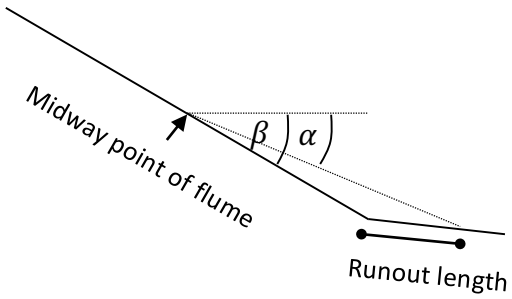

Figure 4.2. Calculation of α and β for comparison of runout lengths. The angles are calculated from halfway down the length of the flume to allow for comparison with data from Prochaska et al. (2008). As the slope of the flume is uniform over its full length, the value of β remains the same for each slope angle.

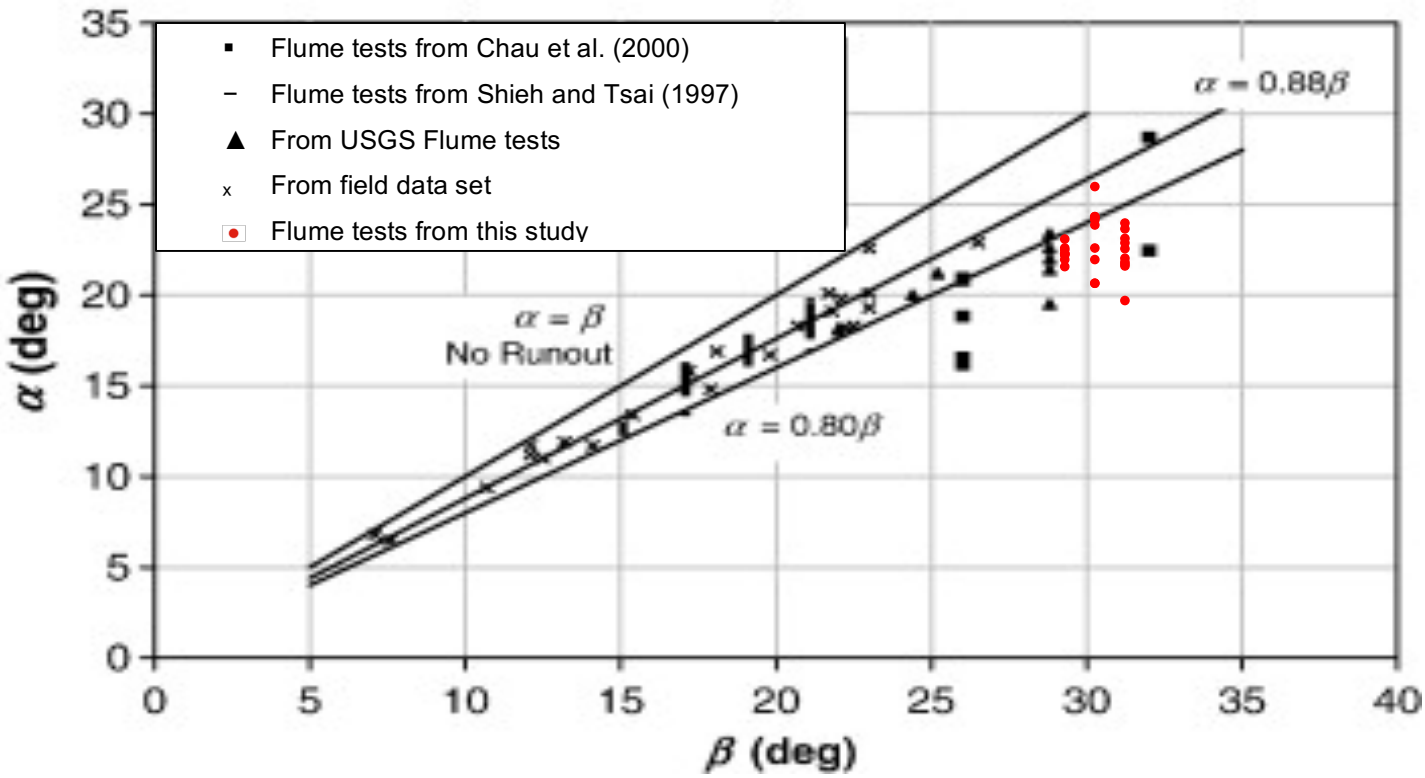

Figure 4.3. Relationship between runout angles, α (degrees), and reach angle, β (degrees). Data from previous flume tests and field data are shown (black markers), as well as the data from the experiments conducted in this study (red markers). Whilst some of the experiments carried out in this research were carried out at the same slope angle as the USGS experiments, due to the non-uniform slope angle of the USGS flume, which reduces in slope angle as the flow nears the runout pad, the data points do no overlap, as the slope is calculated from mid-way down slope here (Adapted from Prochaska et al., 2008).

Figure 4.3 shows that the runout distances for the experiments in this study were longer than expected based upon extrapolations made from field data, although the field data was from debris flows which occurred on lower slope angles than were tested here (Prochaska et al., 2008). Indeed, they tended to be similar, proportionally, to those conducted on larger-scale flumes, with both the small-scale flume experiments carried out here and the USGS large-scale flume experiments producing runout distances longer than predicted based on slope

angle (based on the field data from Prochaska et al. (2008)). As such, the small-scale debris-flow experiments conducted in this research produced results similar to those produced in the USGS experiments in terms of runout length, and so whilst they do not mimic the behaviour of natural debris flows in this respect, this cannot be seen to be a problem unique to small-scale experiments. Overall, it can be demonstrated from the results of this research that slope angle is an important control on debris-flow runout, and as runout is a consideration for hazard management (Hungr, 1995), the sensitivity of the flow to slope angle does highlight a need for variable slope angle experiments, which small-scale flumes offer the potential for.

In this study, the change in velocity with slope angle was statistically significant (Figure 3.15). This is due to the increased gravitational potential energy of the debris-flow material on steeper slopes (which necessarily have a higher starting elevation), which results in the ratio of resisting forces to driving force (factor of safety) acting on the flow to be smaller on steeper slopes (McCombie and Wilkinson, 2002):

$$(\rho_r \cdot g \cdot h) \sin\theta = c + (\rho_r - \rho_w) \cdot g \cdot h \cdot \cos\theta \cdot \tan\phi \qquad [4.3]$$

where ρ_r is the density of the slope material (kg m^{-3}), ρ_w is pore-water pressure (Pa), c is cohesional strength (KPa), g is gravitational acceleration (m s^{-2}), h is the depth of failure (m), θ is slope angle (°), and ϕ is a friction coefficient (°). This highlights the utility of small-scale flume experiments, where slope-angle can be easily varied, as such sensitivity to slope angle results in significant variation in debris-flow behaviour, which is important to consider in hazard management.

There was no clear correlation between slope angle of the channel and the flow depth. This is in support of previous studies: Eu et al. (2017) used a 2.4 m

flume to assess the impact of slope angle and debris-flow composition of debris-flow dynamics, and found no correlation between slope and flow depth. Whilst this cannot be compared with the results of the USGS experiments given that only one slope angle was tested on the USGS flume (31°), the similarity of this result to previous studies performed at different scales suggests that this behaviour scales between debris-flows, and so the experiments conducted here can be asserted to be representative of natural debris-flows.

4.7. Influence of Viscosity

Investigating in more detail the influence of flow composition on debris-flow behaviour (Section 4.1), the mixture composition was intentionally altered for some of the experiments, in order to test the impact of fluid viscosity on debris-flow behaviour. Viscosity has statistically significant relationships with some debris-flow characteristics, including deposit length, deposit width, and debris-flow velocity, which are key indicators of debris flow behaviour tested in this study (Figure 3.18). The morphology of the debris-flows resulting from different mixture viscosities is shown in Figure 3.14. The deposits from the low-viscosity mixtures (below the standard of 0.0025 Pa.s used in the debris-flow experiments in this study) were longer and wider than those produced from the standard mixture, and did not form coarse-grained snouts or lateral levees (Figure 3.12; Figure 3.14). The deposits from the high-viscosity mixtures were shorter than the standard mixtures, and didn't form lateral levees (Figure 3.14). This is likely to be due to changes in the rheology of the flow; in both the high- and low-viscosity flows, there was no clear difference in water-content in the snout and tail of the flow, hence, there was no shouldering apart of the snout by a saturated tail, and so in contrast to the flows produced from the standard mix (Figure 3.1), no levee formation occurred.

However, despite the lack of levee formation in the high-viscosity flows, grain-size segregation was observed, suggesting that some aspects of natural debris-flow behaviour were still present in the debris flows conducted at high viscosities. This is because grain-size segregation is characteristic of debris-flow behaviour (Savage and Iverson, 2003) due to kinematic sieving, buoyancy-related effects due to dilation of the flow material, and assimilation of material during the flow (Naylor, 1980). The changes to the debris-flow deposit morphology suggest that the small changes in debris-flow viscosity in this study were sufficient to alter the rheology of the flow, and hence impact upon debris-flow dynamics, as debris-flow deposits are indicative of in-channel behaviour (Iverson et al., 2010).

The statistically significant relationship of viscosity with deposit width (Figure 3.18) is particularly notable, as other predictors, such as slope angle, do not have such relationships with deposit width. This suggests that viscosity is the main control on the lateral spreading of debris-flow deposits. This supports the results of previous experimental studies, whereby deposit geometry was largely determined by flow composition (de Haas et al., 2015). Indeed, there is also a statistically significant relationship between the interstitial fluid viscosity of the debris-flow mixture and Bagnold number (Figure 3.21). As Bagnold number describes the ratio of collisional forces to viscous forces (Table 1.2), viscosity therefore has an influence on flow behaviour, explaining the influence of viscosity of deposit morphology. The influence of viscosity on the lateral spreading of the debris-flow deposit can explained by the following equation, assuming a simple Bingham model for the rheology of the flow, which is considered appropriate to describe the rheological behaviour of debris-flows (Enos, 1977):

$$\sigma_s = k + \mu_b \varepsilon_s \quad [4.4]$$

where σ_s is the shear stress of the flow (Pa), k is the yield strength, and $\mu_b\varepsilon_s$ is a Newtonian viscosity term made up of viscosity and shear rate. The inclusion of viscosity in the Bingham model for debris-flow rheology explains the correlation between viscosity and deposit width in these experiments (Figure 3.18), as the rheology is directly related to the viscosity of the flow.

The influence of viscosity on debris-flow velocity is important here as debris-flow dynamics are shown to be highly sensitive to viscosity. The velocity of the flows decreased with increasing viscosity (Figure 3.8). This is in contrast to previous findings whereby velocity was observed to decrease with increasing grain-size (Cagnoli and Romano, 2012), as here, the median grain-size of the flows decreased with viscosity. However, in these experiments, the decrease in grain-size was due to an increase in the proportion of fine grains (clay) in the fluid portion of the mixtures as opposed to a decrease in the proportion of coarse-grains (Figure 3.2). Therefore, the increase in clay resulted in an increase in viscosity and therefore a decrease in debris-flow velocity (Davies, 1994). As such, the use of small-scale models such as the one used in this research, which allow for variations in mixture viscosity whilst keeping costs low, is useful as they allow a range of debris-flow compositions to be tested.

4.8. Other factors controlling debris-flow behaviour

Flow depth is thought to be a major control on debris-flow behaviour in natural debris flows (Densmore et al., 2011; Cao et al., 2017). However, this is due to the correlation between local flow depth and magnitude of bed erosion. As such, given that the flume used in the experiments in this study had a rigid bed, there was no erosion, and the increased runout distance of the debris flows with increased velocity was not as a result of increased debris-flow volume. This

explains the lack of correlation of average flow depth with maximum deposit length in the experiments conducted in this research.

However, whilst average flow depth does not necessarily directly correlate with deposit morphology in the small-scale experiments carried out in this research, Iverson et al. (2010) asserts that there is not necessarily a direct relationship between form and process in debris flow dynamics. Therefore, flow depth may still exert control on debris-flow behaviour in these experiments. Indeed, flow depth has a statistically significant relationship with Bagnold number, Savage number, and Friction number (Figure 3.22). As these numbers are key dimensionless parameters used to describe the ratios of forces acting to influence debris flow dynamics (Table 1.2), this suggests that flow depth did exert control on debris-flow behaviour here.

Another factor often incorporated into the prediction of runout length (which is an indicator of debris-flow behaviour) in debris-flows is volume (Bathurst et al., 1997). For example, Ikeya (1981) proposed that runout length could be predicted by (rearranged by Bathurst et al., 1997):

$$L = 8.6(V \tan\theta)^{0.42} \quad [4.5]$$

Where L is runout length (m), V is debris flow volume (m^3), and θ is slope angle (˚). For the experiments conducted in this research, however, this equation underestimates the runout length of the debris flows by an average of 55%, as the volume used for each experiment was constant (0.0092 m^3). Therefore, this represents a discrepancy between natural and small-scale experimental debris flows. However, again, this is likely to be due to the lack of incorporation of bed material into these rigid-bed debris flows. Therefore, such behavioural discrepancies with natural debris flows are likely to be seen in other rigid-bed experiments, regardless of scale. Whilst an increase in slope angle did result in a

larger proportion of the total debris-flow volume being deposited on the runout pad (as increased velocities at higher slope angles reduced the in-channel deposition), this change in volume was therefore not sufficient to influence runout distance, as the thickness of the deposits also varied with volume.

4.9. Debris-Flow Scaling

The scaling relationships between the small-scale debris flow experiments carried out in this study and the large-scale debris flow experiements documented by Iverson et al. (2010) are demonstrated by the comparison of dimensionless parameters presented in Chapter 3. The dimensionless numbers describe characteristcs of debris-flow behaviour irrespective of size, and so if they scaled directly, the dimensionless numbers would be the same across all scales of debris flow. The dimensionless scaling parameters (Table 3.2) demonstrate that there are some differences in behaviour of debris flows at different scales. In the small scale experiments reported here, the key dimensionless parameters which describe debris-flow behaviour (Bagnold number, N_B, and Savage number, N_S) tend to be higher in the small-scale experiments than they are in the large-scale USGS experiments. Although this is to be expected due to the shallow flow depths and high velocities (Haas, 2016), it could be argued that this poses an issue for debris-flow scaling. However, depsite differing from the USGS values for the key dimensionless numbers, the values obtained for the debris flows completed in this research are generally within the ranges expected for natual debris flows. As such, it can be argued, on this comparision alone, that the small-scale flume experimental debris flows was more representative of natural debris flows that the large-scale USGS flume experimental debris flows.

The Friction number, N_F, however, was smaller in some of these experiments than in the large-scale USGS experiments (Table 3.2). This has

important implications for the comparability between debris flows of different scales. Iverson and LaHusen (1993) state that as

$$N_F = \lambda^{-1/2} N_B / N_S \quad [4.6]$$

where N_F>1400, friction dominates viscosity in a debris flow. As this condition is not satisfied in all of the small-scale experiments conducted in this research, other forces are more important in determining the debris-flow behaviour in those flows. This small value for the Friction Number in some of the small-scale experiments is due to the very small flow depths associated with those flows in the small-scale experiments as this meant that the Savage number was proportionally larger than the Bagnold number was in comparison to the dimensionless numbers derived from natural debris flows, and from those from the USGS experiments.

The large grain-size to flow-depth ratio identified in these experiments (Table 3.2) explains the larger-than-expected Savage number in some of the experiments. This highlights a potential scaling issue with small-scale flume debris-flow experiments, as the Savage number describes the force-balances acting in the flow, and so impacts the debris-flow behaivour. However, the large grain-size to flow-depth ratio used in these experiments is actually typical of natural debris flows, which often incorporate large boulders (Takahashi, 1989). The USGS debris-flow mixture has a smaller maximum grain-size proportionally, with gravel-sized particles being used as the maximum grain-size in both the USGS experiments, and the small-scale experiments carried out in this research. As such, as the USGS experiments neglect to include very large grains, which have important influences on debris-flow behaviour (Davies, 1993), the small-scale experiments conducted here may in fact be more representative of natural debris-flows than the large-scale USGS debris-flows are. Furthermore, He et al. (2016) identify boulders as being the main component of impact forces, so the inclusion of

large grains in experimental debris-flows is important if they are to be used to inform models for hazard management.

An analysis of the relationship between debris-flow volume and area based on worldwide data from natural debris flows shows a power-law relationship, whereby the area of inundation increases linearly with debris-flow volume on a logarithmic scale (Griswold and Iverson, 2008). This relationship is also present in the debris flows conducted at a smaller scale (de Haas et al., 2015), and whilst the initial debris flow volume was kept constant in this study, the average inundated area for debris flows conducted is consistent with this relationship (Figure 4.4). This suggests that the scale at which debris-flow experiments are conducted does not affect the representativeness of all aspects of debris-flow behaviour. Such a relationship is important given the use of power-law relationships in hazard prediction (Bovis and Jakob, 1999; Dai and Lee, 2001; Griswold and Iverson, 2008; Li et al., 2011; Reid et al., 2016), and suggests that small-scale experiments are valid for use in hazard management and prediction where debris flows are concerned.

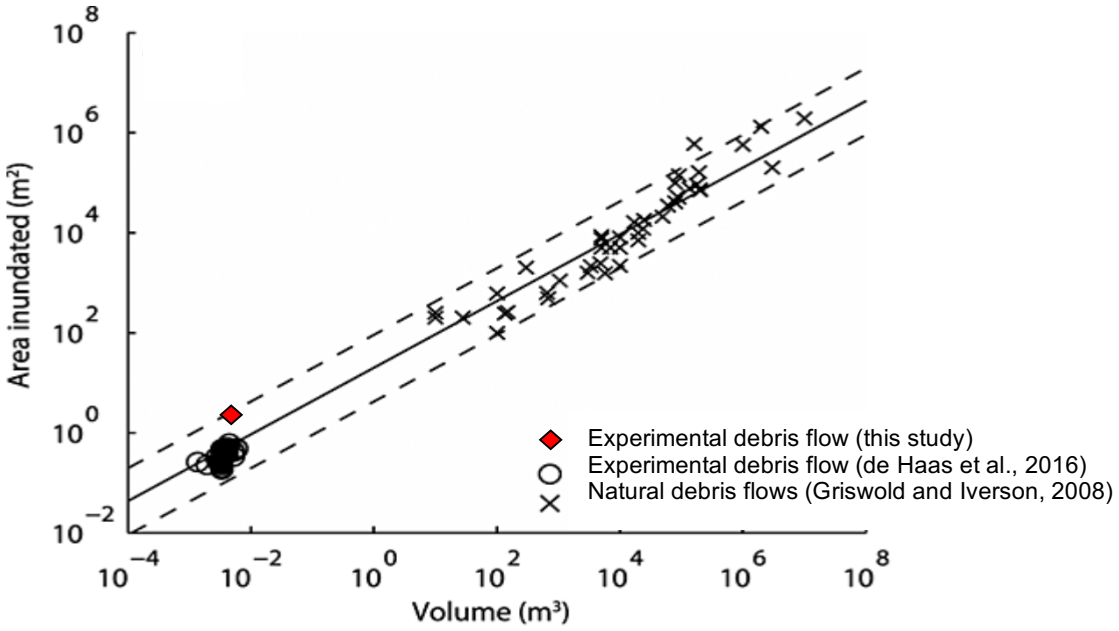

Figure 4.4. Relationship between debris flow volume and area inundated in debris flows at different scales (natural debris flows plotted by Griswold and Iverson, 2008, small-scale debris flow experiments conducted by de Haas et al., 2015 (2 m flume), and small-scale debris flow experiments from this study (8 m flume). (Adapted from de Haas et al., 2016).

A summary of the key results from the experiments which show the similarity of these small-scale experimental debris flows to the large-scale USGS flows and, crucially, to natural debris-flows is shown in Table 4.1. This demonstrates that not only are small-scale experimental debris flows representative of the natural debris flows which they are intended to replicate, but that in many aspects, they are closer replicas of natural debris flows than the large-scale USGS experimental debris flows are.

Table 4.1. Summary of the key characteristics of debris flows from the data collected in this research, compared with data from the USGS flume (Iverson et al., 2010), and from natural debris flows (de Haas, 2016).

Debris-flow parameter	Small-Scale Debris Flows (This Study)	USGS Debris Flows	Natural Debris Flows
Velocity (m s^{-1})	0.68 – 5.13	10	0.1 – 20
Depth (m)	0.008 – 0.03	0.1	0.1 – 10
Bagnold Number	73 - 19134	400	10^0 – 10^8
Savage Number	0.02 - 239.15	0.2	10^{-7} – 10^0
Friction Number	80 - 4678	$2x10^3$	10^0 – 10^5

Overall, whilst there are scaling issues associated with debris-flow experiments carried out in small-scale flumes, they are still useful in progressing debris-flow research. Small flumes allow for a greater range of experiments to be conducted in which key variables can be varied (e.g. slope angle and debris-flow composition). Varying thse parameters allows for both geotechnical/rheological and morphological scalling relationships to be better analysed in a broader experimental framework. Indeed, several of the dimensionless numbers for the debris flows carried out in this research are closer to the typical values of natural debris flows than the large-scale USGS values are. Furthermore, the use of the small-scale flume in these experiments yielded results similar to large-scale experiments and to natural debris flows in terms of the key morphological indicators of debris-flow behaviour.

5. Conclusions

This research has been designed to demonstrate, for the first time, scaling differences between small-scale and large-scale laboratory debris flows. The flexibility of small-scale experiments in comparison to large-scale ones (using the large-scale USGS flume experiments (Iverson et al., 2010) for comparison) has also been demonstrated. Examples are the influence of slope on debris-flow behaviour, which cannot be tested on the USGS flume, and the greater number of experiments that can be carried out in a much shorter period of time when compared to large-scale experiments e.g. it is possible to run c.50 experiments in the small scale flume compared to a single experiment at larger scale. However, to realise these benefits it is important that the behaviour in both small and large scale experiments reproduces actual (prototype) debris flow behaviour. The specific conclusions of this research are as follows:

- For the same initial boundary conditions there is intrinsic variability associated with debris-flow behaviour. For debris flows which occurred under the same initial conditions (including slope angle, mixture composition, and bed conditions), debris-flow behaviour varied considerably. Here, the variation in debris-flow behaviour was manifested in differences in velocities (+/- 43% of the mean), flow depths (+/- 31% of the mean), deposit morphology, and runout distances (+/- 29% of the mean).
- Where the debris-flow mixture was kept the same, the small variations in the proportion of coarse grains in the debris-flow mixture was found to be more significant in influencing the behaviour of the debris flows than the small variations in the proportion of fine grains in the mixture. The proportion of coarse grains in the mixture showed significant relationships (less than the common alpha level) with key behavioural indicators including velocity, runout length, and deposit morphology, whereas the

proportion of fine grains in the mixture did not. This contrasts with previous findings of Iverson et al. (2010).

- The relative composition of the debris-flow mixtures used here was representative of natural flows, despite being scaled down. The bimodality index of the mixture was also similar to that of the USGS mixture (1.79 compared to 2.09), justifying the comparison between the two sets of experiments, as the index is dimensionless so is irrespective of scale. Bimodal grain-size distributions are typical of natural debris flows, so the small-scale debris flows can be considered representative of the prototype.
- The data generated from the experiments conducted in this study compares well with the large-scale USGS experiments documented by Iverson et al. (2010), and with natural debris flows. Roll waves were observed in the small-scale experiments, and with the exception of the very low viscosity flows, lateral levees and coarse-grained snouts formed, which are characteristics typical of natural debris flows.
- Slope has a strong influence over debris-flow behaviour, with velocity and runout distance having statistically significant correlations with slope angle. Small adjustments in slope results in significant changes in debris-flow behaviour whish highlights the need for variable slope angle experiments in debris-flow research, and therefore emphasises an advantage of using small-scale flumes over large-scale ones, where slope angle is fixed. This has implications for numerical modelling, as it requires slope to be reported much more precisely than to two significant figures.
- The runout lengths generated in these experiments were greater than predicted for the slope angle at which they were carried out based upon predictions from natural debris flows but they are similar to those generated by the USGS experiments. Hence this overestimation is not unique to

small-scale debris flow experiments and they provide results comparable to large-scale experiments for a fraction of the cost and time.

- Where debris-flow mixtures of different compositions were tested, debris-flow behaviour was highly sensitive to changes in viscosity, with changes in the interstitial fluid viscosity being sufficient to influence the rheology of the flow, resulting in a lack of levee formation in debris-flow deposits when viscosity was altered by $\pm$ 0.002 Pa.s.
- The key dimensionless numbers for assessing scaling relationships (Bagnold number, Savage number, and Friction number) calculated for the small-scale debris flows in this research were within the ranges expected for natural debris flows.
- There was a greater grain-size to flow-depth ratio in the small-scale experiments than in the large-scale USGS experiments (average of 0.23 compared to 0.10) , and although this resulted in the Savage number of some experiments exceeding values expected of natural flows, this is in fact more representative of natural debris-flow compositions which typically incorporate large boulders.

The small-scale flume debris-flow experiments carried out here produced results similar to both the large-scale USGS results, and crucially, to natural debris flows. The intrinsic variability of debris-flow behaviour identified here raises issues for hazard management of natural debris flows, as it suggests that the initial conditions of a slope are not enough to make accurate predictions of runout length. This uncertainty should be considered when producing models to inform hazard mapping in the future.

6. References

Ancey, C. (2013) Debris Flows. In: Schrefler, B. and Delage, P. (Eds.) *Environmental Geomechanics*. John Wiley and Sons, Hoboken, USA. 1-37.

Anderson, D. M., Reynolds, R. C., Brown, J. (1969) Bentonite Debris Flows in Northern Alaska. *Science*. 164. 173-174.

Arattano, M. & Marchi, L. (2005) Measurements of debris flow velocity through cross correlation of instrumentation data. *Natural Hazards and Earth System Sciences.,* 5. 137-142.

Ashworth, P. J., Peakall, J., Best, J. L. (1996) Physical Modelling in Fluvial Geomorphology: Principles, Applications and Unresolved Issues. In: Rhoads, B. L., Thorn, C. E (Eds.) *The Scientific Nature of Geomorphology*. Proceedings of the 27th Binghamton Symposium, Chapter 9. Wiley, New York. 221-253.

Badoux, A., Graf, C., Rhyner, J., Kuntner, R., McArdell, B. W. (2009) A debris-flow alarm system for the Alpine Illgraben catchment: design and performance. *Natural Hazards.* 49 (3). 517-539

Bagnold, R. A. (1954) Experiments on a gravity-free dispersion of large solid spheres in a Newtonian fluid under shear. *Proceedings of the Royal Society A: Mathematical, Physical and Engineering Sciences*. 225 (1160). 49–63.

Baker, V. R. (1996) Hypotheses and geomorphological reasoning. In: Rhoads, B. L., Thorn, C. E (Eds.) *The Scientific Nature of Geomorphology*. Proceedings of the 27th Binghamton Symposium. Wiley, New York.

Barenblatt, G. I. (1996) *Scaling, Self-similarity, and Intermediate Asymptotics: Dimensional Analysis and Intermediate Asymptotic*s. Cambridge University Press, Cambridge. 386pp.

Bathurst, J. C., Burton, A., Ward, T. J. (1997) Debris Flow Run-Out and Landslide Sediment Delivery Model Tests. *Journal of Hydraulic Engineering.* 123 (5). 410-419.

Benda, L. E. and Cundy, T. W. (1990) Predicting deposition of debris flows in mountain channels. *Canadian Geotechnical Journal.* 24 (7). 409-417.

Bennett. S. J., Ashmore, P., McKenna Neuman, C. (2015) Transformative geomorphic research using laboratory experimentation. *Geomorphology*. 224. 1-8.

Berti, M., Genevois, R., Simoni, A. and Tecca, P.R. (1999) Field observations of a debris flow event in the Dolomites. *Geomorphology,* 29 (3-4). 265-274.

Berti, M., Genevois, R., LaHusen, R., Simoni, A., Tecca, P. R. (2000) Debris flow monitoring in the acquabona watershed on the Dolomites (Italian Alps). *Physics and Chemistry of the Earth, Part B: Hydrology, Oceans and Atmosphere.* 25 (9). 707-715.

Bettella, F., Bisantino, T., D'Agostino, V., Gentile, F. (2012) Debris-flow runout distance: laboratory experiments on the role of Bagonold, Savage, and friction numbers. *Monitoring, Simulation, Prevention and Remediation of Dense and Debris Flows IV* 4. 27.

Blair, T. C. (1999) Cause of dominance by sheetflood vs. debris-flow processes on two adjoining alluvial fans, Death Valley, California. *Sedimentology.* 46 (6). 1015-1028.

Blair, T. C. and McPherson, J. G. (1999) Grain-size and textural classification of coarse sedimentary particles. *Journal of Sedimentary Research.* 69 (1). 6-19.

Blijenberg, H. M. (2007) Applications of physical modelling of debris flow triggering to field conditions limitations posed by boundary conditions. *Engineering Geology*. 91 (25 35).

Blott, S. J. and Pye, K. (2006) Particle size distribution analysis of sand-sized particles by laser diffraction: an experimental investigation of instrument sensitivity and the effects of particle shape. *Sedimentology*. 53 (3). 671-685.

Bolster, D., Hershberger, R. E., Donnelly, R. J. (2011) Dynamic similarity, the dimensionless science. *Physics Today.* 64 (9). 42-47.

Bovis, M. J., and Jakob, M. (1999) The Role of Debris Supply Conditions in Predicting Debris Flow Activity. *Earth Surface Processes and Landforms.* 24. 1039-1054.

Bowman, E., Laue, J., Imre, B., Springman, S. M. (2010) Experimental modelling of debris for behaviour using a geotechnical centrifuge. *Canadian Geotechnical Journal.* 47 (7). 742-762.

Brayshaw, D. and Hasan, M. A. (2009) Debris flow initiation and sediment recharge in gullies. *Geomorphology.* 109 (3-4). 122-131.

Breien, H., Pagliardi, M., De Blasio, F. V., Issler, D. Elverhoi, A. (2007) Experimental studies of subaqueous vs. subaerial debris flows: Velocity characteristics as a function of the ambient fluid. In: Lykousis, V., Sakellariou, D. and Locat, J. (Eds.) *Submarine Mass Movements and Their Consequences*. Springer. 101-110.

Bridgman, P. W. (1922) *Dimensional Analysis*. Yale University Press. New Haven. 112pp.

Burbank, D. W. (2002) Rates of erosion and their implications for exhumation. *Mineralogical Magazine.* 66 (1). 25–52.

Burton, A., Bathurst, J. C. (1998) Physically based modelling of shallow landslide sediment yield at a catchment scale. *Environmental Geology.* 35. 89-99.

Caballero, L., Sarocchi, D., Soto, E., and Borselli, L. (2014) Rheological changes induced by clast fragmentation in debris flows. *Journal of Geophysical Research: Earth Surface.* 119 (9). 1800-1817.

Cagnoli, B., Romano, G. P. (2012) Granular pressure at the base of dry flows of angular rock fragments as a function of grain size and flow volume: A relationship from laboratory experiments. *Journal of Geophysical Research: Solid Earth.* 117. B10202.

Cannon, S. H. (1993) An empirical model for the volume-change behaviour of debris flows. *In:* Shen, H. W., Su, S. T., Wen, F. (Eds.) *Hydraulic Engineering 1993*. 2. 1768-1773.

Cao, C., Song, S., Chen., J., Zheng, L., Kong, Y. (2017) An Approach to Predict Debris Flow Average Velocity. *Water.* 9 (3). 205.

Carrivick, J. L., Smith, M. W., Quincey, D. J. (2016) *Structure from Motion in the Geosciences, New Analytical Methods in Earth and Environmental Science.* John Wiley & Sons. Chichester, West Sussex. 208pp.

Chanson, H., Coussot, P., Jarny, S., Toquer, L. (2004) A Study of Dam Break Wave of Thixotropic Fluid: Bentonite Surges Down an Inclined Plane. (No. CH54/04).

Chau, K. T., Chan, L. C. P., Luk, S. T., Wai, W. H. (2000) Shape of deposition fan and runout distance of debris-flow: effects of granular and water contents.

In: Wieczorek, G. F., and Naeser, N. D. (Eds.) *Proceedings of the Second International Conference on Debris Flow Hazards Mitigation: Mechanics, Prediction and Assessment.* Taipei, Balkema, Rotterdam, Netherlands. 387-395.

Cheng, Y-T, and Cheng, C-M. (2004) Scaling, dimensional analysis, and indentation measurements. *Materials Science and Engineering: R: Reports.* 44 (4-5). 91-149.

Chiarle, M., Lannotti, S., Mortara, G., Deline, P. (2007) Recent debris flow occurrences associated with glaciers in the Alps. *Global and Planetary Change.* 56 (1-2). 123-136.

Coe, J. A., Kinner, D. A., Godt, J. W. (2008) Initiation conditions for debris flows generated by runoff at Chalk Cliffs, central Colorado. *Geomorphology.* 96. 270-297.

Chow, V. T. (1959) *Open Channel Hydraulics*. McGraw-Hill, New York. 680pp.

Contreras, S. M. and Davies, T. R. (2000) Coarse-grained debris-flows: Hysteresis and time-dependent rheology. *Journal of Hydraulic Engineering*. 126 (12) 938-941.

Costa, J. E. (1998) Rheologic, geomorphic, and sedimentological differentiation of water floods, hyperconcentrated flows, and debris flows. In: Baker, V. R., Kochel, R.C., and Patton, R. C. (Eds.) Flood Geomorphology. John Wiley and Sons, New York. Pp. 113-122.

Coussot, P. (1995) Structural Similarity and Transition from Newtonian to Non-Newtonian behaviour for Clay-Water Suspensions. *Physical Review Letters.* 74 (20). 3971-3974.

Coussot, P., Laigle, D., Arattano, M., Deganutti, A., Marchi, L. (1998) Direct Determination of Rheological Characteristics of Debris Flow. *Journal of Hydraulic Engineering*. 865-868.

D'Agostino, V., Cesca, M., Marchi, L. (2010) Field and laboratory investigations of runout distances of debris flows in the Dolomites (Eastern Italian Alps). *Geomorphology*. 115 (3). 294-304.

D'Agostino, V., Bettella, F., Cesca, M. (2013) Basal shear stress of debris flow in the runout phase. *Geomorphology.* 201. 272-280.

Dai, F. C., and Lee, C. F. (2001) Frequency-volume relation and prediction of rainfall-induced landslides. *Engineering Geology.* 59 (3-4). 253-266.

D'Aniello, A. Cozzolino, L., Cimorelli, L., Morte, D. M., Pianese, D. (2015) A numerical model for the simulation of debris flow triggering, propagation and arrest. *Natural Hazards.* 75 (2). 1403-1433.

Davies, T. R. (1986) Large Debris Flows: A Macro-Viscous Phenomenon. *Acta Mechanica.* 63. 161-178.

Davies, T. R. (1990) Debris-Flow Surges – Experimental Simulation. *Journal of Hydrology (New Zealand).* 29 (1). 18-46.

Davies, T. R. (1993) Large and Small Debris Flows – Occurrence and Behaviour: 11-22. *In: International workshop on debris flow.* Kagoshima, Japan. September, 6-8.

Davies, T.R. (1994) Dynamically similar small-scale debris flow models. *In*: *Proceedings of the International Workshop on Floods and Inundations Related to Large Earth Movements*. Edited by University of Trento, IAHS. 11pp.

Davies, C. (2017) Evolution of erosion within a flume: The effects of successive debris flows and channel configuration. MSci Dissertation. *Department of Geography, Durham University.*

Deangeli, C. (2009) Pore Water Pressure Contribution to Debris Flow Mobility. *American Journal of Environmental Sciences.* 5 (4). 486-492.

Densmore, A. L., Schuerch, P., Rosser, N. J., McArdell, B. W. (2011) Erosion and deposition on a debris-flow fan. *America Geophysical Union, Fall Meeting 2011.*

Deubelbeissm Y., Graf, C., Christen, M. (2011) Numerical modelling of debris flows with RAMMS – Alpine case studies*. Mattertal–ein Tal in Bewegung.* 20pp.

Dowling, C. A. and Santi, P. M. (2014) Debris flows and their toll on human life: a global analysis of debris flow fatalities from 1950 to 2011. *Natural Hazards.* 71 (1). 203-227.

Doyle, E.E., Cronin, S. J., Thouret, J.-C. (2011) Defining conditions for bulking and debulking in lahars. *Geological Society of America Bulletin.* 123 (7-8): 1234-1246.

Edwards, A. N. (2014) Roll waves and erosion-deposition waves in granular flows. PhD thesis. *Faculty of Engineering and Physical Sciences, University of Manchester.*

Egashira, S., Itoh, T., Takeuchi, H. (2001) Transition mechanism of debris flows over rigid bed to over erodible bed. *Physics and Chemistry of the Earth, Part B: Hydrology, Oceans and Atmosphere.* 26 (2) 169-174.

Enos, P. (1977) Flow regimes in debris flow. *Sedimentology.* 24. 133-142.

Eu, S., Im, S., Kim, D., Chun, K. W. (2017) Flow and deposition characteristics of sediment mixture in debris flow flume experiments. *Forest Science and Technology.* 13 (2). 61-65.

Fannin, R. J. and Wise, M. P. (2001) An empirical-statistical model for debris-flow travel distance. *Canadian Geotechnical Journal.* 38 (5). 982-994.

Felder, S., and Chanson, H. (2009) Turbulence, dynamic similarity and scale-effects in high-velocity free-surface flows above a stepped chute. *Experiments in Fluids.* 47 (1). 1-18.

George, D. L. and Iverson, R. M. (2011) A two-phase debris-flow model that includes coupled evolution of volume fractions, granular dilatancy and pore-fluid pressure. In: Genevois, R., Hamilton, D. L., and Prestinizi, A. (Eds.) *Fifth International Conference on Debris-flow Hazards Mitigation, Mechanics, Prediction and Assessment.* Casa Editrice Universita La Sapienza, Rome, 415-424.

Ghilardi, P., Natale, L., Savi, F. (2001) Modeling debris flow propagation and deposition. *Physics and Chemistry of the Earth, Part C: Solar, Terrestrial & Planetary Science*. 26 (9). 651-656.

Griswold, J. P., and Iverson, R. M. (2008) Mobility statistics and automated hazard mapping for debris flows and rock avalanches (ver. 1.1, April 2014): U.S. Geological Survey Scientific Investigations Report. 2007-5276. 59pp.

Guthrie, R. H., Hockin, A., Colquhoun, L., Nagy, T., Evans, S. G., Ayles, C. (2010) An examination of controls on debris flow mobility: Evidence from coastal British Columbia. *Geomorphology.* 114. 601-613.

Haas, T. D., Braat, L., Leuven, J. R. F. W., Lokhorst, I. R., Kleinhans, M. G. (2015) Effects of debris-flow composition on runout distance, depositional

mechanisms and deposit morphology in laboratory experiments. *Journal of Geophysical Research: Earth Surface.* 120 (9). 1949-1972.

Haas, T. D. (2016) Life, death and revival of debris-flow fans on Earth and Mars: Fan dynamics and climatic inferences. Faculty of Geosciences, Universiteit Utrechtm The Netherlands. Urecht Studies in Earth Sciences. (USES 95).

Han, Z., Chen, G., Li, Y., Zhang, H., He, Y. (2016) Elementary analysis on the bed-sediment entrainment by debris flow and its application using the TopFlowDF model. *Geomatics: Natural Hazards and Risk.* 7 (2). 764-785.

He, S., Liu, W., and Li, X. (2016) Prediction of impact force of debris-flows based on distribution and size of particles. *Environmental Earth Sciences.* 75. 298.

Henderson, F. M. (1996) Open Channel Flow. The Macmillan Company, New York. 522pp.

Hirano, M. and Iwamoto, M. (1981) Measurement of debris flow and sediment-laden flow using a conveyor-belt flume in a laboratory. *Erosion and Sediment Transport Measurement, Proceedings of the Florence Symposium, Florence, June 1981*. IAHS 133.

Hübl, J. and Steinwedtner, H. (2000) Estimation of Rheological Properties of Viscous Debris Flow Using a Belt Conveyor. *Physics and Chemistry of the Earth (B).* 25 (9). 751-755.

Hübl, J., Suda, J., Proske, D., Kaitna, R., Scheidl, C. (2009) Debris Flow Impact Estimation. *International Symposium on Water Management and Hydraulic Engineering.* Macedonia, 1-5 September. Paper A56.

Hungr, O. (2000) Analysis of debris flow surges using the theory of uniformly progressive flow. *Earth Surface Processes and Landforms.* 25. 483-495.

Hungr, O. (2005) A model for the runout analysis of rapid flow slides, debris flows, and avalanches. *Canadian Geotechnical Journal.* 32 (4). 610-623.

Hungr, O., McDougall, S., Bovis, M. (2005) Entrainment of material by debris flows. In: Jakob, M. and Hungr, O. (Eds.) *Debris-flow Hazards and Related Phenomena*. Springer, Berlin. 135-158.

Hungr, O. (2008) Numerical Modelling of the Dynamics of Debris Flows and Rock Avalanches. *Geomechanics and Tunnelling.* 1 (2). 112-119.

Hurlimann, M., Rickenmann, D., Graf, C. (2003) Field and monitoring data of debris flow events in the Swiss Alps. *Canadian Geotechnical Journal.* 40 (1). 161-175.

Hurlimann, M., Rickenmann, D., Medina, V., Bateman, A. (2008) Evaluation of approaches to calculate debris-flow parameters for hazard assessment. *Engineering Geology.* 102 (3-4). 152-163.

Hurlimann, M., McArdell, B. W., Rickli, C. (2015) Field and laboratory analysis of the runout characteristics of hillslope debris flows in Switzerland. *Geomorphology.* 232. 20-32.

Ilstad, T., Elverhøi, A., Issler, D., Marr, J. G. (2004) Subaqueous debris flow behaviour and its dependence on the sand/clay ratio: a laboratory study using particle tracking. *Marine Geology.* 213 (1-4). 415-438.

Imaizumi, F., Tsuchiya, S., Ohsaka, O. (2016) Field observations of debris-flow initiation processes on sediment deposits in a previous deep-seated landslide site. *Journal of Mountain Science.* 13 (2) 213-222.

Iskender, E. (2016) Evaluation of mechanical properties of nano-clay modified asphalt mixture. *Measurement.* 93. 359-371.

Iverson, R. M., Costa, J. E., LaHusen, R. G. (1992) Debris flow flume at H. J. Andrews Experimental Forest, Oregon. *Open-File Report*. 92-483.

Iverson, R. M. and LaHusen, R.G. (1993) Friction in Debris Flows: Inferences from Large-scale Flume Experiments. *Hydraulic Engineering.* 93. Proc 93 Conference. ASCE. (Eds. Shen, H. W., Su, S. T., and Wen, F.)

Iverson, R. M. (1997) The physics of debris flows. *Reviews of Geophysics*. 35 (3). 245-296.

Iverson, R. M., and Denlinger, R. P. (2001) Flow of variably fluidized granular masses across three-dimensional terrain: 1. Coulomb mixture theory. *Journal of Geophysical Research.* 106(B1). 537–552.

Iverson, R. M. and Logan, M. (2002) Scaling of Experimental Debris Flows and Avalanches. *American Geophysical Union, Fall Meeting.*

Iverson, R. M. (2003) The debris-flow rheology myth. In: Rickenmann and Chen (Eds.) *Debris-Flow Hazards Mitigation: Mechanics, Prediction, and Assessment.* Millpress. Rotterdam. 303-314.

Iverson, R. M., Logan, M., Denlinger, R. P. (2004) Granular avalanches across irregular three-dimensional terrain: 2. Experimental tests. *Journal of Geophysical Research: Earth Surface.* 109 (F1).

Iverson, R. M., Logan, M., LaHusen, R. G., Berti, M. (2006) Effects of the Basal Boundary on Debris-flow Dynamics. *American Geophysical Union.* Fall Meeting, 2006, Vancouver.

Iverson, R. M., Logan, M., LaHusen, R. G, Berti, M. (2010) The perfect debris flow? Aggregated results from 28 large-scale experiments. *Journal of Geophysical Research.* 115. F03005.

Iverson, R. M., Reid, M. E., Logan, M., LaHusen, R. G., Godt, J. W., Griswold, J. P. (2011) Positive feedback and momentum growth during debris-flow entrainment of wet bed sediment. *Nature Geoscience.* 4. 116-121.

Iverson, R. M. and George, D. L. (2014) A depth-averaged debris-flow model that includes the effects of evolving dilatancy. 1. Physical basis. *Proceedings of the Royal Society A.* 470. 20130819.

Iverson, R. M. (2015) Scaling and design of landslide and debris flow experiments. *Geomorphology.* 224. 9-20.

Jakob, M. and Hungr, O. (2005) *Debris Flow Hazards and Related Phenomena*. Springer, Berlin. 739pp.

Johnson, A. M. (1970) *Physical Processes in Geology*. Freeman, Cooper, San Francisco, California. 576p.

Johnson, R. M., and Warburton, J. (2003) Regional assessment of contemporary debris flow activity in Lake District mountain catchments, northern England: occurrence, scale and process. In: Rickenmann, D., Chen, C. L. (Eds). *Debris-Flow Hazards Mitigation: Mechanics, Prediction, and Assessment.* Millpress, Rotterdam, ISBN 90 77017 78 X.

Johnson, C. G., Kokelaar, B. P., Iverson, R. M., Logan, M., LaHusen, R. G., Gray, J. M. N. T. (2012) Grain-size segregation and levee formation in geophysical mass flows. *Journal of Geophysical Research: Earth Surface.*117. F01032.

Julien, P. Y. and Hartley, D. M. (1986) Formation of roll waves in laminar sheet flow. *Journal of Hydraulic Research.* 24 (1). 5-17.

Kaitna, R., Rickenmann, D., Schatzmann, M. (2007) Experimental study on rheologic behaviour of debris flow material. *Acta Geotechnica.* 2 (2). 71-85.

Kaitna, R. and Rickenmann, D. (2007) A new experimental facility for laboratory debris flow inversigation. *Journal of Hydraulic Research.* 45 (6). 797-810.

Kaitna, R., Dietrich, W. E., Hsu, L. (2014) Surface slopes, velocity profiles and fluid pressure in coarse-grained debris flows saturated with water and mud. *Journal of Fluid Mechanics.* 741. 377-403

Kaitna, R., Palucis, M. C., Yohannes, B., Hill., K. M., Dietrich, W. E. (2016) Effects of coarse grain size distribution and fine particle content on pore fluid pressure and shear behaviour in experimental debris flows. *Journal of Geophysical Research: Earth Surface.* 121 (2). 415-441.

Kim, B. B. and Low, D. R. (2004) Depositional processes of the gravelly debris flow deposits, South Dolomite alluvial fan, Owens Valley, California. *Geosciences Journal.* 8 (2). 153.

Larcher, M., Fraccarollo, L., Armanini, A. and Capart, H. (2007) Set of Measurement Data from Flume Experiments on Steady Uniform Debris Flows*. Journal of Hydraulic Research*. 45 (Extra Issue): 59-71.

Li., C., Ma, T., Zhu, X., Li, W. (2011) The power-law relationship between landslide occurrence and rainfall level. *Geomorphology.* 130 (3-4). 221-229.

Li, Y., Wang, B. –L., Zhou, X. –J., Gou, W. –C. (2015) Variation in grainsize distribution in debris flow. *Journal of Mountain Science.* 12 (3). 682-688.

Logan, M., and Iverson, R.M., (2007) (revised 2013) Video documentation of experiments at the USGS debris-flow flume 1992–2006 (amended to include 2007–2013): U.S. Geological Survey Open-File Report 2007–1315 v. 1.3., http://pubs.usgs.gov/of/2007/1315/.

Lorenzini, G., and Mazza, N. (2004) *Debris Flow: Phenomenology and Rheological Modelling*. WIT Press, Southampton. 216pp.

Lowe, D. R., and Guy, M. (2000) Slurry-flow deposits in the Britania Formation (Lower Cretaceous), North Sea: a new perspective on the turbidity current and debris flow problem. *Sedimentology.* 47 (1) 31-70.

Liu, X. (1996) Size of a debris flow deposition: model experiment approach. *Environmental Geology.* 28 (2).

Mainali, A. and Rajaratnam, N. (1994) Experimental study of debris flows. *Journal of Hydraulic Engineering.* 120 (1). 104-123.

Major, J. J. and Pierson, T. C. (1992) Debris Flow Rheology: Experimental Analysis of Fine-Grained Slurries. *Water Resources Research.* 28 (3). 841-857.

Major, J. J. (1997) Depositional Processes in Large-Scale Debris Flow Experiments. *The Journal of Geology*. 105. 345.

Major, J. J., and Iverson, R. M. (1999) Debris-flow deposition: Effects of pore-fluid pressure and friction concentrated at flow margins. GSA Bulletin. 111 (10). 1424-1434.

Marchi, L., Arattano, M., Deganutti, A. M. (2002) Ten years of debris-flow monitoring in the Moscardo Torrent (Italian Alps). *Geomorphology.* 46 (1-2). 1-17.

Martino, R. and Davies, T. R. (2003) Dynamic Friction Coefficient of a Fluid-Solid Mixture. Fast Slope Movements Prediction and Prevention for Risk Mitigation: Naples, May 11-13, 2003, 1. 357-359.

Massey, B. S. (1989) *Mechanics of Fluids* (Sixth Edition). Chapman Hall. 543pp.

McCoy, S. W., Kean, J. W., Coe, J. A., Staley, D. M., Wasklewicz, T. A., Tucker, G. E. (2010) Evolution of a natural debris flow: In situ measurements of flow dyamics, video imagery, and terrestrial laser scanning. *Geology.* 38 (8). 735-738.

McCoy, S. W., Tucker, G. E., Kean, J. W., Coe, J. A. (2013) Field measurement of basal forces generated by erosive debris flows. *Journal of Geophysical Research F: Earth Surface.* 118 (2). 589-602.

Munachen, S. E. (2006) Debris-flow surge dynamics. *Geophysical Research Abstracts.* 8. 10035.

Naylor, M. A. (1980) The Origin of Inverse Grading in Muddy Debris Flow Deposits—A Review. *Journal of Sedimentary Petrology.* 50 (4). 1111-1116.

Paola, C., Straub, K., Mohrig, D., Reinhardt, L. (2009) The unreasonable effectiveness of stratigraphic and geomorphic experiments. *Earth Science Reviews.* 97. 1-43.

Papa, M., Egashira, S., Itoh, T. (2004) Critical conditions of bed sediment entrainment due to debris flow. *Natural Hazards and Earth System Sciences.* 4. 469-474.

Parsons, J. D., Whipple, K. X., Simoni, A. (2001) Experimental Study of the Grain-Flow, Fluid-Mud Transition in Debris Flows. *The Journal of Geology*. 109. pp427-447

Petley, D. N., Hearn, G. J., Hart, A., Rosser, N. J., Dunning, S. A., Oven, K., Mitchell, W, A. (2007) Trends in landslide occurrence in Nepal. *Natural Hazards.* 43. 23-44.

Phillips, C. J. and Davies, T. R. H. (1991) Determining rheological parameters of debris flow material. *Geomorphology.* 4 (2). 101-110.

Pierson, T. C. (1981) Dominant particle support mechanisms in debris-flows at Mt Thomas, New Zealand, and implications for flow mobility. *Sedimentology.* 28. 49-60.

Pierson, T. C. (1985) Effects of slurry composition on debris flow dynamics: Rudd Canyon, Utah. *Delineation of Landslide, Flash Flood, and Debris Flow Hazards in Utah.* Proceedings of a specialty conference at Utah State University, Loga, Utah, June 14-15. 1984. 132-152.

Pierson, T. C. and Scott, K. M. (1985) Downstream Dilution of a Lahar: Transition from Debris Flow to Hyperconcentrated Streamflow. *Water Resources Research.* 21 (10). 1511-1524.

Prochaska, A. B., Santi, P. M., Higgins, J. D., Cannon, S. H. (2008) Debris-flow runout predictions based on the average channel slope (ACS). *Engineering Geology.* 98 (1-2). 29-40.

Prochaska, A. B., Santi, P. M., Higgins, J.D., Cannon, S. H. (2008) A study of methods to estimate debris flow velocity. *Landslides.* 5 (4). 431-444.

Pudasaini, S. P. and Hutter, K. (2007) *Avalanche Dynamics: Dynamics of Rapid Flows of Dense Granular Avalanches.* Springer. Berlin.

Pudasaini, S. P. (2011) Some exact solutions for debris and avalanche flows. *Physics of Fluids.* 23 (4). 043301.

Reid, M. E., Iverson, R. M., Logan, M., LaHusen, R. G., Godt, J. W., Griswold, J. P. (2011) Entrainment of bed sediment by debris flows: results from large-scale experiments. Proceedings of the Fifth International Conference on Debris Flow Hazards Mitigation/Mecahnics, Prediction, and Assessment. Padua, Italy. June 7-11, 2011. *Italian Journal of Engineering Geology and Environment.* Casa Editrice Universita La Sapienza, Rome. 367-374.

Reid, M. E., Coe, J. A., Brien, D. L. (2016) Forecasting inundation from debris flows that grow volumetrically during travel, with application to the Oregon Coast Range, USA. *Geomorphology.* 273. 396-411.

Roberds, Wm. J. and Ho, K. (1997) A Quantitative Risk Assessment and Risk Management Methodology for Natural Terrain in Hong Kong. In: Chen, C. (Ed.) *Debris Flow Hazards Mitigation: Mechanics, Prediction, and Assessment.* Proceedings of the first international conference. August 7-

9, San Francisco, California. American Society of Civil Engineers, New York.

Rombi, J., Pooley, E. J., Bowman, E. T. (2006) Factors influencing debris flow behaviour: An experimental investigation. *In:* Ng, C. W. W., Wang, Y. H., Zhang, L. M. (Eds.) *Physical Modelling in Geotechnics*. Taylor and Francis Group, London. 1604 pp.

Saucedo, R., Macías, J. L., Sarocchi, D., Bursik, M., and Rupp, B. (2008), The rain-triggered Atenquique volcaniclastic debris flow of October 16, 1955 at Nevado de Colima Volcano, Mexico. *Journal of Volcanology and Geothermal Research*. 173. 69–83.

Savage, S. B., Iverson, R. M. (2003) Surge dynamics coupled to pore-pressure evolution in debris flows. In: Rickenmann and Chen (Eds.) *Debris Flow Hazards Mitigation: Mechanics, Prediction and Assessment.* Millpress, Rotterdam.

Savage, W. and Baum, R. (2005) Instability of steep slopes. In: Jakob, M. and Hungr, O. (Eds.) *Debris Flow Hazards and Related Phenomena*. Springer, Berlin.

Scheidl, C., Chiari, M., Kaitna, R., Mülleger, M., Krawtschuk, A., Zimmerman, T., Proske, D. (2013) Analysing Debris-Flow Impact Models, Based on a Small Scale Modelling Approach. *Surveys in Geophysics*. 34 (1). pp121-140.

Scheidl, C., McArdell, B. W., Richenmann, D. (2015) Debris-flow velocities and superelevation in a curved laboratory channel. *Canadian Geotechnical Journal.* 52 (3). 305-317.

Scott, K. M. (1988), Origin, behavior, and sedimentology of lahars and lahar-runout flows in the Toutle-Cowlitz river system. *U.S. Geological Survey Professional Paper.* 1447-A, 72.

Schürch, P. (2011) Debris-flow erosion and deposition dynamics. Durham theses, Durham University. Available at Durham E-Theses Online: http://etheses.dur.ac.uk/3395/

Schürch, P., Densmore, A. L., Rosser, N. J., McArdell, B. W. (2011) Dynamic controls on erosion and deposition on debris-flow fans. *The Geological Society of America.* 39 (9). 827-830.

Seeger, M. Quinton, J., Kuhn, N. J. (2011) Experiments in Earth Surface process research. *Catena*. 01705.

Sharp, R. P. and Nobles, L. H. (1953) Mudflow of 1941 at Wrightwood, Southern California. *Bulletin of the Geological Society of America.* 64. 547-560.

Shieh, C. L., Jiang, J. H. (1992) Study on the judgement of dangerous valley of debris flow. *Proceedings of the 6th Chinese Conference on Hydraulic Engineering.* National Chiao-Tung University, Hsinchu, Taiwan. 262-273.

Sheih, C. L., Tsai, Y. F. (1997) Experimental study of the configuration of debris-flow fan. *In:* Chen, C. I. (Ed.) *Proceedings of the First International Conference on Debris Flow Hazard Mitigation: Mechanics, Prediction, and Assessment.* San Francisco, ASCE, New York. 133-142.

Shih, B. J., Shieh, C.L., Chen, L. J. (1997) The Grading of Risk for Hazardous Debris-Flow Zones. In: Chen, C. (Ed.) *Debris Flow Hazards Mitigation: Mechanics, Prediction, and Assessment.* Proceedings of the first international conference. August 7-9, San Francisco, California. American Society of Civil Engineers, New York.

Silbert, L. E., Ertas, D., Grest, G. S., Halsey, T. C., Levine, D., Plimpton, S. J. (2001) Granular flow down and inclined plane: Bagnold scaling and rheology. *Physical Review E.* 64. 015302.

Smith, M.W., Carrivick, J.L. and Quincey, D.J. (2015) Structure from Motion Photogrammetry in Physical Geography. *Progress in Physical Geography*. 40 (2). 247-275.

Smith, M.W. and Vericat, D. 2015. From experimental plots to experimental landscapes: topography, erosion and deposition in sub-humid badlands from Structure-from-Motion photogrammetry. *Earth Surface Processes & Landforms.* 40. 1656-1671.

Sosio, R. and Crosta, G. B. (2009) Rheology of concentrated granular suspensions and possible implications for debris flow modelling. *Water Resources Research*. 45. W03412.

Stancanelli, L. M., Lanzoni, S., Foti, E. (2015) Propagation and deposition of stony debris flows at channel confluences. *Water Resources Research.* 5100-5116.

Stoffel, M., Mendlik, T., Schneuwly-Bollschweiler, M., Gobiet, A. (2014) Possible impacts of climate change on debris-flow activity in the Swiss Alps. *Climatic Change.* 122 (1). 145-155.

Tiwari, P. C., and Joshi, B. (2016) Rapid urban growth in mountainous regions: The case of Nainital, India. UGEC Viewpoints. Available at: https://ugecviewpoints.wordpress.com/2016/03/29/rapid-urban-growth-in-mountainous-regions-the-case-of-nainital-india/ [Accessed 29/11/16]

Takahashi, T. (1981) Debris Flow. *Annual Review of Fluid Mechanics*. 13. 57-77.

Takahashi, T. (2007) *Debris Flow: Mechanics, Prediction and Countermeasures.* Balkema-proceedings and monographs in engineering, water, and Earth sciences. Taylor and Francis, London; New York. 572 pp.

Turnbull, B., Bowman, E. T., McElwaine, J. N. (2015) Debris Flows: Experiments and Modelling. *Competes Rendus Physique.*16 (1). 86-96.

UN Habitat (2009) Planning Sustainable Cities: Global Report on Human Settlements 2009. *United Nations Settlement Programme.*

Vallance, J. W., and Scott, K. M. (1997) The Osceola Mudflow from Mount Rainier: Sedimentology and hazard implications of a huge clay-rich debris flow, *Geological Society of America Bulletin.* 109 (2).143–163.

Vandre, B. C. (1985) Rudd Creek debris flow. In: Bowles, D. S. (Ed.) Delineation of Landslide, Flash Flood, and Debris Flow Hazards in Utah. Utah Water Resources, Utah State University, Logan, Utah. 117-131.

Van Steijn, H. and Coutard, J. P (1989) Laboratory experiments with small debris flows: Physical properties related to sedimentary characteristics. *Earth Surface Processes and Landforms*. 14. 587-596.

Wang, F., Wu, Y.-H., Yang, H., Tanida, Y., Kamei, A. (2015) Preliminary investigation of the 20 August 2015 debris flows triggered by a severe rainstorm in Hiroshima City, Japan. *Geoenvironmental Disasters.* 2 (17).

Weber, D. and Rickenmann, D. (1999) Physical modelling of debris flow surges and related erosion processes. In: *Hydraulic Engineering for Sustainable Water Resources Management at the Turn of the Millennium*. Proceedings of Int. Association for Hydraulic Research, 28 Biennial Congress, 22-27 August 1999 in Graz, Austria. [CD-ROM]. Graz, Institute for Hydraulics and Hydrology, Technical University. 8 S.

Westoby, M. J., Brasington, J., Glasser, N. F., Hambrey, M. J., Reynolds, J. M. (2012) 'Structure-from-Motion' photogrammetry: A low-cost effective tool for geoscience applications. *Geomorphology.* 179 (15). 300-314.

Wilcock, P. R. (1993) Critical shear stress of natural sediments. *Journal of Hydrological Engineering.* 119. 491-505.

Xiao-qing, C., Yong, Y., Chen, J., De-ji, L. (2014) Characteristics of a drainage channel with staggered indented sills for controlling debris flows. *Journal of Mountain Science.* 11 (5). 1242-1252.

Yalin, S. M. (1971) Theory of Hydraulic Models. Macmillan, London. 288pp.

Young, W. J. (1989) Bedload transport in braided gravel-bed rivers: A hydraulic model study. PhD thesis. *Lincoln College, University of Canterbury*.

Zanuttigh, B., and Lamberti, A. (2007) Instability and surge development in debris flows. *Reviews of Geophysics.* 45 (3) RG3006.

Zhuang, J-q., Cui, P., Peng, J-b., Hu, K-h., Iqbal, J. (2013) Initiation process of debris flows on different slopes due to surface flow and trigger-specific strategies for mitigating post-earthquake in old Beichuan County, China. *Environmental Earth Sciences.* 68 (5). 1391-1403.